Shape & cutoff in superconducting qubits, work fluctuations in correlation creation, & critical commentary

by

Emma McKay

A thesis
presented to the University of Waterloo
in fulfillment of the
thesis requirement for the degree of
Master's of Mathematics
in
Applied Mathematics

Waterloo, Ontario, Canada, 2018

This thesis consists of material all of which I authored or co-authored: see Statement of Contributions included in the thesis. This is a true copy of the thesis, including any required final revisions, as accepted by my examiners.

I understand that my thesis may be made electronically available to the public.

Statement of Contributions

Parts of this thesis have been adapted from Refs. [1, 2], both of which I was the lead author on. In particular, the non-introductory material of Part I is based on [1]. I performed all of the computations and all calculations except those contained in the Appendix A, which were performed by my co-author Adrian Lupascu. I also made the majority of contributions to the writing.

The non-introductory material of Part II is based on [2]. I was the lead author on the publication [2], with my co-author Nayeli A. Rodríguez-Briones, currently a Ph.D. student at the University of Waterloo. I performed most of the computations and figure design, made the majority of contributions to the writing, and led interpretational discussion.

Abstract

Part I

We apply the Unruh-DeWitt model for a qubit interacting with a quantum field to a superconducting qubit. We use the flexibility of this model, as compared to the spin-boson model used widely in the literature, to investigate the effect of an ultraviolet cutoff in the field and the finite size of a qubit on the dynamics of a qubit. In studying these features in the setup of a qubit coupled to an infinite transmission line, we find that both the shape and scale of the ultraviolet cutoff have a significant effect on the qubit's dynamics. For experimentally reasonable parameters, we estimate that using an inaccurate model for the ultraviolet cutoff present in the line could introduce errors in calculation of probability of spontaneous emission of the qubit of around 10%. This is particularly interesting in light of the fact that superconducting lines have natural ultraviolet cutoffs due to the breakdown of superconductivity for high frequency electromagnetic waves.

Part II

We investigate a unitary protocol to create correlations in a bipartite quantum mechanical system. The protocol was initially motivated by its optimal average work cost. We calculate the fluctuations in the work cost and show that for maximal generation of correlations, the fluctuations in the work cost are of the order of the average work cost, making the protocol energetically rather unreliable. We additionally explore some of the nuances of the discussion around work in quantum systems with discussion of the current literature as well as some philosophical motivations of the most widely used definitions of work.

Throughout the thesis, we comment on the motivations for this research and its effect on our world. In doing so, we find multiple ways that supporting the project of developing quantum technology supports injustice. We also model a methodology for engaging with societal and ethical implications of work in theoretical physics.

Acknowledgements

First, an acknowledgement to the land and the people who have been in relationship with it for much longer than I have. The land that I have been living, working, and writing on is the territory of the Anishnaabe, Attawandaron, and Haudenosaunee peoples. All of Kitchener-Waterloo, including the University of Waterloo, is on stolen land. Its history is complicated, and more can be learned by visiting [3]. In 1784, the British Haldimand Proclamation designated six miles on either side of the Grand River to belong to the Haudenosaunee, 950 000 acres. Since that time, activities including squatting and shady land deals have seen over 95% of the Haldimand tract change ownership. The land now under legal care of the University of Waterloo in particular was squatted on by Mennonite farmers.

There are so many ways that I have benefited by being a settler. There is so much that this land has given me. And there is so much harm that settler colonialism, enacted by the state and people of Canada, that has been brought on Indigenous folk. The doing of physics is not separate from this.

The past two years have been a wild time. I've learned so much about physics and knowledge and being a decent human—enough to know that I know barely a thing. And still, I know a few things. I'm completely sure that I would never have grown this much without the people around me. It feels a little strange to write this before it's really over, before the time I'm sure I'll break down in tears and try to deliver a personal message of gratitude to everyone I've known while I sob. But then. These are the limitations of academic procedure.

In no particular order, my deepest gratitude goes to these folks—thank you:

Josh Ruebeck, who won't leave my mind, whose respect I value so much. Your academic honesty, carefulness, and passion is pushing me every day to do better, even in the midst of uncertainty. Thanks for helping me make this thesis into what I wanted it to be. Thanks for your patience as I learn to harmonize.

Carolyn Earnest, for your invaluable insights, your realism, ... for sharing so many of your impressive skills and interests with me. I don't know how to encapsulate how much your education and care has impacted me. Thank you for your friendship. Thank you for working with me.

Simon Daley, for your generosity, your fierce kindness, and always wanting to try to show each other our brains.

John Schanck, for helping me conceptualize of an academia that really prioritizes knowledge and knowledge transfer, for tempering my dramatic criticisms, for working on your

hugs, for sharing art and coffee. (Also for your comments about probability—I don't remember what they were, but they helped me.)

Al Sachs, for your kindness and generosity and that deeply felt smile and every hug! Thank you for sharing so much time with me, teaching me to can, and allowing me to help.

Christian Barna, your friendship sits in just the right place in my heart. Thanks for listening, thanks for growing.

Everyone at FemPhys, thank you for your work! For all your belief in and efforts towards community and a different physics. I am so selfishly reassured by you that my own dreams are not baseless. I am so hopeful that your work is changing this campus, little by little. Thank you especially to Emily Carlson and Hussam Anjum for becoming repositories of knowledge and developing your own ways. Thanks to Cary and Laura and Lindsay for their impressive leadership and all their efforts. Thanks to Jen Reid and Sarah Kaiser for starting this thing. Thanks to the folks at WIPC 2018 for trusting me and wanting to learn what FemPhys is all about! Thanks to Teddy, Alyssa, Ridhee, Sarah, Samra, Oz, Lei, Simon, Morgan, Sherry, Cynthia, Chris, Kailas, Inah, and everyone who has worked on the exec. Our meetings are invariably a highlight in my week. Love y'all.

My colleagues, for your hard work, your encouragement to do better even by virtue of being as good as you are, and your endlessly interesting suggestions: Maria Papageorgiou, Nayeli Rodríguez-Briones (thanks for travelling with me!), Alvaro Ortega, Alvaro Alhambra, Pipo de Ramon (thanks for sharing your giggles!), Nicholas Funai, Daniel Grimmer, Petar Simidzija, Erickson Tjoa, Richard Lopp, and Irene Melgaro-Lermas.

Eduardo, thanks for all your work. I know you supported me in the best way you know how. I really appreciate you engaging in difficult conversations, being open to criticism, and trying to do things differently.

Other folks! Turner, thanks for letting me grow with you. You're a sweetheart. Evan, thanks for showing me your human beatboxing, being Hilarious, for sharing your music and yourself. Lindsay, thanks for talking and cooking. Laura, thanks for doing this academic struggle with me, for sharing your art and your outfits, for inadvertently reminding me to do a land acknowledgement here. Gosh, other folks whose time spent with me I am so grateful for: Briar, Hannah, Parker, Rayne, Julia, Maria, Naye.

Academics: thanks to everyone who engaged with me at RQI-N 2017 after I tried to pick a fight. Thanks to folks at Quantum Thermo 2018, who were so excited and welcoming and did so much for my work on Part II of this thesis. Thanks to Doreen Fraser, whose recent mentoring is invaluable to me. And thanks to folks all over who are doing their damndest to get shit moving in equity in physics, especially Chanda Prescod-Weinstein, Divya Persaud, Katherine Crocker, and Piper Harron, who impersonally taught me a great deal over Twitter. Thanks to Adrian Lupascu for his help with [1]. Thanks to Achim

Kempf, whose soft lecturing voice convinced me I knew something about quantum field theory four years ago, and whose interest in his students has been inspirational. Thanks to Robb Mann, for being a good supervisor to my friends.

Thanks to folks who have made my time at this school run more smoothly, even if I didn't know. Thanks especially to Maren Butcher for being the kindest.

Thanks to all the folks who are (or have been) working hard at making this campus a better place to live and work, many of whom have been a pleasure to work with: Amanda Cook, Lyndia Stacey, Caity Dyck, Sarah Wiley, and I'm sure many more.

Fi: you're the best sister I could ask for. Mom: your support makes my life less stressful every day. Thank you for working so hard to make space for me in excess of all the amazing work you do already. Dad: thanks for passing on your laugh. Cecelia: thanks for being the best big sister you can be. Alastair: I love learning about what you're doing! Thanks for sharing your new family with me. Love y'all.

My deepest gratitude to this land, for its beauty and bounty and being the deepest rooted home I've ever had.

Thanks to you! I hope there's something in this thesis, if you're here to read it, that is at least a little interesting. Thanks for engaging in whatever part you do genuinely, and the work that takes. Thanks for listening.

Dedication

For my friends, and the world we are trying to create together.

Table of Contents

List of Tables

List of Figures

List of Symbols, Part I

$\Box$	d'Alembertian operator, defined under equation (3.1.1)
α_{SB}	non-mode-dependent coupling constant in the spin-boson model
$\hat{a}_k^\dagger$, $\hat{a}_k$	creation and annihilation operators of electromagnetic mode k
$\hat{b}_k^\dagger$, $\hat{b}_k$	alternate creation and annihilation operators for mode k
β_L	a dimensionless parameter, defined in equation (2.2.10)
C	capacitance of a capacitor inserted in parallel with a Josephson junciton
$C_\varepsilon(k)$	a cutoff function with form not specified and scale ε
Δ_{AB}	relative difference between shape or cutoff models A and B
δ_{ij}	Kronecker delta
ε	cutoff scale
e	Euler's number
E_J	Josephson energy, the potential across a Josephson junction
$\tilde{F}$	tilde indicating a Fourier transform, defined in equation (4.2.18)
Φ_{ext}	flux applied externally to a flux qubit
Φ_0	the quantum of flux threading the superconducting flux qubit
$\hat{\Phi}$	magentic flux threading the ring of a superconducting qubit
$F_\sigma(x)$	a smearing function with form not specified and scale σ
Γ	rate of spontaneous decay of the qubit into the field
g_k	coupling constant of mode k to the two-level system in the spin-boson Hamiltonian

$\|g\rangle$, $\|e\rangle$	ground and excited states of the qubit
$\hat{H}$	Hamiltonian; system specified with subscripts
h, $\hbar$	Planck constant, reduced Planck constant
I_c	critical super-current
i	imaginary unit
$\hat{I}$	super-current present in ring of a flux qubit
$J(\omega)$	spectral density function, defined in section 2.1.1
k	mode number (also known as wavenumber) of a field
L	self-inductance of a flux qubit
λ	coupling constant of the UDW interaction
$\|L\rangle$, $\|R\rangle$	basis for left and right wells in the double-well potential
$\hat{\mu}(t)$	monopole moment of the detector
$\|n_{L,k}\rangle$, $\|n_{R,k}\rangle$	Fock states for a mode k associated with the qubit being in state $\|L\rangle$ or $\|R\rangle$
n	an integer, indicating the number of whole loops of the wave function around the ring of a flux qubit
$\hat{\pi}(x,t)$	conjugate momentum of the scalar field, $\hat{\pi} = \partial_t \hat{\phi}$
π	the usual irrational constant
p.v.	Cauchy principal value
P_e	probability of vacuum excitation (or spontaneous emission) of the qubit
$\hat{\psi}$	electron wave function in flux qubit
r	time scale for ramping up and down the interaction
R	resistance of a resistor inserted in parallel with a Josephson junction
$\hat{\rho}$	quantum state, with subscripts q indicating the qubit, π the conjugate momentum, in the initial state, and out the final state
σ_+, σ_-	raising and lowering operators of the qubit
$\hat{\sigma}_x$, $\hat{\sigma}_y$,$\hat{\sigma}_z$	Pauli x, y, and z operators

T	length of constant interaction
$u_k(x,t$	coefficients of creation and annihilation operators in decomposing the scalar field, equation (3.1.4)
$\hat{U}$	voltage drop across a junction
V_b	barrier height in the double-well potential
V	potential for the flux through the flux qubit loop
Ω	qubit frequency
Ω_0	non-renormalized energy gap of a qubit in the double-well potential
ω_k	frequency of electromagnetic mode k
ω_0	frequency of small oscillations in the double-well potential
$W_\sigma[t,t']$	smeared Wightman, defined in equation (4.2.13)
$\chi(t)$	switching function
$\hat{\zeta}_\pm$	location of minima of the double well potential
$\hat{\zeta}$	a useful parameter, defined above equation (2.2.9)

List of Symbols, Part II

$\langle\cdot\rangle$	average (over iterations of a process, usually)
$A_\pm$, $B_\pm$	elements of the final state, equation (5.1.5)
β	the inverse temperature
$C_B(\hat{\rho})$	measure of classical correlations, equation (3.1.4)
E_n	nth eigenenergy
$E(\hat{\rho})$	relative entropy of entanglement, equation (3.1.3)
$\{\|\phi_{m,n}\rangle\}$	generalized Bell states, equation (4.2.3)
F	free energy
$\hat{H}$	a Hamiltonian
I	quantum mutual information, defined in equation (4.1.5)
$I_{\max}$	the maximum mutual information able to be produced by the protocol
λ	protocol parameter
$\{\|n\rangle\}$	energy eigenbasis
$P(W)$	probability distribution over work
$p(\vec{z}(t))$	phase space distibution over phase space points $\vec{z}(t)$
Q	heat

R_i	rotation in subspace S_i
$\hat{\rho}$, $\hat{\rho}'$	initial and final state
$\hat{\rho}_{\mathrm{A}}$	state over the subsystem A, defined under equation (4.1.5)
Σ_W	the standard deviation of the unprojected work probability distribution
S_i	a subspace spanned by a subset of Bell states, equation (4.2.5)
$\sigma_{E_i E_f}$	covariance of initial and final energies, defined in equation (2.2.14)
σ_{E_i}	variance of the enery, defined in equation (2.2.12)
S	entropy (classical Gibbs and von Neumann, dependent on context)
$\hat{\sigma}_Z^{(\mathrm{A})}$	Pauli z operator on subsystem A
$\Delta\sigma_E$	the change in the standard deviation of energy from before to after the protocol
θ, δ, γ, ϕ	real rotation parameters of the unitary
$\hat{\tau}(\beta)$	thermal state of inverse temperature β, equation (4.1.1)
U	total energy of a system
$\hat{U}$	a unitary
$\hat{U}_{\mathrm{corr}}$	correlating unitary, section 4.2
$W_{(I_{\max})}$	work cost of producing the maximum mutual information possible
Z	the partition function, $Z = \mathrm{Tr}[\mathrm{e}^{-\beta H}]$
ω	energy gap of each qubit
σ_W	the standard deviation of the two-time measurement scheme work probability distribution
$\Delta\hat{H}$	the "work operator," defined in section 2.2.2
W	work
$\hat{X}$, $\hat{Z}$	clock operators, equation (4.2.1)

Abbreviations

CQED	circuit quantum electrodynamics
LMI	light-matter interaction
RWA	rotating wave approximation
UDW	Unruh-DeWitt
USC	ultra-strong coupling
UV	ultraviolet

Prologue

Steps Towards a Just Physics

This thesis explores two projects in quantum theory. One concerns using tools developed by quantum field theorists for a simplified setup in superconducting circuits. The other is about the probabilistic work cost of creating correlations between two qubits. Both sit in the literature under the large umbrellas of quantum information, quantum theory, and quantum technology (QTech).

For most of my degree, I did not want to support the development of QTech (for reasons elaborated on below), and held that my research was mostly useless anyway. I have since found that no research has zero impact on the world. Nothing we do is without effect. Consequences of this include the importance of incremental work in science and the fact that the work of my master's degree contributes somehow to the project of QTech.

Instead of ignoring this connection, in this prologue, I analyse it. I will explore what the motivations are for the large scale project of QTech and critique both the realism and political intents of those motivations. I look briefly at existing efforts towards development of QTech which is responsible to society, and provide an example of how this technological project participates in unjust political projects. Finally, I argue for the regular inclusion of critical analysis of our motivations for our research and its effect on the world around us, and begin to demonstrate one method for doing so, which continues throughout the thesis.

The reasons we are developing quantum technology

The motivation given for developing QTech varies to some extent. Popular writers seem keen to dramatize its potential utility [4]. Many scientists discuss in some detail the potential applications in cryptography and simulation, but don't seem to want to discuss the many practical limitations to these proposals [5]. Quantum cryptography is said to lead to communication channels which are resistant to attacks from quantum hackers (though post-quantum cryptography is a promising field, aiming to develop classical cryptography

which is similarly resistant, and will require far less infrastructure to implement). Simulating quantum systems is touted to be able to lead to better understanding and development of drugs, fertilizers, and materials.

There are few publications which make criticisms or are cautionary about the potential of QTech. Some ethical questions are raised by de Wolf in [6], suggestions for a responsible development of technology are made in [7], and Aaronson discusses a few limits of computation in [8]. Major criticisms of the technology itself of course include that the number of algorithms which provide significant speedup over classical computation are few. Simulations of large molecules may even be limited to gate resources which scale like N^6, where N is the number of atoms [9]. Doubts can also be cast on the physical infrastructure needed for a single quantum computer (let alone any kind of network of them)—many millions of physical qubits may be needed to build a computer which can implement Shor's algorithm [10], and weak speedups like those provided by Grover's search algorithm may be made weaker by the physical implementation. This is not to say that the implementations are not possible, but rather to suggest that the endeavour may continue to be very resource intensive and may yield less benefit than is usually discussed (given, of course, that the usual discussion is of the best-case scenario).

de Wolf raises the point that the benefits of QTech are unlikely to be equally distributed across populations [6]. Already, research is concentrated in a few very wealthy areas, and funded primarily by large corporations like Google and IBM and by states like the USA and China. Thus one might expect that any fruits of the technology will primarily benefit the state and those who are able to pay for access to the technology (which includes academics). Beyond this argument, one might wonder whether these benefits of the technology really justify spending our resources on it, whether or not they are distributed equally. If classical computers are capable of implementing quantum-safe cryptography, then why continue to research very expensive and completely new technology which will be difficult to distribute equitably? If fertilizers are already contributing to destructive algal blooms, then why not pursue methods of sustainable food production [11–13]? Our answers needn't always be found in the shiniest new technology.

Exploring new potentially bioactive molecules or properties of known molecules with quantum simulation is a well-discussed reason to develop quantum computers. It's also a rich area for ethical exploration. Undoubtedly, new drugs can be seriously beneficial to many people. But pharmaceutical companies run one of the most profitable and extortionist industries on the planet. Perhaps one of the benefits of quantum computing is that it will increase profit margins of Big Pharma.

Despite these and more general criticisms (expense, resource-intensivity, narrow appli-

cability), support for QTech and computation is prolific.[1] It is an incredibly well-funded area of science and engineering, with at least an informal reputation of being the place to go in order to receive grants. There is minimal popular or funding-agency-level discussion about pitfalls of this huge pursuit. Almost all the press that the field gets is completely positive[2] and optimistic about its utility and impacts.

One piece of the narrative around QTech is that it will be revolutionary in society. In quantum thermodynamics in particular, this narrative is motivated by a strong analogy to classical thermodynamics. Because classical thermodynamics was crucial to the Industrial Revolution, it is argued, quantum thermodynamics will similarly contribute to a substantial revolution in technology and thus society. Arguably, part of the recent expansion of the field is due to this grandiose motivation. Though it is clear that there are genuinely new thermodynamic phenomena and relations to explore in quantum systems, an analogical 'quantum revolution' does not immediately follow. We make a serious inductive jump to assume that the enormity of technological prowess enabled through quantum thermodynamics will be even close to that significant.

A larger analogy is made between computation and quantum computation. Computation changed our society, ergo computation using quantum systems will do the same (but in unfathomable ways)! Incorporating the additional issue of low comprehension of this research by the public and the state, it seems that the attractive, uncritical story that is told about QTech plays a significant role in its receiving so much attention and funds. Both the overhyped narrative and the low public comprehension (among other structural issues) mean that the public have little ability to genuinely contribute to decision-making processes around resource allocation or research focuses.

Existing efforts towards responsible quantum technology

Coenen and Grunwald argue for the development of a strong responsible research and innovation approach to the development of quantum technologies, with the goal of technology that genuinely meets the needs of society and that is embedded into society [7]. Crucial elements of the strategy that they begin to sketch out include not overstating the potential

[1] For instance, the Canada First Research Excellence Fund, which is designed to support large-scale research initiative with "strategic relevance to Canada," has supported all three Canadian QTech research institutes with large grants in 2015 and 2016, totalling $176 million—14% of the total $1.2 billion awarded [14, 15]. This is a comparable amount to funds awarded to research in green energy and more efficient oil sands extraction combined. Note of course that this is a cursory study and does not cover even close to all scientific funding provided by the Canadian state in those years.

[2] Evidence on it being trace preserving unknown.

impact of a field nor its cross-disciplinary utility. This assists in everyone involved having realistic, sustainable expectations which will be more difficult to disappoint.[3]

As analysed by Coenen and Grunwald, many of the extant strategies for the development of quantum technologies do not prioritize responsible research. For instance, the 'Quantum Manifesto' of the European Union addresses public engagement only in terms of educating the general public about quantum technologies [16]. They do not discuss how to engage the public in decision-making or impact-assessment (a critical element of a framework known as 'responsible research and innovation'). The drivers of quantum technology are identified in this manifesto as primarily industry stakeholders.

The most well-developed attempts at creating public involvement in research decisions come from a German report on the nascent applications in the field [17]. The few specific strategies for consultation include considering non-expert, qualitative opinions as important in making policy decisions about technology, as opposed to only valuing the opinions of scientists expert in the physical phenomena and tools used.

The critical analysis in [7] already presents a dramatically different method for technology development than is currently employed. Around us, we can observe the proliferation of dramatized narratives about the impact of quantum technology on our lives; we involve the public only by attempting to disseminate simplified information about our fields of expertise; and the primary role of policy-makers in quantum technology research appears to be the allocation of funds to high-potential areas like quantum cryptography.

In fact, Coenen and Grunwald don't touch on an important part of the role of policy makers in research and innovation. Politicians can and do make decisions about supporting sensationalized narratives and particular technologies for their own political gains. It can benefit a state to be seen nationally and internationally as participating in a field of cutting-edge research—the state may gain a reputation as being technologically advanced, which is invaluable for political and business purposes. This is particular useful when the research relates to state interests like security, and it is clear that much of the narrative around quantum technology is currently about cryptography. Thus, pursuit of security projects like satellite systems of quantum key distribution not only have the effect of furthering development of a (potentially) useful technology for security (with all the inherent consequences of security technology), but also draws on the hyped narratives of quantum technology to lend authority to the state. In this way, sensationalized stories about the potential of QTech serve political purposes. Let's investigate with a case study.

[3] As opposed to sensationalized expectations leading to misapplication of funds and subsequently to dramatic drops in funds when the research does not deliver.

Arctic sovereignty and entangled photons

The Arctic has a long history of being desired by various nation states for its potential business applications. The Northwest Passage has long been desired for more efficient travel around the Americas. Mining has been active in Arctic territories for decades, including for diamonds in Nunavut and gold in Alaska. This desire continues ever stronger today: oil reserves previously under ice are in apparently high demand by the USA, Canada, Russia, and other Arctic nations [18, 19].

Even now, claims to borders and waters are under dispute, with a significant dispute around the Northwest Passage. Canada claims that these waters belong to the state; many other nations consider them international waters [20]. The Canadian state has been implementing strategies to lay definitive claim to this and other Arctic territory for many years, with political intent to expand these strategies [21, 22]. Populations of military personnel and researchers are maintained in Alert, Nunavut, located at the northern tip of Ellesmere Island, making it the northernmost permanently inhabited location in the world [23]. Autonomous submarines have been deployed to make more accurate maps [24], with the explicit goal of continuing the project of Arctic exploration to accurately define the limits of the continental shelf to "obtain international recognition for those limits" [25].

In 1953, 87 Inuit were forcibly relocated from Inukjuak, a community on the northeastern side of Hudson Bay, to new communities named Grise Fiord and Resolute in the High Arctic [26, 27], about 2000 km away. The families were separated en route without prior warning, not provided with enough appropriate supplies for a harsher environment, and were initially told they would be able to choose to move back to their communities, but were never actually offered the opportunity. Various efforts were made by the relocated individuals and their descendents to obtain compensation and an apology. A $10 million fund was created in 1996, with an intentional absence of apology [26]. An apology was officially offered in 2010, 57 years after the relocation and 16 years after the Royal Commission on Aboriginal Peoples recommended an apology which acknowledged that the goal of the relocation included establishing an Arctic presence for the benefit of the Canadian government [28]. The Canadian government continues to cite Inuit presence as a legitimizing factor in its efforts to make land and water claims [22, 29]. This was undoubtedly a project of Arctic sovereignty.

In 2018, the Department of National Defence awarded a $2.7 million contract to a research group at the Institute for Quantum Computing for contributions to the development of a quantum radar system to be deployed in the Arctic [30]. The government media release identifies the project as one which supports Arctic sovereignty: "Surveillance solutions support the Government of Canada's ability to exercise sovereignty in the North,

and provide a greater awareness of safety and security issues, as well as transportation and commercial activity in Canada's Arctic" [30].

The research itself is primarily concerned right now with the development of a source of entangled photons. One could make conservative judgements about whether advertised technological goals are genuinely achievable; certainly, the implementation of a long-distance radar system using sensitive photonic devices in harsh conditions seems tricky. Even if the research funded by this grant does not lead to a technology which directly supports the state's land and water claims, participating in the grant program adds credence to the sovereignty effort in at least two ways. First, internationally reported tech and geopolitical news stories share information about the grant, contributing to Canada's reputation as a technologically proficient nation with the ability to fund cutting-edge military projects [31]. Second, this reputation is additionally built by researchers sharing their extant authority in quantum technology, which has an already established reputation of scientific and technical interest. Thus, even if the advertised technological goal fails, the efforts of these researchers are supporting the interests of the Canadian state.

If the development of a quantum radar eventually succeeds, then local researchers will have assisted in the advancement of Canada's military capabilities, and in particular made substantive contributions to the military's ability to detect stealth aircraft in the internationally desired and geopolitically contentious High Arctic.

These two narratives about forcible relocation and quantum technology are tied by their role in Canadian Arctic sovereignty. The analysis presented about the political motivations surrounding the quantum radar project does not rely on the High Arctic Relocation for validity. But the project *does* implicitly and additionally support the appropriation of Indigenous land claims by the Canadian government. Indigenous land claims have not been internationally acknowledged as important in sovereignty claims until really quite recently [21], and the Canadian government has treated Inuit and Indigenous people in seriously harmful ways for a long time. It is now part of their policy that the historical presence of Inuit people in the Arctic justifies *Canada's* land and water claims (rather than claims by the Inuit nations themselves). Uncritical acceptance of grant funds and participation in a narrowly defined military project supports Canada's claims to Arctic sovereignty, supports their methodology in doing so, and supports the end goals of further exploitation of northern resources.

Enacting just physics

What does it matter if the research of quantum physicists and nanoscale engineers contributes to a specific political interest, whether it is resource extraction, political repute, or

displacement of Indigenous people? In the usual story we tell as physicists, our research is well-justified if it addresses a theoretical question deemed interesting by our peers, or if it contributes to technological development deemed worthwhile by grant-awarding agencies. Why do our stories end there? We don't actively consider which specific political interests are beneficial or harmful to support. Our reluctance to engage in critical analysis of the impacts of our work on the world around us is enacted through the limits we set on our formal discussion. These limits cyclically discourage folks to engage in critical analysis. Often, these limits are justified by arguing that societal effects from research projects are not the responsibility of researchers, or arguing that those effects are not in the domain of the research itself, and that therefore they are irrelevant to the objects of study.[4]

I'm arguing for the inclusion of critical analysis in our practice of our science. We can expand our stories to regularly involve analysis of the effects of our science, and why we're doing it in the first place.[5] We can then make ethical judgements about the impact of our work. Why wouldn't we? As humans, we can all take responsibility for actions that might affect other humans and our planet. We know there are pressing issues on our planet—among them significant inequities between white folks and people of colour, Western and non-Western folks, and men and women, as well as dramatic misuse of resources leading to global climate crisis. When the impact of uncritical development of QTech could include support of inappropriate management of mining resources, complicity in conflict surrounding those metals, support of Arctic sovereignty explicitly for the purposes of resource extraction, and more, why would we want to stay uncritical? Why would we pretend to be neutral, when continuing the way we are clearly supports these non-neutral stances and activities?

Steps can be made towards honesty in our daily practice. We can start with communication within particular academic circles, especially with folks better versed in these issues, like academics in science and technology studies and philosophy of science. We can use methodologies like responsible research and innovation frameworks to spread the power of decision-making in science [7]. We can be self-critical and honest about outcomes at conference presentations. We can brainstorm ways to support folks who have already been trying this methodology and been penalized by grant-awarding agencies. We can develop goals which have the potential to address issues of inequity, or at least minimal potential

[4]The most widely-used argument supporting this point is that science ought to be value-neutral and therefore separate from political analysis (even as it clearly contributes to political projects) [32]. Otherwise, one could argue that physicists should probably not be the folks responsible for studying the impacts of their work as they do not have the relevant expertise—this is a problem that should probably be addressed through education of physicists and collaboration with folks appropriately trained [33].

[5]For instance, grants are more available in one area than another, or they require certain technological spins on research to be awarded. And then—why are those the goals of the grant awarding agencies?

to continue or worsen inequity. We can allow our goals of equity and justice to influence choices that we make in science, without the concern that they will lessen the accuracy of the science itself [34]. We can make a project of justice and physics [35].

A step towards responsibility: the effects of my own contributions

Here's a step towards a more just physics: we can be very realistic about the motivation for and results of our work in our writing. Usually, introductions give context and motivation to a problem; they construct the space in the literature that the work is aiming to fill. This gives the sense that the primary and perhaps only effect of doing the work is filling the hole that the introduction excavates. As might be expected of folks who must advertise and advocate for the validity of their own work, the effect of the work is also generally presented as exclusively positive and constructive. Criticisms of the work are constrained to notes about future work that must be done, or are made by folks who did not author the paper. The impression we get just from the way that we write is that our work is all reasonably significant and that its region of influence is limited to physics and possibly technological advances, which are further implicitly presented as definitely positive.

Instead, we can try to not just construct *one* compelling motivation to consider the problem, but to identify all the relevant motivations for why one would care about it. What technological projects are being supported by the relevant body of literature? Are there potentially negative effects of those projects? What effects will the work likely have on its immediate fields? What goals did the physicists themselves have for the project, including career-motivated goals? In this way, we can begin to build a clearer picture of the place physics has in our world.

Being more honest and accurate about the effects of our work has a bonus effect of addressing the disparity between the way physics is done and the way people think that it is done. Most physicists, at least on some level, believe that much of physics is done by singular pieces of work with dramatic effect. Certainly our field still acts like this, when a paper published in a journal like *Nature* adds so much credence to a job application. In reality, many advances in physics cannot be readily traced back to a single contributor. Growth of knowledge often comes over long periods of time, in the midst of a community of researchers, with many inaccurate claims made along the way. Many incremental pieces of work construct knowledge about a field [36, 37]. Work which ends up being untrue or unhelpful for a particular problem can actually be very useful; it's great to know which avenues of solution won't be productive. Our writing process erases these contributions to scientific knowledge, as publishing is generally reserved for so-called positive results. Some folks are more affected by this discrepancy between appearances and reality than others.

Women of colour, for instance, are at much higher risk of receiving disproportionately less professional acknowledgement than their white or male colleagues. The appearance is that these scientists are worse at science, when in reality, parts of the publishing and citing processes are structurally discriminating against their contributions. These scientists may, then, be more likely to believe that they *are* worse at science, especially if they have negative results. This has a real effect of women of colour leaving science.

In this thesis, I will try to enact these steps towards the physics I would like to see. We will start with some general comments about the effects of the two studies of this thesis. In the introductory and concluding chapters of each part, more analysis will be conducted dealing with the specifics of each study.

A general and honest assessment of my works is that they make incremental contributions to their respective fields. The details of these contributions can be found in the concluding chapters of Parts I and II.

There are effects of these studies beyond the immediate and direct impacts on the fields that they are contributing to. Here are a few. First, by studying quantum physics with the advertised intent of contributing to the development of quantum technology, I and my collaborators are endorsing the project of QTech in a substantive way. We are being complicit in the advertised narrative around QTech, discussed above—that it is important, that it will be useful, that it is a worthwhile expenditure of resources. This effect will be elaborated on below.

Second, we are personally benefitting from participating in this narrative. I benefitted from advertising my quantum thermodynamics project as useful for QTech by way of having won an NSERC CGS-M grant, which allowed me to continue my studies for the past eight months without having to work as a teaching assistant. QTech is heavily and positively advertised at the Institute for Quantum Computing, where I and my collaborators work. The IQC is well-funded, which translates into nicer office space and more and fancier work parties than the majority of other graduate students at the University of Waterloo.

Finally, like any physics project that participates in the usual process of applying for grant money and reporting one's findings in a sufficiently acceptable journal, we also support the standard methodology for physics. We accepted grant money from the Canadian state to contribute to a project which they have particular political interest in. We published our work in *Physical Review*, and reported positively on it at conferences. We did not attempt to make substantive changes to a system which some of us have made critiques of over the course of my time working on these projects.

This project of identifying context and making societally relevant critiques of my own work is the first step in a project to amend the methodology of physics by doing it differently. It continues in Parts I and II.

Part I

Finite sizes and smooth cutoffs in superconducting circuits

Chapter 1

Introduction

There are a couple of ways that we can motivate the problem of this part of the thesis. One way is from a big picture, starting with physical situations as basic as the interaction of light and matter, motivated by some wonder and awe, and making some claims about the generality and power of our models. Then, we carve out a particular space, a set of parameters and methods that haven't been addressed in the literature before, and in the context of this powerful model that we've already introduced, we construct an interesting problem. There's utility in this usual way of introduction, so we'll do that first. Another way to motivate the problem is telling the story of how I came upon the problem and how it was motivated to me. We'll do that motivation next. Finally, we can look back and update the motivation of the study once we have its results—we can comment on what it ended up being for after all. We'll address this motivation in chapter 5, after we have the results of the study.

We can begin with the motivation from a big picture: we are interested in the interaction of light and matter. It's super ubiquitous. It's very cool. It's literally a part of you, reading this thesis, right now: your eyes seeing the light coming from the screen (or the WiFi communicating with your screenreader), your skin feeling the warmth of the sun, your energy from plants powered by light. Those are classical interactions, at least for the most part, but the light-matter interaction (LMI) doesn't lose its importance in quantum regimes. We only collect information about light via its interaction with pieces of the world we have "direct" control over, that is, pieces of matter. Even in quantum regimes, we like light—it illuminates the world, it's how we communicate, and it carries information about our universe and its history.

We have a wonderful theory to describe light. We quantize the classical electromagnetic field to give quantum electrodynamics, a quantum field theory. In this formulation, we

consider light existing across a free domain to be made up of infinitely many continuous harmonic oscillators, one for every frequency.

To be able to interact with this everpresent field, we as fundamentally limited beings must use matter. In our theory of light, we can couple a simple matter system to the modes of the field. Often, we use the simplest matter systems possible—two-level quantum systems, also known as qubits. The interaction of light with matter changes properties of the matter in ways that we can directly observe. Most commonly, we look for changes in the state of our qubit. Its transition between its two energy levels (ground and excited) can be observed through recorded signals such as clicks. Recording in this way the transition probability (or, more likely, calculating it) gives us some information about the field.

Now, we (as in, my supervisor, myself, and other theorists in our field) often explore "fundamental" scenarios of the LMI in this way. We do things like set up a qubit or two in an infinite vacuum and let them interact with the electromagnetic field for a second, or send them accelerating in the infinite universe forever [38, 39]. Well. We do the math we believe corresponds to these scenarios, at least. We employ the Unruh-DeWitt (UDW) model, a flexible and powerful model that utlizes the first principles of the LMI [40]. Incorporated into the model are tools to define the ultraviolet cutoff of the frequencies involved in the interaction, the spatial extent of the interaction, and how the interaction is turned on and off.

We were motivated to explore an application of the UDW model grounded, perhaps, in a slightly more accessible portion of reality—the lab. In superconducting circuits, we have all of these features of the UDW model: the LMI, with a finite spatial extent, an ultraviolet cutoff, and an interaction which is switched on and off. Further, superconducting qubits (originally, and still, sometimes, called artificial atoms) provide a unique kind of playground for those of us interested in the LMI. These qubits can interact with the electromagnetic field contained in wires at strengths far exceeding that of a natural atom to the electromagnetic field, called ultra-strong coupling (USC) [41–44]. This can provide unprecedented ability to study features of the LMI, especially since we can turn the interaction on and off in a controlled way, allowing for the exploration of non-adiabatic and short interaction times [42].

Typically, some variant of the spin-boson model is employed to analyse these setups [44–46]. Often, this model is simplified with assumptions known as the rotating wave approximation (RWA) and single- or few-mode approximations. In these simplified cases, systems can be solved exactly. This is, for instance, where our description of Rabi oscillations comes from [47]. In the USC regime, however, the RWA is no longer valid [43, 48, 49]. Further, stronger coupling necessarily makes contributions from higher frequency modes more relevant, encouraging the re-evaluation of the use of single-mode approximations [50].

The UDW model makes a good candidate for avoiding making these approximations, as it incorporates from the start all frequencies of the field and avoids making the RWA.

Beyond investigating these approximations, there are natural features of superconducting qubit and transmission line (i.e. a wire) warranting exploration. Though the spin-boson model already requires some form of an ultraviolet cutoff, there has been little consideration afforded to the presence of a natural ultraviolet cutoff originating in the superconducting medium [46]. Superconducting wires are not able to transmit very high frequency modes, but it is not known exactly how this decay behaves. In regimes where high frequency modes play a more significant role in interactions with a qubit, such as short-time and strongly coupled regimes, it seems plausible that the form of the ultraviolet cutoff may actually effect dynamics. In this case, it is important to understand exactly what this impact could be.

Additionally, though superconducting qubits have finite spatial extent, their shapes have been neglected almost completely in analysis of superconducting circuits. Similarly to the ultraviolet cutoff, it would be highly nontrivial to attempt to derive the form of this spatial extent from first principles. Given the well-developed tools to deal with spatial extents of detectors in the UDW model, and indeed the significant interest in how shapes do actually affect dynamics of qubits [51, 52], it seems fitting that we explore how the finite shape of a superconducting qubit may affect its dynamics.

The above set of motivations is mostly technical, and outlines what about the problem is interesting to study given already that the LMI is interesting, or that superconducting qubits are worthwhile technology to develop. We thus justified why we should study this problem in terms of societal interests and goals; there is a substantial number of people who are interested in the development of quantum technology, and thus our pursuing this problem which is useful for that goal is a good thing. Another group of motivations to pursue this problem has to do with personal interest. We as researchers may feel personally and individually motivated to ask questions about qubits and the LMI. In some deep, subtle, and potentially subconscious ways, though, societal interests also shape what folks find personally interesting. There are at least two ways this is relevant here. First, widely-discussed and well-advertised fields tend to attract researchers. The content of these fields may personally interest most (if not all) of those attracted researchers, but undoubtedly positive and excited discussion *about* the content plays an important role in cultivating interest. Second, a field being popular makes it easier to publish in it. Researchers must publish to continue to be researchers, so it makes sense that ability to publish would influence on some level the research decisions of academics.

In the case of this particular study, personal motivations which may have influenced the decision to pursue this particular problem include that it would be the closest to

experiment that our group had ever researched in, which my supervisor communicated as being appealing to him. Superconducting qubits are quite popular right now, which may have encouraged our engaging with the field, both because the ideas and researchers were accessible and because it seemed that other folks were interested in details of these systems. It might be nice also for the community of relativistic quantum information, a fairly new and growing niche field, to have UDW model to be used in a wider variety of situations and get exposure from a community that it is not usually exposed to.

Finally, my supervisor suggested that I study this problem in 2016. I accepted his suggestion, partially because it sounded more feasible than the other project he suggested, partially because it sounded interesting, and partially because I trusted his judgement on the value of the problem.

Having outlined to the best of our ability our motivations, let us continue with the details of the study. In this part of the thesis, we will investigate the effect of ultraviolet (UV) cutoffs, spatial extents, and their respective scales on the dynamics of a superconducting qubit interacting with a 1+1D open transmission line. Since the exact forms of these features are unknown, we will compare a selection of plausible forms to develop an understanding of the importance of using an accurate description of the feature. We will focus in the short-time and non-adiabatic interaction regimes, based on the intuition that both features will become more important in these regimes, and with the knowledge that short-time interactions are relevant in experimental settings for those who wish to create low photon number states [45, 53–55].

The study described here proceeds as follows: we use the UDW model to study a qubit interacting with an open (i.e. infinite) transmission line, where the qubit takes on one of several nontrivial shapes and sizes, and the transmission line has one of several UV cutoffs and cutoff scales. This study in the ultrastrong coupling regime will calculate the probability of vacuum excitation of the qubit and spontaneous emission into the line, investigating the effect of the size of the qubit, the shape model, the cutoff scale, the cutoff model, and adiabaticity and length of the interaction on these probabilities. We will show that in the adiabatic and especially in the adiabatic and short-time regime, neglecting to use the correct cutoff model can introduce inaccuracies in a model's predictions of the order of 10%.

This part of the thesis is organized as follows. In chapter 2, we contextualize our study in the extant tools and literature of the spin-boson model. We discuss the spin-boson Hamiltonian, how ultraviolet cutoffs are employed in the model, coupling constants, the RWA, and currently employed methods of solution. We also discuss how the physical systems making up a particular type of superconducting qubits may be approximated as two-level systems. In chapter 3, we introduce the model we utilize for the study, the UDW

model. We give a brief review of quantum field theory, history and applications of the model, and how spatial smearings and ultraviolet cutoffs have been utilized in the model. We also provide a thorough relationship between the UDW model and the spin-boson model, including a relationship between their coupling constants. In chapter 4, we detail our specific scenario and results. We give the relevant physically-inspired parameters and provide reasonable forms for the qubit's spatial extent and the line's ultraviolet cutoff. We calculate the time evolution of the qubit, and give the results in terms of sensitivity of the qubit's dynamics to the shape and cutoff models, the size and cutoff scale, and to the cutoff models as a function of adiabaticity and interaction duration. Finally, in chapter 5, we discuss some conclusions and limitations of the study, and revisit what it was all for in the first place.

Chapter 2

The Spin-Boson Model and Superconducting Qubits

Artificial atoms have adjustable coupling strengths which can be orders of magnitude larger than the coupling between a hydrogen atom and the electromagnetic field (see, e.g. [43]). As such, they are of interest to those who study the light-matter interaction (LMI). We can use these systems to study particular features of the LMI that might be too small to detect in a natural atom-field interaction.

Superconducting qubits are among the most popular artificial atoms right now, used in applications from generating single- and few-photon states (i.e. states with low expectation values of the number operator) to exploring quantum heat engines [56, 57]. They also feature at least two characteristics which can have nontrivial impact on the LMI—a natural ultraviolet cutoff and a non-trivial spatial distribution. Further, these features are not simple to describe. In simple atoms, at least, we can write down the electronic shape of the atom, or its spatial crosssection of interaction. In artificial atoms, where there are billions of atoms, we just don't have that. We're not able to derive the electromagnetic spatial distribution of the qubit from first principles. Are there signatures in the LMI of this spatial cross-section that give us an idea of the shape without needing the detailed knowledge of the electronic structure? We can ask the same question of the ultraviolet cutoff, which depends in superconducting materials in a highly nontrivial way on the breakdown of Cooper pairs at high frequencies. Thus, the superconducting qubit interacting with light provides us not only with a place to study features of the LMI, but is in fact provides new features for us to study.

We have powerful tools to study the interaction of an atom with a field, incorporating features like ultraviolet cutoffs and spatial distributions, in the Unruh-DeWitt (UDW)

model. There are already plenty of tools to study the way that a superconducting qubit interacts with a transmission line, though, so it behooves us to justify the use of the UDW model. To do this, we first need to be familiar with the tools already used, and see how they do or do not already address the features that we're interested in.

Variants of the spin-boson model are generally employed to study qubits interacting with light [58], including the rotating wave approximation Jaynes-Cummings model [45, 59, 60]. Often, hard cutoffs (including single-mode approximations) are used [45, 61]. When a qubit couples to a continuum of modes, ultraviolet cutoffs are already employed in the spin-boson model [46, 50]. These cutoffs are not necessarily motivated by the high-frequency decay of mode amplitude cause by the breakdown of superconductivity, but from requiring that certain quantities are not UV divergent.

In this chapter, we give an overview of the spin-boson model in section 2.1. We discuss ultraviolet cutoffs used in the model in subsection 2.1.1; we will see that an exponential cutoff is commonly used, and that it has a physical impact which is quite well documented [44]. We'll discuss coupling constants and regimes in section 2.1.2, use of the rotating wave approximation in section 2.1.3, and methods of solution for the model in section 2.1.4. To ensure our use of the spin-boson model as a tool to study superconducting qubits, we also require justification that the circuits, as anharmonic oscillators, are well-approximated by a two-level system. We thus give a derivation of the equation of motion of a flux qubit and approximate it as a two-level system in section 2.2.

2.1 The spin-boson Hamiltonian

As a general framework, the spin-boson model is widely employed to describe two-level systems interacting with a bosonic environment. In particular, the full and modified Hamiltonians have been used extensively to describe on-chip qubits interacting with finite and open transmission lines. Here, we detail the basics of the model, including the Hamiltonian, spectral density functions, and coupling regimes. We use as primary references for this section [46, 58].

We consider a two-level system coupled to a bath of harmonic oscillators. The full Hamiltonian for this system may be written as

$$\hat{H}_{\mathrm{SB}} = \Omega\hat{\sigma}_z + \sum_k \omega_k \hat{a}_k^\dagger \hat{a}_k + \hat{\sigma}_x \sum_k g_k(\hat{a}_k^\dagger + \hat{a}_k), \tag{2.1.1}$$

where $\hat{\sigma}_x$ and $\hat{\sigma}_z$ are the Pauli x and z operators, Ω is the transition frequency of the qubit, the $\hat{a}_k^\dagger$ and $\hat{a}_k$ are the creation and annihilation operators of the bath with mode frequency ω_k, and the g_k are the mode-dependent coupling constants of the interaction.

2.1.1 Ultraviolet cutoffs in the spin-boson model

Information about how the bath couples to the spin system is encoded in the coupling constants g_k, and is usually expressed by writing a spectral density function $J(\omega)$. This function relates the mode coupling strength to the frequency of the mode. Commonly, the bath is considered to be Ohmic, that is, to have a linear spectral density function

$$J(\omega) = \frac{2\pi}{\hbar^2} \sum_k g_k^2 \delta_{\omega\omega_k} = \pi\omega\alpha_{\mathrm{SB}}, \tag{2.1.2}$$

as in the Supplementary Information of [44], where $\omega_k = ck$ is the frequency of mode k, with c the speed of light, $\delta_{\omega\omega_k}$ is a Kronecker delta, and α_{SB} a coupling constant, to be discussed in detail below. This is an appropriate spectral density function for low frequencies—for high frequencies, we require that the coupling strength go to zero. This ultraviolet cutoff is introduced not from considerations of what frequencies the environment can sustain (as we do in this work), but rather from requiring that certain physical quantities remain UV-convergent. A number of different analytic forms of cutoff are employed for convenience, including Gaussian, sharp, exponential, and Lorentzian decay [46]. Though a Lorentzian decay is inspired by the Drude model of conductivity [62], in practice these cutoffs are explicitly not engaging with the microscopic origins of the mode-dependence of the coupling; this is well-justified for Markovian setups, i.e., when the relevant scales of interaction are much longer than scales of the bath [63]. In other words, only when the timescale of the interaction is comparable to the inverse cutoff frequency will the particular functional form of the cutoff matter. In particular, we see that in experiments that make single mode and few mode approximations, a cutoff is not used at all, with little to no detriment to theoretical predictions [45, 60, 61, 64].

As will be shown in chapter 4, the ultraviolet cutoff and the Fourier transform of the spatial smearing of an interaction function in the same way—they both decide what modes of the field are a part of the interaction. It makes sense, then, to ask what shape is taken for the qubit in the spin-boson model. In fact, a shape is generally not explicitly assumed. Rather, there is implicitly an assumption of a pointlike smearing of the qubit, as shown in detail in section 3.3.

2.1.2 Coupling constants and regimes

Once we consider coupling to a continuum of modes, the way in which we cut off high frequencies begins to matter, and in a nontrivial way. Coupling to an environment of harmonic oscillators renormalizes the qubit frequency—it shifts the peak frequency of emission

of the qubit into its environment [50]. This is a physical signature of the coupling which is readily measured. Ultrastrong experiments have found very good agreement with the predicted value of this renormalized frequency using an exponential cutoff (see figure 4b in [44]). Still, there is an absence of first principle justification for using an exponential cutoff and investigations into how cutoffs additionally affect short-time dynamics of qubit-line interactions. It is in this niche that we will settle our project, with more details on how this work fits into the literature in chapter 4.

We wish to establish a particular form for the modal coupling constants. Looking again at equation (2.1.2) with the goal of isolating g_k, we have

$$\sum_k g_k^2 \delta_{\omega\omega_k} = \frac{\hbar^2}{2}\omega\alpha_{\mathrm{SB}}. \tag{2.1.3}$$

To find the value of each g_k, we can split the sum over modes up, making the reasonable assumption that the frequency ω on the left hand side is constituted of a weighted sum of frequencies, $\omega = \sum_k \omega_k \Delta\omega_k$ where $\Delta\omega_k = \omega_{k+1} - \omega_k$, the difference in frequency between neighbouring modes, serves as a weighting function. This gives

$$g_k^2 = \frac{\hbar^2}{2}\omega_k\Delta\omega_k\alpha_{\mathrm{SB}}, \tag{2.1.4}$$

for the contribution of each g_k. Thus the modal coupling strength is given by

$$g_k = \hbar\sqrt{\frac{\alpha_{\mathrm{SB}}\omega_k\Delta\omega_k}{2}}. \tag{2.1.5}$$

The coupling constant α_{SB} indicates both the strength of the field-qubit coupling and the effective phase of the field—that is, in different regimes of the coupling, the nature of the interaction changes significantly. Phase transitions are observed at $\alpha_{\mathrm{SB}} = 1/2$ and 1 [44, 58]. More concretely, in the discrete mode spin-boson model, α_{SB} is a measure of the coupling strength Γ/Ω, where Γ is the rate of spontaneous decay of the qubit into the field and Ω is the transition frequency of the qubit. The exact relationship of α_{SB} and Γ/Ω depends on the regime of coupling strength. For instance, under the rotating wave and Born-Markov approximations, the exact relationship $\Gamma/\Omega = \pi\alpha_{\mathrm{SB}}$ holds. This is very accurate when $\Gamma/\Omega \lesssim 0.1$. For larger such ratios, this becomes a lower bound: $\Gamma/\Omega > \pi\alpha_{\mathrm{SB}}$. An exact relationship between Γ/Ω and α_{SB} has been derived using non-perturbative methods in [65].

We can identify two extreme coupling regimes. One regime is $\Gamma/\Omega \ll 1$, so that $\alpha_{\mathrm{SB}} \ll 1$; this is the regime in which the rotating wave approximation is valid. We will

discuss this approximation and some issues with it briefly below. The ultrastrong coupling regime, on the other hand, is where $\Gamma \sim \Omega$, in particular, $\Gamma/\Omega \gtrsim 0.1$ [42, 44, 65]. This is the regime of particular interest for us. Note the use of the word "ultrastrong" here indicates an interaction much stronger than the naturally present interactions between light and matter, i.e. that between an atom and light. In [44], the ratio Γ/Ω reaches values well over 1; the coupling constant α_{SB} exceeds $1/2$.

2.1.3 Rotating wave approximation

It is not infrequent for researchers to make use of the rotating wave approximation (RWA). This is an approximation made on the interaction Hamiltonian of a two-level system interacting with a single harmonic oscillator,

$$\hat{H}_{\mathrm{int}} = g\hat{\sigma}_x(\hat{a}^\dagger + \hat{a}) = g(\hat{\sigma}_+ + \hat{\sigma}_-)(\hat{a}^\dagger + \hat{a}), \tag{2.1.6}$$

where $\hat{\sigma}_+ = |g\rangle\langle e|$ and $\hat{\sigma}_- = |e\rangle\langle g|$, wherein so-called counter-rotating terms $\hat{\sigma}_+\hat{a}^\dagger$ and $\hat{\sigma}_-\hat{a}$ are ignored. This results in the commonly used (e.g. [45, 66]) RWA Jaynes-Cummings Hamiltonian,

$$\hat{H}_{\mathrm{int}} = g(\hat{\sigma}_+\hat{a} + \hat{\sigma}_-\hat{a}^\dagger). \tag{2.1.7}$$

The approximation is incredibly useful—it allows one to exactly solve the single-mode spin-boson system [47]. It's only applicable in certain regimes, however.

Let us review justification for making this approximation. We can write the interaction Hamiltonian (2.1.6) in the interaction picture,

$$\begin{aligned}\hat{H}_{\mathrm{int}} &= g(\mathrm{e}^{\mathrm{i}\Omega}\hat{\sigma}_+ + \mathrm{e}^{-\mathrm{i}\Omega}\hat{\sigma}_-)(\mathrm{e}^{\mathrm{i}\omega}\hat{a}^\dagger + \mathrm{e}^{-\mathrm{i}\omega}\hat{a}) \\ &= g(\mathrm{e}^{\mathrm{i}(\omega+\Omega)}\hat{\sigma}_+\hat{a}^\dagger + \mathrm{e}^{-\mathrm{i}(\omega-\Omega)}\hat{\sigma}_+\hat{a} + \mathrm{e}^{\mathrm{i}(\omega-\Omega)}\hat{\sigma}_-\hat{a}^\dagger + \mathrm{e}^{-\mathrm{i}(\omega+\Omega)}\hat{\sigma}_-\hat{a}).\end{aligned} \tag{2.1.8}$$

When the frequency of the qubit Ω is very close to the frequency of the harmonic oscillator ω, then the terms $\mathrm{e}^{-\mathrm{i}(\omega-\Omega)}\hat{\sigma}_+\hat{a}$ and $\mathrm{e}^{\mathrm{i}(\omega-\Omega)}\hat{\sigma}_-\hat{a}^\dagger$ will be oscillating with a very small frequency in comparison to the other two terms, $|\omega - \Omega| \ll \omega + \Omega$. This justifies neglecting the terms $\mathrm{e}^{\mathrm{i}(\omega+\Omega)\hat{\sigma}_+\hat{a}^\dagger}$ and $\mathrm{e}^{-\mathrm{i}(\omega+\Omega)}\hat{\sigma}_-\hat{a}$ as their rapid oscillations will quickly be averaged over in any interactions longer than those of the order of $(\omega - \Omega)^{-1}$.

Under what regimes does the approximation fail? Notice the presence of the single-mode approximation here, and in particular the assumption that $\Omega \sim \omega$. In the process of spontaneous emission, where the two-level system begins in the excited state, this approximation can be justified by noting that quanta are emitted from the qubit at the qubit's frequency Ω. In the process of vacuum excitation, where the two-level system begins in

the ground state, there is no such dominant frequency, making this crucial assumption in the RWA unjustifiable and the approximation inaccurate.

We have also assumed that the coupling is Ohmic, as in equation (2.1.2), which is a very good approximation for weak coupling of the two-level system to the harmonic oscillator. For stronger coupling, with $\alpha_{\mathrm{SB}} \gtrsim 0.1$, the frequency dependence of the interaction changes, as discussed in 2.1.2. In fact, the Ohmic spectral density becomes super-Ohmic, rendering the RWA unjustifiable. As discussed in section 2.1.1, the assumption of an Ohmic spectral density only applies for low frequencies—at high frequencies, the coupling must decay. This means the RWA cannot hold there either. Further, using the RWA even introduces issues with casuality [51].

2.1.4 Methods of solution

When we make the rotating wave approximation, we can exactly solve the spin-boson model. The existence of an exact solution for low-strength couplings is one of the reasons that the spin-boson model is so ubiquitous. However, for strong couplings, neither the RWA nor perturbation methods work. In order to make accurate predictions for these regimes, which are only becoming more common experimentally, we need to employ other methods of solution. At least two methods have been used to good effect: matrix product states [50] and the dynamical polaron ansatz [65]. The results of [65] have been corroborated by the experiments in the ultrastrong coupling regime of [44].

2.2 Flux qubits: approximate two-level systems

In the previous section, we considered a two-level system coupled to an open transmission line. Here we provide more detail on what actually makes up the two-level system. Superconducting qubits are generally, in fact, anharmonic oscillators which, in certain regimes, can be approximated well as a two-level system. We will look at a canonical example of such an approximation: the flux qubit, diagrammatically shown in figure 2.1. We study this particular qubit (as opposed to a charge or phase qubit) because of its ability to facilitate stronger couplings [42, 46]. The basic flux qubit consists of a Josephson junction interrupting a ring of superconducting material, through which is threaded a magnetic flux. More common implementations of flux qubits utilize three or four junctions in a single loop; the two-level approximation made in these cases is similar [67, 68]. Again, we employ [46] as a primary reference in this section.

To see how we consider this circuit to be a two-level system, we will set up the equation

of motion and potential of the electron wave function phase $\hat{\psi}$ the junction. The Josephson junction is a nonlinear inductor which will be shown to act as an anharmonic oscillator, with a much larger gap between the second and third energy levels than between the first and second. We will thus see how the potential can be well-approximated by a double-well potential, and thus in certain regimes can be further approximated by a two-level system.

To do this, we first need Josephson's two relations. The first relates the magnetic flux threading the ring, $\hat{\Phi}$, to the phase difference of the electron (Cooper pair) wave function across the junction, $\hat{\psi}$,

$$\hat{\psi} = 2\pi \left(n - \frac{\hat{\Phi}}{\Phi_0} \right), \tag{2.2.1}$$

where $2\pi n$ is the phase change of the wave function around the entire ring and Φ_0 is the flux quantum, $\Phi_0 = h/2e$, with e the charge of the electron. We can additionally break up the flux through the ring into two parts: the externally applied flux $\hat{\Phi}_{\text{ext}}$ and the flux created by the super-current $\hat{I}$ present in the ring, given by $L\hat{I}$ where L is the self-inductance of the ring,

$$\hat{\Phi} = \hat{\Phi}_{\text{ext}} + L\hat{I}. \tag{2.2.2}$$

The super-current is produced by Cooper pairs sliding around the superconducting ring (seeing as how it is a zero-friction environment) and is related to the phase across the junction by

$$\hat{I} = I_c \sin \hat{\psi}, \tag{2.2.3}$$

where I_c is a parameter describing the critical super-current, determined by properties of the junction. It is related to the Josephson energy E_J (the potential across the junction) and the flux quantum by

$$E_J = \frac{I_c \Phi_0}{2\pi}. \tag{2.2.4}$$

In practice, Josephson junctions are not inserted into a superconducting loop alone. Instead, they are shunted, that is, inserted in parallel with, other circuit elements. Resistively shunted junctions are those which are shunted by a capacitor and a resistor, as in figure 2.1. This splits the supercurrent, i.e. the total current around the ring, into three parts:

$$\hat{I} = I_c \sin \hat{\psi} + \frac{\hat{U}}{R} + C\dot{\hat{U}}, \tag{2.2.5}$$

where $\hat{U}$ is the voltage drop across the junction (and thus also across the shunting elements), R is the resistance of the resistor, and C is the capacitance of the capacitor.

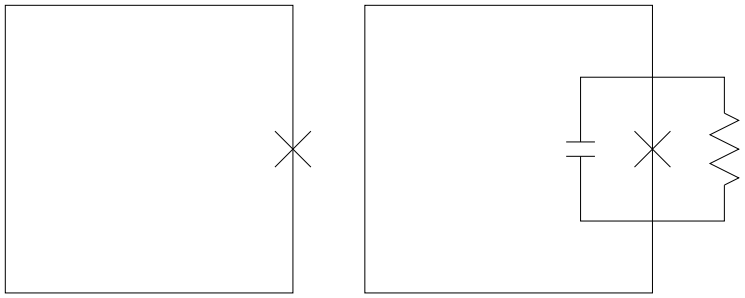

a) b)

Figure 2.1: Schematic diagrams of single-junction flux qubits. a) A Josephson junction, marked by an "X", in a superconducting loop. b) A resistively shunted Josephson junction. The junction is placed in a loop in parallel with a capacitor and a resistor.

Josephson's second relation is

$$\dot{\hat{\psi}} = 2e\frac{\hat{U}}{\hbar}, \tag{2.2.6}$$

relating the voltage drop across the junction $\hat{U}$ to the rate of change of the phase change across the junction $\hat{\psi}$. Combining Josephson's two relations and substituting in to the current equation 2.2.5 to find an equation of motion for the flux $\hat{\Phi}$, we arrive at

$$C\ddot{\hat{\Phi}} + \frac{\dot{\hat{\Phi}}}{R} + \frac{\partial V(\hat{\Phi})}{\partial \hat{\Phi}} = 0, \tag{2.2.7}$$

with the potential V defined as

$$V(\hat{\Phi}) = \frac{1}{2L}(\hat{\Phi} - \hat{\Phi}_{\text{ext}})^2 - E_J \cos\left(\frac{2\pi\hat{\Phi}}{\Phi_0}\right). \tag{2.2.8}$$

We now wish to see how this potential lends itself to a two-level approximation. To this end, we enforce that $2\hat{\Phi}_{\text{ext}}/\Phi_0 = 1$. When this is the case, the potential $V(\hat{\Phi})$ is symmetric about $\hat{\zeta} = 2\pi\hat{\Phi}/\Phi_0 - \pi$, and can be rewritten as

$$V(\hat{\zeta}) = \left(\frac{\hat{\zeta}^2}{2\beta_L} + \cos\hat{\zeta}\right) E_J, \tag{2.2.9}$$

where

$$\beta_L = \frac{2\pi L I_c}{\Phi_0} = \frac{4\pi^2 L E_J}{\Phi_0^2} \tag{2.2.10}$$

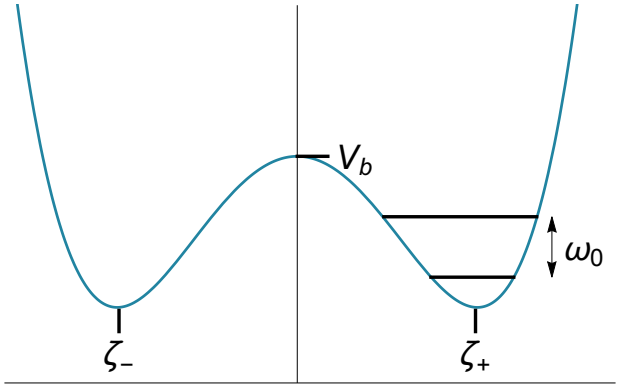

Figure 2.2: The double well potential V_{quart} of a superconducting qubit.

is a dimensionless parameter. We can take $\hat{\zeta}$ to be small and expand $V(\hat{\zeta})$ in a power series up to the fourth power:

$$V_{\text{quart}}(\hat{\zeta}) = \left(1 - \frac{1}{2}\left(1 - \frac{1}{\beta_L}\hat{\zeta}^2 + \frac{\hat{\zeta}^4}{24}\right)\right). \tag{2.2.11}$$

If the parameter $\beta_L > 1$, then this potential is a symmetric double well, with degenerate minima at

$$\hat{\zeta} = \hat{\zeta}_\pm = \pm\sqrt{6(1 - \beta_L^{-1})} \tag{2.2.12}$$

and barrier height

$$V_b = \frac{3}{2}\left(1 - \beta_L^{-1}\right)^2 E_J. \tag{2.2.13}$$

This symmetric double well potential is shown in figure 2.2. The two wells correspond to the current running clockwise and counterclockwise in the ring.

We can find the energy gap between the approximate ground and excited states using the instanton method, explained in some detail in [46]. The energy gap Ω_0 of the qubit (in a symmetric double-well potential) can be expressed in terms of the barrier height as

$$\Omega_0 = 8\sqrt{\frac{2V_b\omega_0}{\pi\hbar}}\exp\left(\frac{-16V_b}{3\hbar\omega_0}\right), \tag{2.2.14}$$

where ω_0 is the frequency of small oscillations in each well. For a superconducting qubit which is not interacting with a transmission line or other environment, then, we can write the Hamiltonian approximating the qubit as a two-level system as follows:

$$\hat{H}_{\text{q}} = -\frac{1}{2}\hbar\Omega\left(|L\rangle\langle R| + |R\rangle\langle L|\right), \tag{2.2.15}$$

where we've written the renormalized qubit frequency Ω and are using the basis $\{ |L\rangle, |R\rangle \}$ corresponding to being in the left and right wells. This renormalization arises from coupling the qubit to an environment, which modifies the transition probability $\langle L|R\rangle$. For a non-interacting qubit, there is only one such transition frequency. When we consider the qubit interacting with a bath of harmonic oscillators, we must consider the joint state of the system. We use the spin-boson Hamiltonian

$$\hat{H} = \Omega\hbar\hat{\sigma}_x + \sum_k \hbar\omega_k \hat{a}_k^\dagger \hat{a}_k + \hat{\sigma}_z \sum_k g_k(\hat{a}_k^\dagger + \hat{a}_k), \tag{2.2.16}$$

We write our states as $|L\rangle \prod_k |n_k\rangle \equiv \prod_k |n_{L,k}\rangle$, including the state of the qubit and the state of the harmonic oscillator for all modes k. In fact, we can divide the oscillator part of the Hamiltonian into parts associated with the two-state system being the left or right states. Then, the oscillator has two ground states, $|0_{L,k}\rangle$ and $|0_{R,k}\rangle$. These are not orthogonal. Assuming that we are in the vacuum state $|0_k\rangle$ for each mode, the transition amplitude between the two ground states must be calculated as

$$\Omega = \Omega_0 \prod_k \langle 0_{R,k}|0_{L,k}\rangle \,. \tag{2.2.17}$$

Coupling to a bath of harmonic oscillators thus changes the way that the two-state system can transition. The amplitude is modified by what is called the Franck-Condon factor,

$$\Omega = \Omega_0 \exp\left(-\frac{1}{2}\sum_k \frac{g_k^2}{\omega_k^2}\right). \tag{2.2.18}$$

When we couple to a continuum of modes, we can write this renormalized transition amplitude as

$$\Omega = \Omega_0 \exp\left(-\frac{1}{2}\int_0^\infty \mathrm{d}\omega \frac{J(\omega)}{\omega^2}\right), \tag{2.2.19}$$

with $J(\omega)$ the spectral density as in 2.1.2. This integral can be tricky; it is IR divergent when $J(\omega) \propto \omega^s$ with $s \leq 1$. This is physically due to assuming that the coupling is adiabatic, in the sense that the bath immediately responds to any change in the qubit. It is managed by using this relation to lessen the contribution of low-frequency modes:

$$\Omega_\mathrm{r} = \Omega_0 \exp\left(-\frac{1}{2}\,\mathrm{p.v.}\int_0^\infty \mathrm{d}\omega \frac{J(\omega)}{\omega^2 - \Omega_\mathrm{r}^2}\right), \tag{2.2.20}$$

where p.v. denotes taking the Cauchy principal value of the integral. For an Ohmic spectral density with exponential cutoff

$$J(\omega) = \omega \mathrm{e}^{-\omega/\varepsilon}, \tag{2.2.21}$$

the renormalized qubit frequency is

$$\Omega_{\mathrm{r}} = \Omega_0 \left(\frac{\Omega_0}{\varepsilon} \right)^{\alpha_{\mathrm{SB}}/(1-\alpha_{\mathrm{SB}})}. \tag{2.2.22}$$

This shifted frequency is observed in experiment, as in, for instance, [44].

As a final note, this derivation uses the basis $\{ |L\rangle, |R\rangle \}$ of the wells. Switching to the energy eigenbasis, $\{ |g\rangle, |e\rangle \}$, and setting $\hbar = 1$ as in the rest of this thesis, we can write the spin-boson Hamiltonian for this system of qubit coupled to a transmission line in an identical fashion to (2.1.1),

$$\hat{H}_{\mathrm{SB}} = \Omega \hat{\sigma}_z + \sum_k \omega_k \hat{a}_k^\dagger \hat{a}_k + \hat{\sigma}_x \sum_k g_k (\hat{a}_k^\dagger + \hat{a}_k). \tag{2.2.23}$$

Chapter 3

The Unruh-DeWitt Model

A generalization of the light-matter interaction to fields interacting with matter is found in the Unruh-DeWitt (UDW) model, now ubiquitous in the field of relativistic quantum information. First introduced by Unruh [39] and simplified by DeWitt [69], this model of a two-level system interacting with a quantum field has facilitated operational investigation of characteristics of fields. The proliferation of this model is motivated by this operational property, in addition to the fact that it captures the essential features of the light-matter interaction. Properties of a quantum field like light which are calculated by considering the field to be free raise a number of questions: are these properties really observable? Are they artifacts of the method of calculation? The UDW model circumvents these issues by ensuring any calculated effects are in principle observable, by nature of being properties of a two-level system. We can rest easy knowing that we are able to measure and interact with two-level systems, and that therefore the predictions of the model are physical in an operational sense.

In this chapter, we first review in section 3.1 quantum field theory for scalar fields in flat spacetime. We follow this in section 3.2 with a review of the Unruh-DeWitt model, including some history of its development and important conceptual issues (including notions of particles and causality issues of detectors). We finish with a demonstration of the equivalence of the spin-boson model and the UDW model under certain conditions in section 3.3.

3.1 Quantum field theory: scalar fields in flat spacetime

In this study, we will make use of the powerful framework of quantum field theory. Specifically, we utilize the UDW model coupled to the conjugate momentum of a massless scalar field in 1+1D, for two reasons. One, that qubits which couple to the current of a line do in fact couple to the conjugate momentum of the field and two, that the conjugate momentum is IR-safe in 1+1D, allowing for ease of computation. Here, we review the essentials needed for this purpose. A more complete review may be found in e.g. [70–72], used as primary references for this section. Additional brief pedagogical reviews can be found in [73–76].

A field theory, at its roots, aims to describe the dynamics of fields over space and time. We can thus begin with the physically motivated Klein-Gordon equation—a wave equation in space and time:

$$\Box\phi(x,t) = 0, \tag{3.1.1}$$

where $\Box = \partial_t^2 - \partial_x^2$ is the d'Alembertian operator. Solutions to this equation minimize the action

$$S = \frac{1}{2}\int \mathrm{d}x \int \mathrm{d}t \left((\partial_t\phi)^2 + (\partial_x\phi)^2\right). \tag{3.1.2}$$

We can quantize the field by imposing the canonical commutation relations on the field ϕ and its conjugate momentum $\pi = \partial_t\phi$ and writing hats:

$$\begin{aligned} &[\hat{\phi}(x,t), \hat{\pi}(y,t)] = \mathrm{i}\delta(x-y), \\ &[\hat{\phi}(x,t), \hat{\phi}(y,t)] = 0, \\ &[\hat{\pi}(x,t), \hat{\pi}(y,t)] = 0. \end{aligned} \tag{3.1.3}$$

We can express a general solution to this free field equation in terms of plane waves,

$$\hat{\phi}(x,t) = \int \mathrm{d}k \, \left(u_k^*(x,t)\hat{a}_k^\dagger + u_k(x,t)\hat{a}_k\right) \tag{3.1.4}$$

where the $\hat{a}_k^\dagger$ and $\hat{a}_k$ are the creation and annihilation operators, respectively, of each mode k. The coefficients $u_k(x,t)$ of the $\hat{a}_k^\dagger$ and $\hat{a}_k$ are partially determined by requiring that the commutation relations (3.1.3) be satisfied. The commutation relations of the field operator and its conjugate momentum require that the creation and annihilation operators satisfy

$$\begin{aligned} &[\hat{a}_k^\dagger, \hat{a}_{k'}] = 2\pi\delta(k-k'), \\ &[\hat{a}_k^\dagger, \hat{a}_{k'}^\dagger] = 0, \\ &[\hat{a}_k, \hat{a}_{k'}] = 0, \end{aligned} \tag{3.1.5}$$

and that the coefficients u_k are complete and orthonormal with respect to the Klein-Gordon inner product, given by

$$(u, v) = \mathrm{i} \int \mathrm{d}x \ (u^*(\partial_t v) - (\partial_t u^*)v) \,. \tag{3.1.6}$$

One set of coefficients which satisfy this are the plane waves,

$$u_k(x, t) = \frac{1}{2\sqrt{\pi \, |k|}} \mathrm{e}^{-\mathrm{i}(|k|t - kx)}. \tag{3.1.7}$$

We can thus write the free field in a plane wave mode expansion as

$$\hat{\phi}(x, t) = \frac{1}{2\sqrt{\pi}} \int \mathrm{d}k \, \frac{1}{\sqrt{|k|}} \left(\hat{a}_k^\dagger \mathrm{e}^{\mathrm{i}(|k|t - kx)} + \hat{a}_k \mathrm{e}^{-\mathrm{i}(|k|t - kx)} \right). \tag{3.1.8}$$

In the rest of this work, we will be interested not in the field but in its conjugate momentum $\hat{\pi}(x, t)$. We do this to avoid difficulties with the IR divergence of the field $\hat{\phi}(x, t)$ in 1+1D—the Wightman function of $\hat{\phi}(x, t)$ is IR divergent, with ambiguities arising in how to calculate the transition probability of a detector [77–79]. Coupling to the conjugate momentum instead of the field amplitude avoids such ambiguities [78]. From this mode expansion of the field, we can immediately write the same for its conjugate momentum by taking the partial derivative with respect to time:

$$\hat{\pi}(x, t) = \frac{1}{2\sqrt{\pi}} \int \mathrm{d}k \, \sqrt{|k|} \left(\mathrm{i}\hat{a}_k^\dagger \mathrm{e}^{\mathrm{i}(|k|t - kx)} - \mathrm{i}\hat{a}_k \mathrm{e}^{-\mathrm{i}(|k|t - kx)} \right). \tag{3.1.9}$$

3.2 The Unruh-DeWitt model

As discussed above, calculations about a field can seem ethereal without a connection to a system that we can directly measure. The Unruh-DeWitt model was developed to deal with this difficulty by investigating the behaviour of a matter system coupled to a quantum field. In this section, we briefly review some major applications of the model, detail the model itself, and discuss aspects and consequences of its use of spatial smearing.

3.2.1 History & applications

The first and most celebrated result that makes use of the UDW model is the Unruh effect, initially described by Fulling, Davies, and Unruh [39, 80, 81]. The effect is this: when a

detector coupled to a field in flat spacetime undergoes constant acceleration for all time, it thermalizes, transitioning to the excited state as if it were interacting with a thermal background with a temperature proportional to the acceleration.

Entanglement in quantum fields is a particularly slippery concept. The operational approach provided by the UDW model alleviates conceptual difficulties with how to appropriately divide spacetime (i.e. avoids divergences associated with ultraviolet scale correlations) [82]. Instead of considering entanglement between areas of spacetime, entanglement harvesting considers entanglement which can be generated between two UDW detectors which each interact with the same quantum field [38, 83–85]. This setup has been employed many times; for instance, entanglement harvesting has been investigated using model of a real atom coupled to the electromagnetic field [40]; using quadratically coupled detectors [86]; and in coherent background states [87, 88]. A variety of backgrounds and worldlines of detectors have additionally been investigated [89–91]. The protocol has even been extended to a sustainable repeated method called, entertainingly, entanglement farming [92]. Additional applications of the model include quantum seismology [93], assessing attacks on randomness generated by measuring an atom [94], and investigating information transfer in cosmology [95]. Some nice reviews of application and more on the UDW model include [96–98].

Additional uses of this model include the interrogation of the idea of a particle in quantum field theory—rather than a property of a free field, the particle becomes "that which a particle detector detects" [69]. This definition is one of few in physics which makes very explicit the role of the detector in the physical phenomenon of interest. It brings into question to which quantum object the concept of particle belongs. Can it really belong to a field if we require that a detector be present? It surely can't only belong to the detector, as the field has to be around to make the detector click. This operational approach to an aspect of quantum field theory has significance in the ontology of quantum objects [99–101].

3.2.2 Hamiltonian

In this model we have a very flexible and powerful framework with which to calculate, sometimes non-perturbatively, dynamics of matter coupled to a quantum field. The model typically couples a two-level first-quantized system, often called a *detector* (i.e. a qubit) to a scalar bosonic field. The model is flexible in the specification of the spatial extent of the detector, called the *smearing*, and the time-dependence of the interaction of the detector

and the field, called the *switching function*. The typical UDW interaction Hamiltonian is

$$\hat{H} = \lambda\, \hat{\mu}(t)\, \chi(t) \int \mathrm{d}x\, F_\sigma(x)\, \hat{\phi}(x,t), \tag{3.2.1}$$

where λ is a coupling constant denoting some measure of the strength of the interaction, $\hat{\mu}(t) = \mathrm{e}^{\mathrm{i}\Omega t}\, |e\rangle\langle g| + \mathrm{e}^{-\mathrm{i}\Omega t}\, |g\rangle\langle e|$ is the monopole moment of the detector (describing its single internal degree of freedom) with energy gap Ω, $\chi(t)$ is the switching function (describing how the interaction turns on and off), $F_\sigma(x)$ is the spatial smearing function with characteristic size σ, and $\hat{\phi}(x,t)$ is the amplitude of a scalar field. In order to avoid dealing with the IR divergence of the field in 1+1D, the UDW Hamiltonian we will make use of here couples not to the scalar field but to its conjugate momentum, $\hat{\pi}(x,t)$, written in equation (3.2.3),

$$\hat{H} = \lambda\, \hat{\mu}(t)\, \chi(t) \int \mathrm{d}x\, F_\sigma(x)\, \hat{\pi}(x,t). \tag{3.2.2}$$

For a variety of reasons (discussed below), one may choose to make use of an ultraviolet cutoff in the conjugate momentum, which modulates the dependence of the amplitude of $\hat{\pi}$ on the mode k. We will here use the following expression for the conjugate momentum used in the interaction Hamiltonian, which incorporates such a cutoff:

$$\hat{\pi}(x,t) = \frac{1}{2\sqrt{\pi}} \int \mathrm{d}k\, C_\varepsilon(k) \sqrt{|k|} \left(\mathrm{i}\hat{a}_k^\dagger \mathrm{e}^{\mathrm{i}(|k|t - kx)} - \mathrm{i}\hat{a}_k \mathrm{e}^{-\mathrm{i}(|k|t-kx)} \right), \tag{3.2.3}$$

where $C_\varepsilon(k)$ is the cutoff function and ε is its characteristic scale. Note the distinction here between cutting off the field itself (which would modify the canonical commutation relations, (3.1.3)) and having an ultraviolet cutoff in the interaction of the field with a detector.

3.2.3 Spatial smearings and ultraviolet cutoffs

We have in our UDW Hamiltonian a spatial smearing $F_\sigma(x)$ and an ultraviolet cutoff $C_\varepsilon(k)$. In chapter 4, we study how these spatial and mode dependencies affect qubit dynamics in a simple superconducting setup of a flux qubit coupled to a 1D wire. Here, we review a variety of motivations for including these terms in UDW and field theory models and interesting themes therein.

Ultraviolet cutoffs have been used for decades for the regularization of ultraviolet divergences of field amplitudes and correlators (see, among many others, [71]) and, more recently, entanglement entropy [102, 103]. This regularization is often used as a theoretical tool to get around problems with infinite energies and correlations at infinitely small

scales; often, once an integration over momentum is done, the sharp UV cutoff is taken to infinity. Some physicists argue that such an ultraviolet cutoff is in fact a natural scale [104–106]. In particular, an application of quantum theory to causal structure indicates fluctuations of causal order near the Planck scale, potentially demonstrating a need for a universally present sharp cutoff [107, 108]. Ultraviolet cutoffs are also introduced from more readily accessible physical motivations. For instance, atoms are effectively transparent to very high-frequency modes, encouraging the use of few- and single-mode approximations in quantum optics and cavity quantum electrodynamics [43, 61]. Mediums can also introduce cutoffs; both optical fibres and superconducting wires have damping effects on high-frequency modes [109].

In its initial formulation, the UDW model used a Dirac delta smearing to produce a pointlike detector [39, 69]. Problems with this pointlike smearing were identified in [110], namely that it produced a non-Lorentz invariant quantity for the instantaneous transition rate of a detector. Spatially smeared fields were introduced to resolve the issue, with the size of the smearing sometimes being taken to zero after the calculation was performed [52, 110, 111]. There has since been wide usage of smeared detectors, motivated both by physical reality (i.e. atoms are not pointlike [47]) and analytic simplicity of expressions [40, 112, 113]. Note that the use of a spatial smearing is, also, covariant [114].

We have a good deal of evidence supporting the consideration of these two factors of the Hamiltonian hand in hand. As argued in [115] and as employed in [71], the Fourier transform of a spatial smearing function is effectively equivalent to a soft ultraviolet cutoff. We will see this concretely in section 4.2.

Finally, we note that the inclusion of factors affecting the spatial and modal distribution of an interaction is not trivial. Concretely, smearing a detector in space means that it is nonlocal; anything which affects the detector will be felt simultaneously across its spatial profile. Cutting off high-frequency modes sharply has a similar effect. Both factors can thus introduce acausal behaviour into field theories [51, 116]. This appears as a potentially frustrating fact—if smearings and cutoffs are physically justified, shouldn't they be causal? In [51], acausal terms are shown to be superexponentially suppressed in leading order perturbation theory for smearing functions which are strongly concentrated, such as Gaussians. Additionally, it is shown that hard UV cutoffs are unfixably acausal[1]. It is straightforward to surmise that soft UV cutoffs have similar restrictions as smooth spatial smearings—they need only be sufficiently widely supported to have minimal acausal effect.

[1]This fact may be remediated by the use of a sharp UV cutoff to avoid issues with fluctuating causal structure, which would itself address pressing causality issues [107].

3.3 Relating the Unruh-DeWitt and spin-boson models

In chapter 2, we introduced the spin-boson model as a widely used model for two level systems (i.e. the spin) interacting with light (i.e. the bosons). Here, we will show how the Unruh-DeWitt model (3.2.2) corresponds to the spin-boson model.

To begin with, we consider the interaction Hamiltonian of the spin-boson model, written in the Schrödinger picture, as in section 2.1,

$$\hat{H}_{\text{int}} = \hat{\sigma}_x \sum_k g_k(\hat{b}_k + \hat{b}_k^\dagger), \tag{3.3.1}$$

where the sum is over all bosonic modes (i.e. a sum over the wavenumber k), the $\hat{b}_k$ and $\hat{b}_k^\dagger$ are annihilation and creation operators for mode k, and g_k is the strength of the coupling between the qubit and mode k. We reviewed in section 2.1 the relationship between the modal coupling strength g_k and the Ohmic spectral density function

$$J(\omega) = \frac{2\pi}{\hbar^2} \sum_k g_k^2 \delta_{\omega\omega_k} = \pi\omega\alpha_{\text{SB}}, \tag{3.3.2}$$

giving

$$g_k = \hbar\sqrt{\frac{\alpha_{\text{SB}}\omega_k\Delta\omega_k}{2}}, \tag{3.3.3}$$

where $\Delta\omega_k = \omega_{k+1} - \omega_k$. We will use this relationship to express the coupling constant λ of the UDW model in terms of the coupling constant α_{SB} of the spin-boson model.

To fully relate the UDW model, which uses a continuum model of the electromagnetic field, to the spin-boson model, we will substitute this expression for the modal coupling strength into the spin-boson interaction Hamiltonian (3.3.1) and take the continuum limit. Substituting the expression for g_k in terms of α_{SB}, we have

$$\hat{H}_{\text{int}} = \hat{\sigma}_x \frac{\hbar}{\sqrt{2}} \sum_k \sqrt{\alpha_{\text{SB}}\omega_k\Delta\omega_k}(\hat{b}_k + \hat{b}_k^\dagger). \tag{3.3.4}$$

In order to properly take the continuum limit, we need a factor of $\Delta\omega_k$ to multiply our whole expression, rather than the $\sqrt{\Delta\omega_k}$ that we have right now. Then, we can take $\Delta\omega_k \to \mathrm{d}\omega_k$ straightforwardly. So, we take

$$\hat{H}_{\text{int}} = \hat{\sigma}_x \frac{\hbar}{\sqrt{2}} \sum_k \Delta\omega_k \sqrt{\alpha_{\text{SB}}\omega_k} \left(\frac{\hat{b}_k}{\sqrt{\Delta\omega_k}} + \frac{\hat{b}_k^\dagger}{\sqrt{\Delta\omega_k}} \right), \tag{3.3.5}$$

We can conveniently take this extra factor of $\sqrt{\Delta\omega_k}$ in the denominator into the creation and annihilation operators as $\hat{b}_k/\sqrt{\Delta\omega_k} \to \hat{a}_k$, where the $\hat{a}_k$ are the new continuum annihilation operators. Taking the continuum limit $\Delta\omega_k \to \mathrm{d}\omega_k$, this gives

$$\hat{H}_{\mathrm{int}} = \hat{\sigma}_x \frac{\hbar}{\sqrt{2}} \int_{-\infty}^{\infty} \mathrm{d}\omega_k \sqrt{\alpha_{\mathrm{SB}}\omega_k}(\hat{a}_k + \hat{a}_k^\dagger). \tag{3.3.6}$$

Now, rewrite this interaction Hamiltonian in the interaction picture:

$$\hat{H}_{\mathrm{int}} = \hat{\mu}(t) \frac{\hbar}{\sqrt{2}} \int_{-\infty}^{\infty} \mathrm{d}\omega_k \sqrt{\alpha_{\mathrm{SB}}\omega_k} \big(\mathrm{i}\hat{a}_k^\dagger \mathrm{e}^{\mathrm{i}(|k|t-kx)} - \mathrm{i}\hat{a}_k \mathrm{e}^{-\mathrm{i}(|k|t-kx)}\big), \tag{3.3.7}$$

where the qubit degree of freedom is now encapsulated by $\hat{\mu}(t) = \mathrm{e}^{\mathrm{i}\Omega t} |e\rangle \langle g| + \mathrm{e}^{-\mathrm{i}\Omega t} |g\rangle \langle e|$. The difference now between this Hamiltonian and that of the UDW model is the lack of switching, spatial smearing, and UV cutoff. We can introduce these features by noting that this is the Hamiltonian obtained if we take uniform switching, $\chi(t) = 1$, pointlike smearing, $F_\sigma(x) = \delta(x)$, and uniform cutoff, $C_\varepsilon(k) = 1$. With these choices, the following is equivalent to (3.3.7):

$$\hat{H}_{\mathrm{int}} = \hat{\mu}(t)\chi(t) \frac{\hbar}{\sqrt{2}} \int_{-\infty}^{\infty} \mathrm{d}x\, F_\sigma(x) \int_{-\infty}^{\infty} \mathrm{d}\omega_k C_\varepsilon(k) \sqrt{\alpha_{\mathrm{SB}}\omega_k} \big(\mathrm{i}\hat{a}_k^\dagger \mathrm{e}^{\mathrm{i}(|k|t-kx)} - \mathrm{i}\hat{a}_k \mathrm{e}^{-\mathrm{i}(|k|t-kx)}\big). \tag{3.3.8}$$

Generalizations of the switching $\chi(t)$, the smearing $F_\sigma(x)$, and the cutoff $C_\varepsilon(k)$ can then be introduced to the spin-boson model in this way. This does of course result in a different model than the one we started with in this section in equation (3.3.1).

This is very nearly the Hamiltonian we have written for the UDW model, in equation (3.2.2). We finally recall that $\omega_k = ck$, and that in our UDW model, we have taken $c = \hbar = 1$, and will continue to do so for the rest of the thesis:

$$\hat{H}_{\mathrm{int}} = \hat{\mu}(t)\chi(t) \frac{1}{\sqrt{2}} \int_{-\infty}^{\infty} \mathrm{d}x\, F_\sigma(x) \int_{-\infty}^{\infty} \mathrm{d}k\, C_\varepsilon(k) \sqrt{\alpha_{\mathrm{SB}}\,|k|} \big(\mathrm{i}\hat{a}_k^\dagger \mathrm{e}^{\mathrm{i}(|k|t-kx)} - \mathrm{i}\hat{a}_k \mathrm{e}^{-\mathrm{i}(|k|t-kx)}\big). \tag{3.3.9}$$

Comparing this with the UDW interaction Hamiltonian,

$$\hat{H}_{\mathrm{int}} = \frac{\lambda}{2\sqrt{\pi}} \hat{\mu}(t)\chi(t) \int_{-\infty}^{\infty} \mathrm{d}x\, F_\sigma(x) \int_{-\infty}^{\infty} \mathrm{d}k \sqrt{|k|} \big(\mathrm{i}\hat{a}_k^\dagger \mathrm{e}^{\mathrm{i}(|k|t-kx)} - \mathrm{i}\hat{a}_k \mathrm{e}^{-\mathrm{i}(|k|t-kx)}\big), \tag{3.3.10}$$

we can write the coupling constant λ in terms of the physical parameter α_{SB}:

$$\lambda = \sqrt{2\pi\alpha_{\mathrm{SB}}}. \tag{3.3.11}$$

Practically speaking, we can have $0 < \alpha_{\mathrm{SB}} \lesssim 1$ in experiment, corresponding to $0 < \lambda < \sqrt{2\pi}$ [44]. Taking, for instance, $\lambda = 0.1$ gives $\alpha_{\mathrm{SB}} = 2 \times 10^{-3}$; taking $\alpha_{\mathrm{SB}} = 0.1$ corresponds to $\lambda = 0.8$.

Later in our investigation, we will take the UDW coupling constant to be $\lambda = 0.1$, as a somewhat arbitrary choice. This in fact does not quite qualify as ultrastrong coupling—for that, we require at least $\lambda = 0.3$. However, the results that we cite are relative differences, which do not depend on the specific value of λ—the only requirement we make of λ is that it is small enough for us to be able to use perturbation theory. Higher values of λ do increase the transition probabilities we investigate. These transition probabilities scale like λ^2. Additionally, it is evident from equation (3.3.11) that existing technology allows for much stronger couplings than $\lambda \sim 0.1$. We do not investigate this regime, which would require the use of non-perturbative methods. We speculate, however, that our results only become stronger with much stronger coupling. That is, we expect that accurate choice of ultraviolet cutoff in analysis of ultrastrong coupling of a superconducting qubit to the continuum only becomes more important as the strength of the coupling exceeds the perturbative regime of the UDW model.

This completes the relationship of the spin-boson and Unruh-DeWitt models.

Chapter 4

Finite Sizes and Smooth Cutoffs in Superconducting Circuits

Let us now particularize to a simple system of a qubit coupled to an open transmission line. We'll use the parameters and study of the physical system provided by the spin-boson model and superconducting experiments in combination with the theoretical power of the Unruh-DeWitt model to study this 1+1D system.

We are interested in a number of properties here. First, there is an ultraviolet cutoff in the transmission line which arises from the breakdown of Cooper pairs at high frequencies. This naturally present cutoff implements a mode-dependence in the strength of the interaction between qubit and line. The prospect of deriving the functional behaviour of this mode-dependence from first principles is foreboding, due to the complicated nature of the phenomenon. Indeed, as of the time of this writing, little has been published on this endeavour. Rather, an ultraviolet cutoff has always been assumed for continuum spin-boson models. In many iterations of the model, an exponential cutoff is assumed. This is used to derive a renormalized qubit frequency, which can be observed in experiment [44]. However, in absence of detailed knowledge of the functional behaviour of the ultraviolet cutoff, it seems prudent to be aware of any consequences that may arise from assuming an inaccurate cutoff model in ultrastrong coupling to the continuum.

Second, the qubit has a physical shape and size which is nontrivially related to the spatial extent of its interaction with the transmission line. This finite size has not been fully considered in the literature—it has, rather, been treated as negligible for observable dynamics based on its very small spatial extent. This assumption, as we will see, is perfectly justified, but we nonetheless conduct a thorough investigation on how the shape and size of the qubit affect observable dynamics. We are partially motivated by the fact that the shape

of a qubit, like the ultraviolet cutoff, has been shown to have nontrivial effects on qubit dynamics [117]. Notably, both of these properties can affect causality of an interaction [51].

Finally, we are particularly interested in the effects of ultraviolet cutoffs and qubit shapes in short-lived and quickly switched interactions. As we will see, effects from these properties are much more significant in the short and non-adiabatic regimes. These types of interactions are interesting for a number of reasons. Practically, they are very useful for generation of so-called single photon states (i.e. states with low expectation value of the number operator), which have uses in quantum communication and information processing [53, 54]. These states, being very narrowly distributed in Fock space (i.e. in expectation value of the number operator), have wide distributions in frequency space, leading us to expect that they are more susceptible to effects coming from high-frequency decay of interaction strength.

We have seen in previous sections the power of the UDW model in incorporating spatial smearings, interactions switchings, and ultraviolet cutoffs in the interaction of a qubit and a field. We have also seen the explicit relationship between the spin-boson model and the UDW model. In the context of the ultrastrong coupling regime, where the rotating wave approximation is no longer valid and factors such as the ultraviolet cutoff and the qubit shape are no longer trivially negligible, we can use the UDW model to readily incorporate cutoffs and qubit shapes into our predictions. Specifically, we will investigate in the perturbative regime the impact of the shape and size of the qubit, the shape and scale of the ultraviolet cutoff, and the duration and adiabaticity of the switching on probabilities of spontaneous emission and vacuum excitation of the qubit.

In section 4.1, we discuss scales and plausible functional forms of the qubit shape, transmission line UV cutoff, and time-dependence of the interaction. In section 4.2, we set up the UDW Hamiltonian and detail our perturbative time evolution calculations. In section 4.3, we discuss the method and results of our study, with some remarks about consequences.

4.1 Scales and functional dependencies of the problem

We will establish five scales in this problem, summarized in table 4.1: the energy gap of the qubit Ω, the length scale of the qubit σ_0, the scale of the cutoff ε_0, and scales of adiabaticity and length of the interaction r_0 and T_0.

	Physicality	Approx. value	Scaled to Ω
Ω	energy gap of qubit	10 GHz	Ω
ε_0	cutoff scale	50 GHz	5Ω
σ_0	physical size of qubit	10 μm	$10^{-4}\Omega^{-1}$
r_0	adiabaticity	0.1 ns	Ω^{-1}
T_0	interaction duration	0.1 ns	Ω^{-1}

Table 4.1: Scales of the problem.

Superconducting qubits typically have gaps between 1 and 20 GHz [49, 118–121]. We will take the gap to be $\Omega = 10$ GHz, and will use this as the reference scale of the problem.

The physical size and shape of a qubit is straightforward to measure, but the relationship of the qubit's spatial extent to the spatial extent of its interaction with the electromagnetic field in the line is nontrivial; one could think of an oddly shaped classical capacitor and the fringing of its fieldlines. We will take as a scale the length of the qubit, typically around 10 μm. We will call this scale σ_0. For the shape, we will investigate four symmetric functions which decay as $x \to \infty$: Gaussian, Lorentzian, quartic, and sharp shapes.

The scale of the cutoff is again fairly straightforward to measure. This is the approximate frequency above which microwave modes do not propagate through the transmission line. This frequency is approximately 75 GHz for aluminum, a typical material used for superconducting transmission lines. Calculations in [44] to renormalize the transition frequency of a qubit coupled to an aluminum line are additionally consistent with a cutoff scale of 50 GHz. In this paper, we take 50 GHz as a scale for the cutoff, and call it ε_0. The functional behaviour of the cutoff, as noted, is highly nontrivial to derive from first principles. To some degree, permittivity may be investigated using the Drude model, though this model is built for conductors and semi-conductors as opposed to superconductors [62].

We are investigating a finite-time interaction with realistic switching, as has been previously implemented with switchable coupling [42, 44]. We are interested in the effects from both duration of the interaction and its adiabaticity, so we employ two time parameters: a ramp-up time r describing how quickly the interaction is switched on and off and a duration length T describing how long the interaction remains at maximum strength. Both of these scales are tunable in practice and can, in principle, be as short as 0.01 ns. We take $r_0 = T_0 = 0.1$ ns as our scales. We will explore around these scales in both adiabatic and non-adiabatic regimes and short and long interaction regimes.

The switching function ought to be both experimentally implementable and analytically amenable; we choose the following function which fits these requirements and has both an

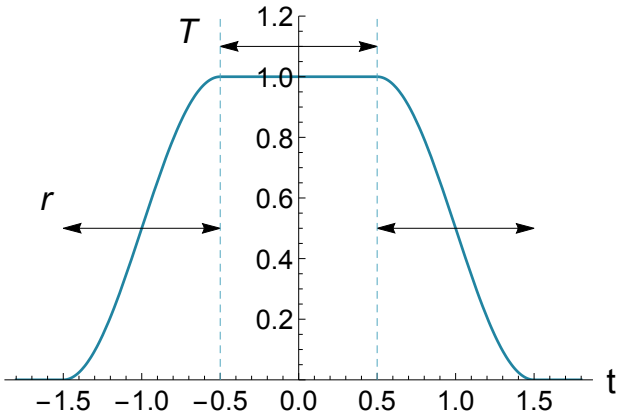

Figure 4.1: The interaction strength has time-dependent strength, called the switching $\chi(t)$. The switching used here is cosine-ramped, with a half-period cosine of period $2r$ on either side of a constant-strength interaction for duration T.

adiabaticity and duration scale,

$$\chi(t) = \begin{cases} \frac{1}{2} + \frac{1}{2}\cos\left(\frac{\pi}{r}\left(t + \frac{T}{2}\right)\right) & t \in \left[-\frac{T}{2} - r, -\frac{T}{2}\right) \\ 1 & t \in \left[-\frac{T}{2}, \frac{T}{2}\right] \\ \frac{1}{2} + \frac{1}{2}\cos\left(\frac{\pi}{r}\left(t - \frac{T}{2}\right)\right) & t \in \left(\frac{T}{2}, \frac{T}{2} + r\right] \\ 0 & \text{otherwise} \end{cases}, \tag{4.1.1}$$

shown in figure 4.1. This switching function has ramping given by half-period cosine functions. In an experimental setting, the implementation of any switching function is accomplished through approximating it with constant voltage on discrete intervals and then transforming it through a filter into an analog signal. It is difficult to preserve pulse shapes through transmission from the generator to the switchable coupler between the qubit and transmission line, due to distortion. It is thus desirable to have a switching function which can be accurately discretized and has an achievable analog bandwidth [122, 123]. The cosine switching function (4.1.1) meets these requirements. We note that the inclusion of scales of duration and adiabaticity means that we expect the results of this study to be applicable to other switching shapes as well.

4.2 Model and time evolution of the qubit

We are able to include the features of finite size, smooth cutoff, and time-dependent interaction strength in our model of the qubit-line system by using the UDW model, first detailed in chapter 3. Its equivalence to the frequently-used spin-boson model was shown in section 3.3. The Hamiltonian is

$$\hat{H}_{\text{int}}(t) = \lambda\, \chi(t)\hat{\mu}(t) \int \mathrm{d}x\, F_\sigma(x)\hat{\pi}(x,t), \tag{4.2.1}$$

with λ the coupling strength, $\chi(t)$ the time-dependent switching of the interaction, $\mu(t) = \mathrm{e}^{\mathrm{i}\Omega t}\left|e\right\rangle\left\langle g\right| + \mathrm{e}^{-\mathrm{i}\Omega t}\left|g\right\rangle\left\langle e\right|$ is the qubit's internal degree of freedom, $F_\sigma(x)$ is the spatial smearing function with characteristic length σ, and $\hat{\pi}(x,t) = \partial_t\hat{\phi}(x,t)$ is the conjugate momentum of a scalar field $\hat{\phi}$. Coupling to $\hat{\pi}(x,t)$ here is as a qubit coupling to the current of a 1D wire. The conjugate momentum can be expanded in plane waves as

$$\hat{\pi}(x,t) = \frac{1}{2\sqrt{\pi}} \int \mathrm{d}k\, C_\varepsilon(k)\sqrt{|k|}\left(\mathrm{i}\hat{a}_k^\dagger \mathrm{e}^{\mathrm{i}(|k|t - kx)} + \text{H.c.}\right), \tag{4.2.2}$$

where the $\hat{a}_k^\dagger$ and $\hat{a}_k$ are the creation and annihilation operators for each mode k and $C_\varepsilon(k)$ is the ultraviolet cutoff function, which weights the contribution of each mode k, with characteristic scale ε.

We will use this model to time-evolve the system to calculate the transition probability of the qubit in situations of spontaneous emission and vacuum excitation. We will begin with each part initially in its free ground state,

$$\hat{\rho}_{\text{in}} = \hat{\rho}_{\text{in},\pi} \otimes \hat{\rho}_{\text{in,q}} = \left|0\right\rangle\left\langle 0\right| \otimes \left|g\right\rangle\left\langle g\right|, \tag{4.2.3}$$

which will give us the transition probability of vacuum excitation, i.e. $\left|g\right\rangle \to \left|e\right\rangle$. The calculation for spontaneous emission is exactly the same as what follows, but with $\Omega \to -\Omega$, which effectively makes the state we label ground into the excited state (making this calculation give the transition probability for $\left|e\right\rangle \to \left|g\right\rangle$).

The unitary describing this evolution is given by the time-ordered exponential of the Hamiltonian,

$$\hat{U} = \mathcal{T}\exp\left(\int_{-\infty}^{\infty} \mathrm{d}t\hat{H}_{\text{int}}(t)\right) = \mathcal{T}\exp\left(\int_{-T-r}^{T+r} \mathrm{d}t\hat{H}_{\text{int}}(t)\right), \tag{4.2.4}$$

where $\mathcal{T}$ is the time-ordering operator. We are able to rewrite the limits of integration given that $\chi(t)$ has compact support on $[-T-r, T+r]$. We must solve this system perturbatively,

so we expand the unitary $\hat{U}$ in a Dyson series:

$$\hat{U} = \mathbb{1} \underbrace{-\mathrm{i}\int_{-\infty}^{\infty} \mathrm{d}t\, \hat{H}_{\mathrm{int}}(t)}_{\hat{U}^{(1)}} \underbrace{-\int_{-\infty}^{\infty} \mathrm{d}t \int_{-\infty}^{t} \mathrm{d}t'\, \hat{H}_{\mathrm{int}}(t)\hat{H}_{\mathrm{int}}(t')}_{\hat{U}^{(2)}} + \mathcal{O}(\lambda^3). \tag{4.2.5}$$

We can thus write the evolution as

$$\hat{\rho}_{\mathrm{out}} = \hat{U}\hat{\rho}_{\mathrm{in}}\hat{U}^{\dagger} = \hat{\rho}_{\mathrm{in}} + \hat{\rho}^{(1)}_{\mathrm{out}} + \hat{\rho}^{(2)}_{\mathrm{out}} + \mathcal{O}(\lambda^3), \tag{4.2.6}$$

where

$$\hat{\rho}^{(1)}_{\mathrm{out}} = \hat{U}^{(1)}\hat{\rho}_{\mathrm{in}} + \hat{\rho}_{\mathrm{in}}\hat{U}^{(1)\dagger}, \tag{4.2.7}$$

$$\hat{\rho}^{(2)}_{\mathrm{out}} = \hat{U}^{(1)}\hat{\rho}_{\mathrm{in}}\hat{U}^{(1)\dagger} + \hat{U}^{(2)}\hat{\rho}_{\mathrm{in}} + \hat{\rho}_{\mathrm{in}}\hat{U}^{(2)\dagger}. \tag{4.2.8}$$

The state of the qubit is then given by tracing out the field on this final state:

$$\hat{\rho}_{\mathrm{q,out}} = \mathrm{Tr}_{\pi}[\hat{\rho}_{\mathrm{out}}] = \hat{\rho}_{\mathrm{q,in}} + \hat{\rho}^{(1)}_{\mathrm{q,out}} + \hat{\rho}^{(2)}_{\mathrm{q,out}} + \mathcal{O}(\lambda^3). \tag{4.2.9}$$

We will now show that $\hat{\rho}^{(1)}_{\mathrm{q,out}}$ is zero for any initial state where the field is in a Fock state. The first order state is

$$\begin{aligned}
\hat{\rho}^{(1)}_{\mathrm{q,out}} &= \mathrm{Tr}_{\pi}\left[\hat{U}^{(1)}\hat{\rho}_{\mathrm{in}} + \mathrm{H.c.}\right] \\
&= \mathrm{Tr}_{\pi}\left[-\mathrm{i}\lambda\int_{-\infty}^{\infty}\mathrm{d}t\chi(t)\hat{\mu}(t)\int \mathrm{d}x F_{\sigma}(x)\hat{\pi}(x,t)\hat{\rho}_{\mathrm{in}} + \mathrm{H.c.}\right] \\
&= -\mathrm{i}\lambda\int_{-\infty}^{\infty}\mathrm{d}t\chi(t)\hat{\mu}(t)\int \mathrm{d}x F_{\sigma}(x)\hat{\rho}_{\mathrm{q,in}}\mathrm{Tr}_{\pi}\big([\hat{\pi}(x,t),\hat{\rho}_{\pi,\mathrm{in}}]\big),
\end{aligned} \tag{4.2.10}$$

where we've taken scalar factors and factors living only in the qubit's Hilbert space ($\hat{\mu}(t)$) out of the partial trace over the field and rewritten the sum over Hermitian conjugates as the commutator of $\hat{\rho}_{\pi,\mathrm{in}}$ and $\hat{\pi}$. Now, it's straightforward to see that the zero-point correlation function $\mathrm{Tr}_{\pi}([\hat{\pi},\hat{\rho}_{\pi,\mathrm{in}}])$ vanishes:

$$\begin{aligned}
\mathrm{Tr}_{\pi}\big([\hat{\pi},\hat{\rho}_{\pi,\mathrm{in}}]\big) &= \sum_n \langle n|\,\hat{\pi}\,|0\rangle\,\langle 0|n\rangle - \langle n|0\rangle\,\langle 0|\,\hat{\pi}\,|n\rangle \\
&= \langle 0|\,\hat{\pi}\,|0\rangle - \langle 0|\,\hat{\pi}\,|0\rangle \\
&= 0.
\end{aligned} \tag{4.2.11}$$

Thus the leading order contribution to the final state is of second order in λ, $\hat{\rho}^{(2)}_{\mathrm{q,out}}$.

We will find an explicit expression for $\hat{\rho}^{(2)}_{\mathrm{q,out}}$, beginning by substituting the interaction Hamiltonian (4.2.1) into the expression for the second order term (4.2.8), and tracing over the modes of the field:

$$\hat{\rho}^{(2)}_{\mathrm{q,out}} = -\lambda^2 \mathrm{Tr}_\pi \left(\int_{-\infty}^{\infty} \mathrm{d}t \int_{-\infty}^{\infty} \mathrm{d}t' \, \chi(t)\,\chi(t')\,\hat{\mu}(t)\,\hat{\rho}_{\mathrm{q,in}}\,\hat{\mu}(t') \int \mathrm{d}x \int \mathrm{d}x' F_\sigma(x) F_\sigma(x') \hat{\pi}(x,t) \hat{\rho}_{\pi,\mathrm{in}} \hat{\pi}(x',t') \right.$$
$$\left. + \int_{-\infty}^{\infty} \mathrm{d}t \int_{-\infty}^{t} \mathrm{d}t' \, \chi(t)\,\chi(t')\,\hat{\mu}(t)\,\hat{\mu}(t')\,\hat{\rho}_{\mathrm{q,in}} \int \mathrm{d}x \int \mathrm{d}x' F_\sigma(x) F_\sigma(x') \hat{\pi}(x,t) \hat{\pi}(x',t') \hat{\rho}_{\pi,\mathrm{in}} + \mathrm{H.c.} \right). \tag{4.2.12}$$

Let us introduce the smeared Wightman function[1] $W_\sigma[t,t']$ in the goal of simplifying the above expression:

$$W_\sigma[t,t'] = \int \mathrm{d}x \int \mathrm{d}x' F_\sigma(x) F_\sigma(x') \mathrm{Tr}_\pi[\hat{\pi}(x,t) \hat{\rho}_{\pi,\mathrm{in}} \hat{\pi}(x',t')]. \tag{4.2.13}$$

This allows us to rewrite the second order term of the state as

$$\hat{\rho}^{(2)}_{\mathrm{q,out}} = -\lambda^2 \left(\int_{-\infty}^{\infty} \mathrm{d}t \int_{-\infty}^{\infty} \mathrm{d}t' \chi(t)\,\chi(t')\,\hat{\mu}(t)\,\hat{\rho}_{\mathrm{q,in}}\,\hat{\mu}(t') W_\sigma[t',t] \right. \tag{4.2.14}$$
$$\left. + \int_{-\infty}^{\infty} \mathrm{d}t \int_{-\infty}^{t} \mathrm{d}t' \chi(t)\,\chi(t')\,\hat{\mu}(t)\,\hat{\mu}(t')\,\hat{\rho}_{\mathrm{q,in}} W_\sigma[t,t'] + \mathrm{H.c.} \right).$$

Using that $\hat{\rho}_{\mathrm{q,in}} = |g\rangle\langle g|$ and $\hat{\mu}(t) = \mathrm{e}^{\mathrm{i}\Omega t}|e\rangle\langle g| + \mathrm{e}^{-\mathrm{i}\Omega t}|g\rangle\langle e|$, we have

$$\hat{\rho}^{(2)}_{\mathrm{q,out}} = \int_{-\infty}^{\infty} \mathrm{d}t \int_{\infty}^{\infty} \mathrm{d}t' \, \chi(t)\,\chi(t')\, W_\sigma[t',t] \mathrm{e}^{\mathrm{i}\Omega(t-t')} |e\rangle\langle e| \tag{4.2.15}$$
$$- 2 \int_{-\infty}^{\infty} \int_{-\infty}^{t} \mathrm{d}t' \, \chi(t)\,\chi(t')\, \mathrm{Re}\big[W_\sigma[t,t']\big] \cos\big(\Omega(t-t')\big) |g\rangle\langle g| \,.$$

Let us now focus on simplifying the smeared Wightman $W_\sigma[t,t']$. The trace over the modes of the field simplifies to an expectation value of $\hat{\pi}(x,t)\hat{\pi}(x',t')$ on the state $\hat{\rho}_{\pi,\mathrm{in}} = |0\rangle\langle 0|$:

$$W_\sigma[t,t'] = \frac{1}{4\pi} \int \mathrm{d}x \int \mathrm{d}x' F_\sigma(x) F_\sigma(x') \int \mathrm{d}k \int \mathrm{d}k' C_\varepsilon(k) C_\varepsilon(k') \tag{4.2.16}$$
$$\times \sqrt{|k|\,|k'|}\, \langle 0| \left(\hat{a}^\dagger_k \mathrm{e}^{\mathrm{i}(|k|t - kx)} - \mathrm{H.c.} \right) \left(\hat{a}'^\dagger_k \mathrm{e}^{\mathrm{i}(|k'|t - k'x')} - \mathrm{H.c.} \right) |0\rangle \,.$$

[1] Normally, the Wightman function (and smeared versions of it, that is, ones which include spatial smearing) is the two-point correlator of the field amplitude $\hat{\phi}$. The smeared Wightman we use here is of course the two-point correlator of the field's conjugate momentum $\hat{\pi}$, or the smeared momentum Wightman function. We'll just call it the smeared Wightman.

The modes k' coincide with k, as $\langle 0|\, \hat{a}_k \hat{a}_k'^{\dagger}\, |0\rangle = \delta(k-k')$, giving

$$W_\sigma[t,t'] = \frac{1}{4\pi}\int \mathrm{d}k \int \mathrm{d}x\, F_\sigma(x) \mathrm{e}^{\mathrm{i}kx} \int \mathrm{d}x'\, F_\sigma(x') \mathrm{e}^{\mathrm{i}kx'} C_\varepsilon^2(k)\, |k|\, \mathrm{e}^{-\mathrm{i}|k|(t-t')}. \tag{4.2.17}$$

Notice that we have here the Fourier transform of the spatial smearing,

$$\tilde{F}_\sigma(k) = \int \mathrm{d}x F_\sigma(x) \mathrm{e}^{\mathrm{i}kx}, \tag{4.2.18}$$

and that we use only real symmetric smearings, so that $\tilde{F}_\sigma(k) = \tilde{F}_\sigma(-k)$. The smeared Wightman becomes

$$W_\sigma[t,t'] = \frac{1}{4\pi}\int \mathrm{d}k \tilde{F}_\sigma(k) C_\varepsilon^2(k)\, |k|\, \mathrm{e}^{-\mathrm{i}|k|(t-t')}. \tag{4.2.19}$$

Substituting this expression for the smeared Wightman into (4.2.15) now gives the expression for the final state of the qubit, general in choice of smearing, UV cutoff, and switching functions:

$$\begin{aligned}\hat{\rho}^{(2)}_{\mathrm{q,out}} = \frac{1}{4\pi}\int \mathrm{d}k\, \tilde{F}_\sigma^2(k) C_\varepsilon^2(k)\, |k| \Bigg(&\int_{-\infty}^{\infty} \mathrm{d}t \int_{-\infty}^{\infty} \mathrm{d}t' \chi(t)\, \chi(t')\, \mathrm{e}^{\mathrm{i}(|k|+\Omega)(t-t')}\, |e\rangle\, \langle e| \\ &-2\int_{-\infty}^{\infty} \mathrm{d}t \int_{-\infty}^{t} \mathrm{d}t' \chi(t)\, \chi(t')\, \cos\big(-|k|\,(t-t')\big) \cos\big(\Omega(t-t')\big)\, |g\rangle\, \langle g| \Bigg).\end{aligned} \tag{4.2.20}$$

Now, since $\hat{\rho}^{(2)}_{\mathrm{q,out}}$ is a perturbation to a quantum state $\hat{\rho}_{\mathrm{q,in}}$, as in $\hat{\rho}_{\mathrm{q,out}} = \hat{\rho}_{\mathrm{q,in}} + \hat{\rho}^{(2)}_{\mathrm{q,out}} + \mathcal{O}(\lambda^3)$, we must have that $\hat{\rho}^{(2)}_{\mathrm{q,out}}$ is traceless. Thus the coefficient of $|e\rangle\langle e|$ must be the same as the negative of $|g\rangle\langle g|$ in equation (4.2.20), and we can rewrite the second order perturbation as

$$\hat{\rho}^{(2)}_{\mathrm{q,out}} = -P_e\, |g\rangle\, \langle g| + P_e\, |e\rangle\, \langle e|\,, \tag{4.2.21}$$

where P_e is the leading order probability of vacuum excitation of the qubit,

$$P_e = \frac{1}{4\pi}\int \mathrm{d}k\, \tilde{F}_\sigma^2(k) C_\varepsilon^2(k)\, |k| \int_{-\infty}^{\infty} \mathrm{d}t \int_{-\infty}^{\infty} \mathrm{d}t' \chi(t)\, \chi(t')\, \mathrm{e}^{\mathrm{i}(|k|+\Omega)(t-t')}. \tag{4.2.22}$$

We can particularize to our choice of smearing, given in equation (4.1.1), and express the t and t' integrals in closed form:

$$\begin{aligned}P_e = \frac{\lambda^2}{4\pi}\int_{-\infty}^{\infty} \mathrm{d}k\, \tilde{F}_\sigma^2(k) C_\varepsilon^2(k)\, |k| \Bigg(&\frac{-\mathrm{i}\pi^4}{2} \frac{\mathrm{e}^{-\mathrm{i}(k+\Omega)(2r+T)/2}}{(k+\Omega)^2(\pi - r(k+\Omega))^2(\pi + r(k+\Omega))^2} \\ &\times \left(1+\mathrm{e}^{\mathrm{i}r(k+\Omega)}\right)\left(-1+\mathrm{e}^{\mathrm{i}(k+\Omega)(r+T)}\right)\left[\sin\left(\frac{(k+\Omega)(2r+T)}{2}\right) + \sin\left(\frac{T(k+\Omega)}{2}\right)\right]\Bigg).\end{aligned} \tag{4.2.23}$$

This expression contains all the information about the qubit's dynamics that we need. Given a particular spatial smearing of the qubit, an ultraviolet cutoff of the modes in the line, and time scales of the switching, we can use (4.2.23) to calculate the probability that the qubit will undergo vacuum excitation. If we replace Ω with $-\Omega$, (4.2.23) gives the probability of spontaneous emission. We can thus investigate the effects on qubit dynamics of each of these properties.

In this expression for the probability of vacuum excitation, we see that although the Fourier transform of the spatial smearing and the ultraviolet cutoff describe different physical properties of the system, they affect the qubit dynamics in the same way. This justifies the heuristic view where the ultraviolet cutoff determines what modes of the field are available to participate in the interaction and the Fourier transform of the spatial smearing determines what modes of the field the qubit can 'see'. We thus regard the product $\tilde{F}^2_\sigma(k)C^2_\varepsilon(k)$ as an *effective form factor* of the qubit, where both $\tilde{F}_\sigma(k)$ and $C_\varepsilon(k)$ contribute equally to the modes of the field which participate in the interaction between qubit and line.

4.3 Results

We now analyse the effects on qubit dynamics of particular shapes and sizes of qubit, cutoff models and scales, time scales of the switching. We'll focus on the impact of the effective form factor on the probability of spontaneous emission and vacuum excitation as a function of the ramp-up time r and the interaction duration T.

We discussed the characteristic scales of the problem (i.e. the length scale of the qubit, the scale of the ultraviolet cutoff, and characteristic times for ramp-up and constant interaction strength) in section 4.1. We will investigate a range around each of these characteristic scales to analyse the importance of precise knowledge or tuning of each of them.

There are four smearing models that we will consider: Gaussian, Lorentzian, sharp decay, and quartic decay. The form of these models are written in table 4.2. Note that these smearing functions are normalized, so that the qubit has an 'area' of one. There are also four ultraviolet cutoff models that we will consider: Gaussian, Lorentzian, sharp decay, and exponential decay. These are written in table 4.3. Note that the cutoff models assume that the interaction strength is constant up to the frequency of the qubit.

We compare the effect of the each of these properties using the relative difference Δ_{AB} between shape or cutoff models A and B over a range of sizes, cutoff scales, ramp-up times,

Smearing	Notation	$F_\sigma(x)$
Gaussian	$F_{\mathrm{G},\sigma}(x)$	$(\sigma\sqrt{\pi})^{-1}\mathrm{e}^{-x^2/\sigma^2}$
Lorentzian	$F_{\mathrm{L},\sigma}(x)$	$\dfrac{\sigma}{2\pi}\dfrac{1}{x^2+\sigma^2/4}$
Quartic decay	$F_{\mathrm{Q},\sigma}(x)$	$\dfrac{\sigma^3}{4\sqrt{2}\pi}\dfrac{1}{x^4+\left(\frac{\sigma}{2}\right)^4}$
Sharp decay	$F_{\mathrm{S},\sigma}(x)$	$\sigma^{-1}\Theta\left(x+\dfrac{\sigma}{2},-x+\dfrac{\sigma}{2}\right)$

Table 4.2: Spatial distributions.

Cutoff	Notation	$C_\varepsilon(k)$
Gaussian	$C_{\mathrm{G},\varepsilon}(k)$	$\begin{cases}\exp\left(-\frac{(\lvert k\rvert-\Omega)^2}{2\varepsilon^2}\right) & \lvert k\rvert>\Omega\\ 1 & \lvert k\rvert<\Omega\end{cases}$
Lorentzian	$C_{\mathrm{L},\varepsilon}(k)$	$\begin{cases}\frac{\varepsilon^2}{\left(\lvert k\rvert-\Omega\right)^2+\varepsilon^2} & \lvert k\rvert>\Omega\\ 1 & \lvert k\rvert<\Omega\end{cases}$
Exponential	$C_{\mathrm{E},\varepsilon}(k)$	$\begin{cases}\exp\left(\frac{\Omega-\lvert k\rvert}{\sqrt{2}\varepsilon}\right) & \lvert k\rvert>\Omega\\ 1 & \lvert k\rvert<\Omega\end{cases}$
Sharp decay	$C_{\mathrm{S},\varepsilon}(k)$	$\Theta\big(k+\Omega+\varepsilon,-k+\Omega+\varepsilon\big)$

Table 4.3: Cutoff models.

and interaction times,

$$\Delta_{\text{AB}} = \frac{|P_{e,\text{A}} - P_{e,\text{B}}|}{\max(P_{e,\text{A}}, P_{e,\text{B}})}, \tag{4.3.1}$$

e.g. the relative difference between the exponential and sharp cutoff models is denoted as Δ_{ES}. The relative difference estimates the error generated by analyzing data using an incorrect model. We can judge whether the impact of a property like the shape model is significant by looking at the relative difference in transition probabilities of the qubit between different models.

In the following subsections, we assess the effect on vacuum excitation and spontaneous emission of the components of the effective form factor (i.e. shape and cutoff models and their respective scales) and of the two time scales of the interaction (ramp-up time and duration). In section 4.3.1, we see that the particular choice of shape model in fact makes negligible contributions to the effective form factor in comparison to the cutoff model. In section 4.3.2, we show that within orders of magnitude, the size of the qubit is neglible, while the effect of the cutoff scale is quite significant. Finally, in section 4.3.3, we detail how the effect of the choice of cutoff model changes with the adiabaticity and duration of the interaction between the qubit and line.

4.3.1 Sensitivity to shape and cutoff models

Here we compare the impact of the cutoff model $C_\varepsilon(k)$ and the qubit's shape model $F_\sigma(x)$ on the probability of vacuum excitation and spontaneous emission over a range of cutoff scales and sizes, for fixed interaction time scales $r = r_0$ and $T = T_0$. The relative difference between probability of spontaneous emission calculated with different cutoff models is plotted in figure 4.2, panels c and d; differences between shape models is plotted in figure 4.2, panels a and b.

The difference effected by the choice of cutoff model is at least two orders of magnitude larger than that effected by the choice of shape for cutoff scales up to at least $20\varepsilon_0$, as seen by comparing panels b and c of figure 4.2. The effect of the cutoff model dominating over that of the shape model persists for qubit sizes within at least an order of magnitude of σ_0, as shown in panels a and d of figure 4.2.

We expect this dominance of the cutoff model from our expression for the transition probability of the qubit, equation (4.2.23). We identified the effective form factor $\tilde{F}_\sigma(k)^2 C_\varepsilon(k)^2$ as a regulator of shape (or modes) of the interaction—thus the Fourier transform of the shape and the cutoff model contribute equally to the k integrand. The scale of the cutoff is, however, about 4 orders of magnitude larger than that of the shape. We

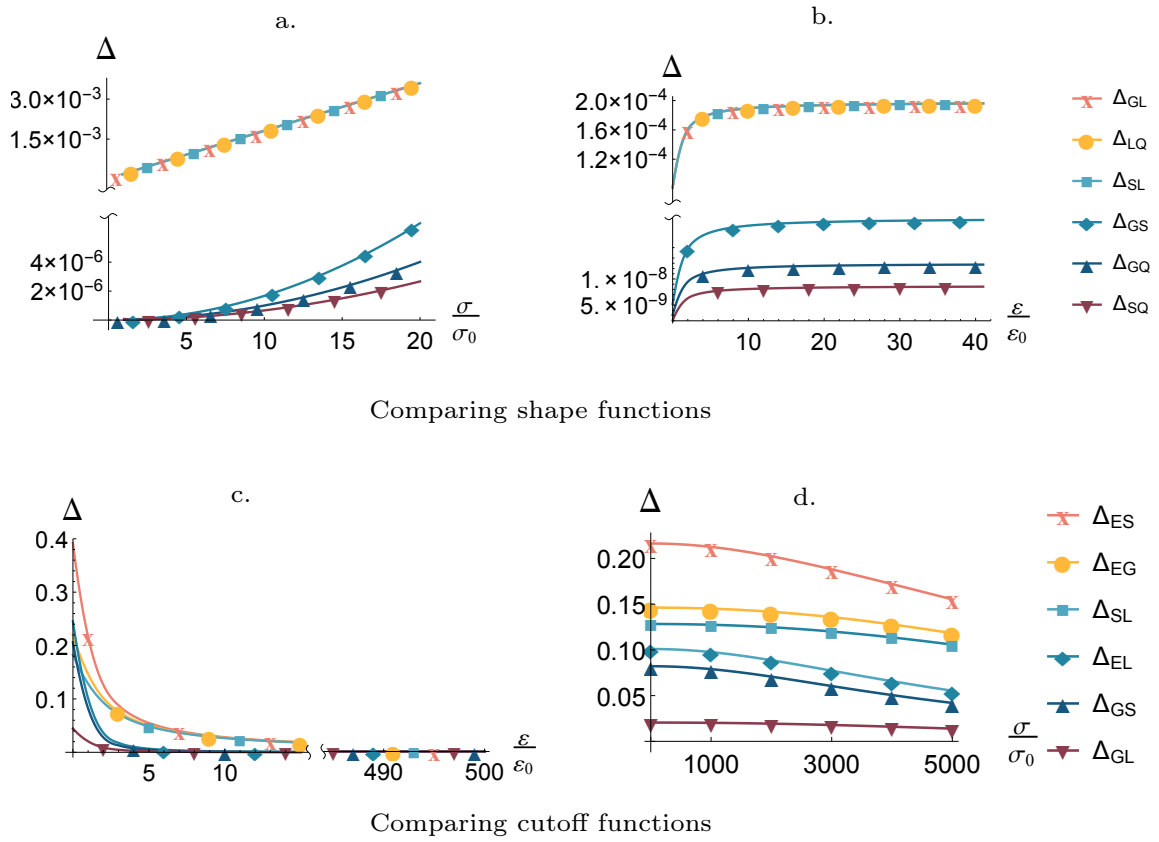

Figure 4.2: Relative difference of spontaneous emission probabilities when comparing **a)** shape functions over a range of sizes σ, **b)** shape function over a range of cutoff scales ε, **c)** cutoff functions over a range of cutoff scales ϵ, and **d)** cutoff functions over a range of sizes σ. Markers are included to distinguish lines. Markers indicate which pair of shape functions or cutoff functions are being compared, and are listed in the legends to the right of figures b and d. The interaction times are fixed at $r = r_0$ and $T = T_0$. Shapes are compared using exponential cutoff and cutoffs using Gaussian shape. Sizes are compared while the cutoff is kept constant at ε_0 and cutoff scales while the size is kept constant at σ_0. The behaviour of the vacuum excitation probabilities is similar.

would thus anticipate that changes to the cutoff model have a much larger impact on qubit dynamics than changes to the shape model.

Thus the effect of the shape function on the qubit dynamics is negligible as compared with the effect of the cutoff model. Given this irrelevance of the qubit shape for the regime studied, for the rest of this investigation, we choose the shape to be Gaussian for purely aesthetic reasons.

4.3.2 Sensitivity to size and cutoff scale

Here, we assess the impact on qubit dynamics of the physical size of the qubit σ and the cutoff scale ε. We again analyse the processes of spontaneous emission and vacuum excitation with the interaction timescales fixed.

The relative difference between different cutoff models is effectively insensitive to the size of the qubit σ, as seen in figure 4.2d. In fact, a relative difference of just 10^{-6} in the probability of spontaneous emission is seen between sizes of $0.1\sigma_0$ and $10\sigma_0$. In other words, the Fourier transform of the qubit's shape is effectively flat for a wide range of frequencies. Thus, as long as the size of the qubit as seen by the transmission line, σ, is within a couple of orders of magnitude of the physical size of the qubit, σ_0, the specific value will have a negligible effect on the dynamics. In view of the fact that the effective form factor of the qubit is largely independent of σ for a wide range of values, we will set $\sigma = \sigma_0$ for the rest of the investigation.

In contrast, figure 4.2c shows high sensitivity to the cutoff scale—a relative difference of 0.7 in the transition probability is seen between cutoff scales of $0.1\varepsilon_0$ and $10\varepsilon_0$. Note also that this relative difference between pairs of cutoffs decreases as ε increases. This is expected; as the cutoff scale goes to infinity, all probabilities calculated with different cutoff models converge to the cutoff-free value.

In many contexts, an exponential cutoff is a standard choice when an ultraviolet cutoff is needed. We note that the transition probability calculated with an exponential cutoff is slower to converge to the cutoff-free value than the other cutoff models considered here. This can be attributed to the fast decay of the exponential cutoff, and notably its lack of inflection, in contrast to the Gaussian and Lorentzian cutoff models. This fact should perhaps be considered in the context of an exponential cutoff often being used by default, for example, as an *ad-hoc* soft cutoff—it is possible that this choice of cutoff may lead to inaccuracies in predictions if the physical ultraviolet cutoff does not decay so rapidly.

From this set of observations, we can conclude that for the two scales of the effective form factor, the specific value of the size is irrelevant to qubit dynamics in comparison to the cutoff scale.

Combining the observations from this and the previous subsection, we conclude that for the parameter regimes in table 4.1, the effective form factor of the qubit is dominated by the cutoff model and cutoff scale as compared to the effects of the shape model and size. This corroborates the current practice of treating the shape of the qubit as negligible.

4.3.3 Sensitivity to cutoff models as a function of adiabaticity and interaction duration

We have now established that for typical superconducting qubit setups in the ultrastrong coupling regime, the cutoff model and cutoff scale dominate the effective form factor of a qubit interacting with a superconducting transmission line. In this subsection, we move on to the particulars of the effect of the choice of cutoff model. As discussed above, the exact functional form of the UV cutoff function in a realistic scenario is complex to obtain from first principles, as it involves the complicated interplay of electrodynamics and quasiparticle physics.

We thus ask the question of how much we should care about the particular way in which in the transmission line loses its ability to trap higher frequency modes when we make predictions. In other words, will the experiment be sensitive to the particular shape of the cutoff function or just its scale? How much do the microscopics of the superconductor impact the outcome of experiments? Does it really matter if the effective coupling strength decays exponentially with the mode frequency or with any other shape?

In particular, we focus on the relative difference in transition probabilities calculated using different cutoff models for different choices of ramp-up time r and constant interaction time T (recall the switching function given in equation (4.1.1)), with fixed cutoff scale $\varepsilon = \varepsilon_0$. This will narrow down the regimes for which one must consider the actual form of the mode-dependency of the interaction.

In figure 4.3, we plot the relative difference in probability of spontaneous emission between different cutoff models for a range of ramp-up and constant interaction times; we plot the same for vacuum excitation in figure 4.4. There are several features to be noted. First, in the non-adiabatic ($r \lesssim r_0$) and short time ($T \lesssim T_0$) regime, the choice of cutoff model has a very significant effect on both transition probabilities, with relative differences between particular pairs of cutoff models often reaching well above 10%. Second, in the adiabatic limit ($r \gg r_0$), this effect vanishes. For adiabatic switching, all cutoffs look the same. Finally, in the long-time regime ($T \gg T_0$), we see different behaviours for the excitation and emission probabilities. The effect of the cutoff on the probability of spontaneous emission vanishes for long-time and non-adiabatic interactions; it does not

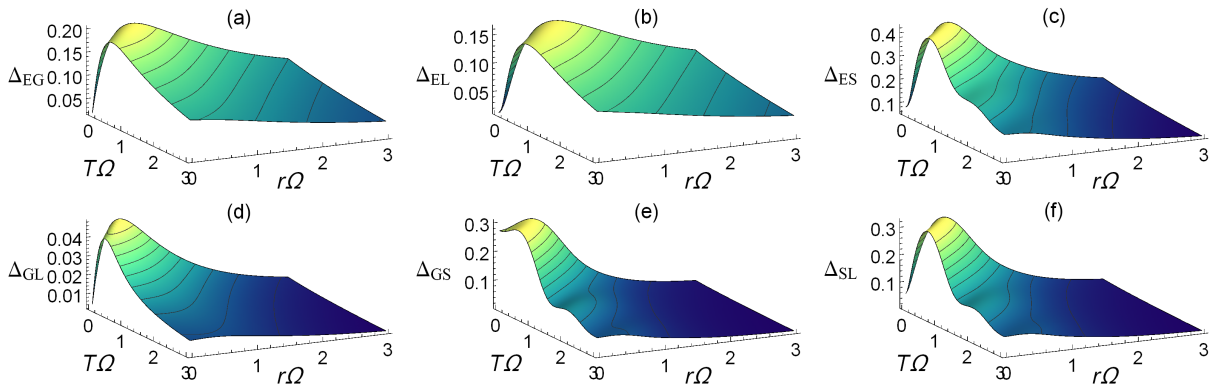

Figure 4.3: Relative difference of probability of spontaneous emission comparing **a)** exponential and Gaussian, **b)** exponential and Lorentzian, **c)** exponential and sharp, **d)** Gaussian and Lorentzian, **e)** Gaussian and sharp, and **f)** sharp and Lorentzian cutoff functions across a range of ramp-up and constant interaction times r and T. Here we take the size to be σ_0, the shape to be Gaussian, and the cutoff scale to be ε_0.

vanish in the same regime for the probability of vacuum excitation. That is, in long-time and non-adiabatic interactions, the effect of a particular choice of cutoff is a relative difference of even 10%. This persistent effect can be seen in figure 4.5.

There are small differences in the behaviour of the relative differences for vacuum excitation and spontaneous emission. We find that the choice of cutoff has a more noticeable effect on the probability of excitation as compared to emission. We can justify this by thinking of the frequencies involved with each process. In spontaneous emission, the qubit emits into the line at its own frequency Ω. In vacuum excitation, there is no such dominant frequency—fluctuations in the field at all frequencies can contribute to the process of exciting the qubit. Thus we would expect the strength of higher frequency modes to be have a more significant effect on excitation than on emission. This can be seen in the comparison of figures 4.4 and 4.3.

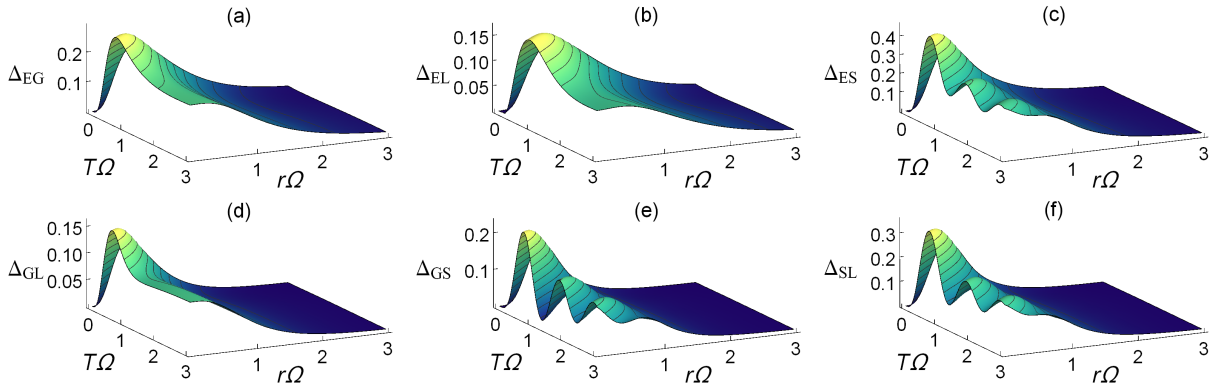

Figure 4.4: Relative difference of probability of vacuum excitation comparing **a)** exponential and Gaussian, **b)** exponential and Lorentzian, **c)** exponential and sharp, **d)** Gaussian and Lorentzian, **e)** Gaussian and sharp, and **f)** sharp and Lorentzian cutoff functions across a range of ramp-up and constant interaction times r and T. Here we take the size to be σ_0, the shape to be Gaussian, and the cutoff scale to be ε_0. Notice the slightly higher relative differnces here as compared to probabilities of spontaneous emission in figure 4.3. This is attributable to there not being a dominant frequency in the process of vacuum excitation (where the qubit's frequency is the dominant frequency of spontaneous emission) and thus modifications to the strength of higher frequency modes through a cutoff being more important.

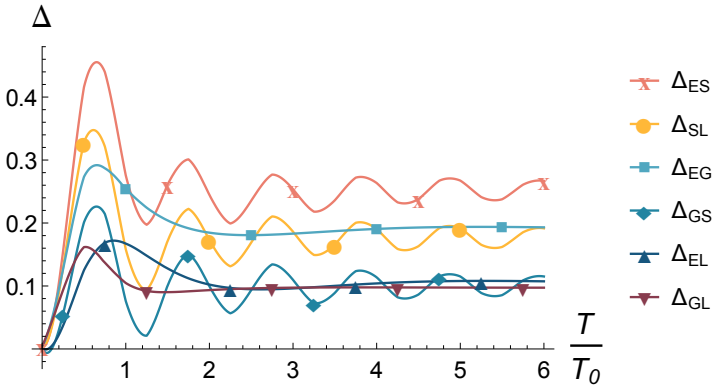

Figure 4.5: Relative difference of vacuum excitation probability between pairs of cutoff functions across a range of interaction times T, for fixed size σ_0, shape (Gaussian), cutoff scale ε_0, and ramp-up time $r = 0.1r_0$. Markers are included to distinguish lines.

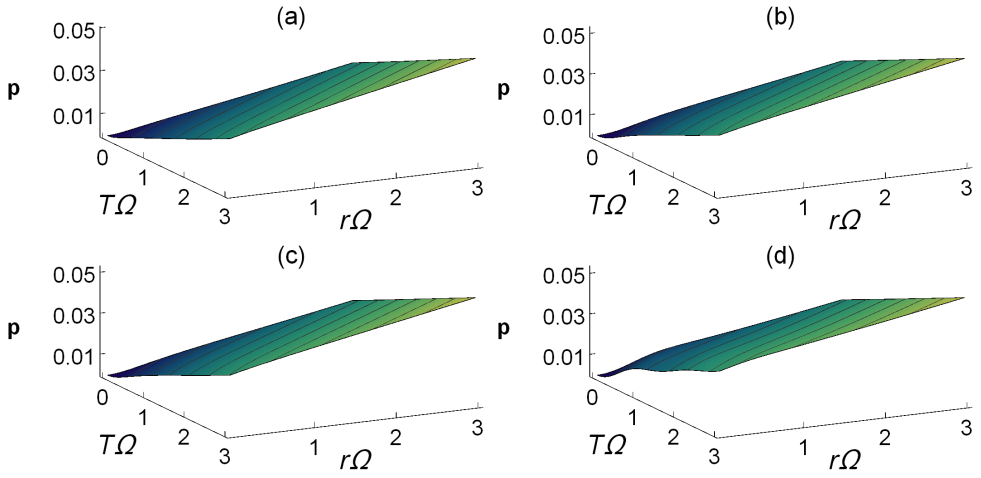

Figure 4.6: Probability of spontaneous emission for different cutoff models: **a)** exponential, **b)** Gaussian, **c)** Lorentzian, and **d)** sharp, plotted across a range of ramp-up and constant interaction times r and T. Here we take the size to be σ_0, the shape to be Gaussian, and the cutoff scale to be ε_0.

We end this section with some discussion of the implementation and relevance of the timescales where the choice of cutoff matters to the predictions made by our model. There are certainly difficulties associated with attempting to implement highly non-adiabatic switchings, namely the ramp-up and ramp-down times of a signal generator and distortions to fine pulse shapes from various sources. The fastest arbitrary waveform generators can output switching waveforms with ramp-up and ramp-down times of the order of 20 ps. Other types of pulse generators have even shorter ramping time, but lack fine control of the pulse shape. Distortion effects can come from dispersion and reflection of pulses at interconnects between room temperature equipment and a cold tunable coupler between the qubit and transmission line. This distortion can currently be managed to be less than 0.1 ns (see experiments in [122]). Reduction of such distortion below 0.1 ns may be possible with significant investments in custom setups. As in table 4.1, we take $r_0 = T_0 = 0.1$ ns. Thus, experiments exploring regimes where the ramp-up and constant interaction times of a superconducting qubit and transmission line are of the order of 0.1 ns are currently feasible, with some difficulty. Finally, we note that coupling elements are usually designed to work in the adiabatic regime; specialized attention must therefore be made to optimizing these elements for non-adiabatic pulse shapes.

The absolute value of the probability of vacuum excitation and spontaneous emission are shown for different choices of cutoff models across ranges of ramp-up and interaction times

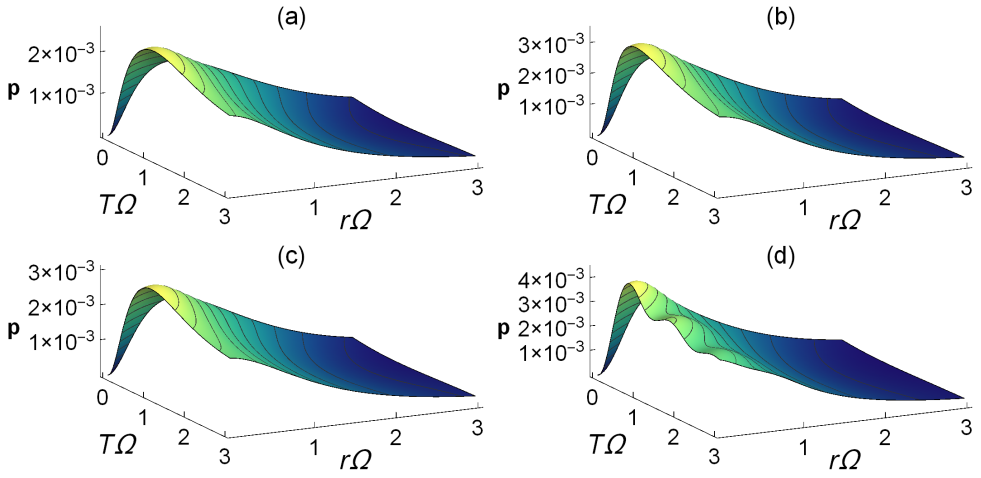

Figure 4.7: Probability of vacuum excitation for different cutoff models: **a)** exponential, **b)** Gaussian, **c)** Lorentzian, and **d)** sharp, plotted across a range of ramp-up and constant interaction times r and T. Here we take the size to be σ_0, the shape to be Gaussian, and the cutoff scale to be ε_0.

in figures 4.7 and 4.6 respectively. The probability of spontaneous emission is large enough ($\sim 1\%$) for short interaction and ramp-up times that making observations of differences between cutoff models seems plausible. On the other hand, the probability of vacuum excitation is vanishingly small—only about 0.1% chance of excitation for long interaction times and short ramp-up times, making direct observation of the effect of the cutoff model less likely.

The regimes where observations may be made of the dependence of transition probabilities on the behaviour of the cutoff are plausibly within reach of current superconducting qubit technology. For non-adiabatic switching especially, a poor choice of cutoff model can introduce significant errors in the theoretical analysis of the setup.

Chapter 5

Discussion, limitations, and conclusions

5.1 Discussion

In this part of the thesis, we have studied a simple scenario of a superconducting qubit coupled to an open transmission line, and asked about the importance of the finite size of the qubit and the ultraviolet cutoff of the transmission line in specific transition probabilities of the qubit. Usually, these types of setups are analysed using the spin-boson model and variants therein, which we reviewed in chapter 2. In order to study the impact of a spatial distribution, which are not present in the spin-boson model, we employed the UDW model, reviewed in chapter 3.

In chapter 4, we laid out the details of the investigation. We calculated the transition probability of a qubit beginning in the excited and ground states for a variety of shapes and sizes, cutoff models and scales, and adiabaticities and interaction durations. The factors of cutoff and shape were investigated in tandem due to their similar contribution to the transition probability (4.2.23), making up an effective form factor determining the shape of the interaction. Motivated by the difficulty of determining the functional form of the shape and cutoff from first principles, we considered several plausible forms for each and identified in what regimes of interaction this choice made a difference to the probabilities of vacuum excitation and spontaneous emission. We made a similar investigation for the scale of the shape (i.e. the size) and the cutoff scale.

We found that, in the parameter regime of table 4.1, the cutoff scale dominates significantly over the size, as may be expected from their difference in magnitude: the cutoff scale, $\varepsilon_0 = 5\Omega$, is several orders of magnitude smaller than the size of the qubit in frequency

space, $\sigma_{0,k} = 10^4\Omega$, meaning that its effect is more readily visible for frequencies of the order of Ω. The cutoff scale was found significant impact on the transition probabilities. We additionally found that the shape is negligible as compared to the cutoff model, for similar reasons. This corroborates the practice already present in the literature of considering the finite size effects to be negligible.

Taking the cutoff scale to be given, the cutoff model was found to have particular importance in the non-adiabatic and short-time switching regimes, with this effect persisting for non-adiabatic and long-time interactions in the case of vacuum excitation. The choice of cutoff model may affect predictions in this regime by well over 10%. We emphasize that this experimental regime is feasibly accessible with current switching technologies. Thus, though the specifics of an ultraviolet cutoff present due to complex microscopic physics and the breakdown of superconductivity are difficult to derive, there are experimentally attainable regimes where they must nonetheless be considered.

5.2 Limitations

There are some limitations to this study. First, we use perturbation theory. In fact, our results only hold for a certain portion of the USC regime. Other methods have been developed to accurately predict dynamics in the USC regime, like the dynamical polaron ansatz [65]. In very strong coupling regimes, studies like this demonstrate qualitatively different behaviour; for instance, the spontaneous emission rate decreases in the very strong ($\alpha_{\mathrm{SB}} \gtrsim 0.3$) regime (see figure 2 of [65]). In the coupling regime where our studies overlap, our investigation is at least conceptually corroborated by this study. For very short interaction times, this method finds a dependence on the cutoff of spontaneous emission (see figure 3 of [65]). One could make this analysis nonperturbative for very short couplings (those with interaction times much shorter than the time scale of the qubit, Ω^{-1}) by approximating the switching as a delta function. We would not, however, expect the probability of emission or excitation to be observable in this case.

Additionally, our study is partially motivated by the inclusion of different cutoff models. The spin-boson model in fact already includes at least some model of ultraviolet cutoff for continuum cases, and this is observed in the renormalization of the qubit frequency, seen in studies such as [44]. Our study brings significant flexibility in this; it is arguably easier to study different cutoff models in the UDW model as opposed to the spin-boson model.

Finally, we were motivated to study the impact of the cutoff and shape specifically in the context of a qubit coupled to an infinite line. In practice, qubits are more frequently coupled to a resonator, which is then coupled to a transmission line. Among other studies,

[50] couple a flux qubit to a cavity and get very good agreement with the spin-boson model, which they solve using matrix product states. This suggests that there are relatively niche areas where the application of our model is more useful than the spin-boson model, using techniques of solution which already exist.

5.3 Conclusions

In this work, we have provided a thorough relationship between the Unruh-DeWitt and spin-boson models, including relating their coupling constants. We applied the UDW model to a physically-motivated setup, and were able to find that for very short and non-adiabatic interactions, the way in which the coupling strength is cut off for high frequencies may be detectable in experiment. We were able to corroborate the current practice of taking the spatial extent of the qubit to be negligible, even at very short timescales. These perturbative results are quite strong in the lower range of the ultra-strong coupling regime, which may suggest that these effects are even more readily observable for stronger couplings. We may say rather confidently that, at least for quickly-switched interactions of a qubit and an open transmission line, the ultraviolet cutoff matters.

5.4 Motivations, Revisited

The results of Part I are that the dynamics of a qubit coupled to a scalar field can tell something about the form of an ultraviolet cutoff in that field when the interaction between the two is quite strong, is short, and is rapidly switched on and off.

We set out to investigate a very particular part of a physical scenario that we initially motivated as fundamental and thus naturally interesting, and that is one genuine effect of our study—we studied a niche theoretical setup. But what effect does it genuinely have to contribute a niche theoretical study?

Our results tell quantum field theorists that the form they choose to write for an ultraviolet cutoff (which they may use for several purposes) for a field can affect the dynamics of a qubit interacting with that field. They also tell folks designing and working with superconducting qubits that their models may need a little updating if this regime become widely used (and straightforward to access). There is perhaps some applicability for similar situations with ultraviolet cutoffs present in fiber optic cables in photonics experiments. No substantive change in the near future is likely to arise in any of these fields—the region of applicability of these results is small. They require strong coupling between a qubit and

a field and very fast interactions to be relevant at all. There are applications of this regime, though, (the most likely of which to me seems to be the creation of narrow-frequency states in the field, e.g. [53]) so it is possible the results have a little utility.

In addition to these effects of this study, our analysis from the Prologue applies. Contributing to literature which is involved with the large-scale goal of developing quantum technology implicitly supports that goal and the trends in how it is being worked towards. We participated in the usual publishing process, and spoke mostly about the motivation for this study in an uncritical way. The methodology of physics is of course more than how we write and talk about it. Contributing to the study of superconducting devices supports the usage of resources in the field; devices make significant use of metals, which are often mined in seriously dangerous conditions, amidst violent conflict, and have been involved in some of the worst environmental disasters on the planet.[1] Encouraging the development of new technology not only condones the current methods for resource extraction (and minimal methods for resource recycling) but the expansion of such extraction and the other industries which currently produce consumer technology. This includes venture capital economies and tech mega-companies, which are proud to encourage the proliferation of precarious labour in places like Canada and low-wage high-toxicity labour in places like China [132].

We are left to conclude this part not with a nice bow on a problem for which the only relevant scope is physics, isolated from the world. Rather, though the hole we initially carved out in the introduction has been filled, we leave new spaces empty. How can the people who study quantum systems, through the study itself, become more cognizant of their effects on the world? How can we move past the small steps presented in and around this study? How can we move to ensure we contribute more to an equitable world than not?

[1]For instance, recent spills of tailing ponds in British Columbia and Brazil. The Sanmarco spill in Minas Gerais, Brazil displaced over a thousand people and spilled well over 32 million cubic metres of toxic waste into a river, the basin of which is home to 3.2 million people [124]. Adequate cleaning has not been carried out [125]. Coltan mining in the Democratic Republic of the Congo is a significant source of funds for a brutal civil war responsible for at least 5 million deaths. The mineral is used in cell phones. There is little way for manufacturers to be sure that they have not purchased coltan from the DRC [126]. See also [127–131].

Part II

Work cost fluctuations in correlation creation

Chapter 1

Introduction

Studies of quantum thermodynamics are often motivated with an analogy to classical thermodynamics, as discussed in the Prologue. The story goes like this. We introduce classical thermodynamics as something with serious power:

> Thermodynamics is arguably the most general physical theory ever developed, with utlity in systems as disparate as steam engines, computers, and galactic formation. It is a framework built to identify what operations are physically allowable, and, if they are, how much they will cost. It additionally brings together concepts rich in interpretational issues, like entropy, probability, and how our knowledge affects how we can interact with the world.

This story already has issues. Whenever we talk about physics as powerful, we invoke at least two concepts. One is that the technology produced by physics is powerful and, moreover, desirable. In a similar fashion to the criticisms raised in the Prologue of the potential effects of quantum technology, there are also issues with the technology made possible with thermodynamic knowledge. The steam engine may have been a factor in bringing about the Industrial Revolution and a great many improvements to a great many lives, but that also means that it has played a role in the casual use of electric and mechanical power in our lives—in the widespread and frequently catastrophic (and ever more so) use of fossil fuels. When we invoke the narrative that thermodynamics is technologically powerful, we celebrate all of the effects we have assigned to it.

Another concept of power is that theories like thermodynamics are widely applicable to a huge variety of situations, and that this is laudable. Thermodynamics is highly abstracted, and while it is certainly impressive that it applies to (as far as we can tell) all physical systems, it is also the case that valuing abstraction in physical theories means

valuing decontextualization. This is an invaluable methodology in physics. We strip down a system to what we believe are its indispensable parts, which makes mathematical analysis possible. Often this works fantastically well. It's just also true that there are other methodologies which deal in all of the context of objects of study, which acknowledge the context as generally indispensable. To understand physics' place in our world, for instance, we cannot dispense with its relationship to technology and so on. It isn't necessarily a problem to have multiple methodologies which value context in different ways, but it is a problem when the methodologies of physics are seen as somehow fundamentally more powerful. This type of narrative is really widespread—that physicists are connected more deeply to the secrets of the universe because we study abstracted objects like entropy. Certainly physics has specific usages which make it special, but it is not necessarily a more universal way of knowing because it cares so little about details [33].

The analogy of quantum to classical thermodynamics is sometimes made explicit, continuing perhaps as:

> Thermodynamics in the quantum realm presents a new frontier, with rich insights to be had in this wildly different physical theory. Like the industrial revolution brought about by the study of engines, we can expect impactful new technologies to be developed through understanding new phenomena.

Of course, making even an indirect analogy between the advances that may come from quantum thermodynamics and those which are already attributed to classical thermodynamics is a significant inductive jump. It assumes, among other things, that thermodynamics in quantum systems is different enough from classical systems that dramatic insights will be made. It also assumes that the effect of quantum technologies will be somehow comparable to the effect of engines (perhaps something like a 'quantum revolution'). There is more evidence for the former assumption than the latter. The important point is this: we cannot take for granted that the impact of thermodynamics will continue to be as significant as we have made it out to be thus far.

Though we have painted this motivation as problematic, it *is* nevertheless one reason that folks study problems in quantum thermodynamics. There are other reasons, too. For instance, in trying to write down thermodynamic considerations for quantum systems, many classic thermodynamic issues are brought up anew, in the wildly different context of quantum probabilities. We can ask questions like: how can we measure the energy of a system that is in a superposition of two energy eigenstates?

With these motivations in mind, we can give a little context to the field of quantum thermodynamics. It is popular, and growing. It is little difficult to draw out storylines for such a young and active field. There are so many paths of research, different desires, and

varying interpretations of results. This introduction does not aim to be a review of quantum thermodynamics. For this, please see the excellent and thorough reviews [133, 134] as well as chapters of the upcoming book [135], chapters of which include a review of quantum work [136].

A taste of some interesting questions being asked in the field right now: is von Neumann entropy the thermodynamic entropy [137]? Are info-theoretic quantities really thermodynamic ones [138–140]? How can we define work? Does it even make sense as a scalar quantity [141]? What aspects of classical thermodynamics should we try to preserve? Which ones should we let go of [142, 143]?

A very particular problem in this wide range is about correlations and their relationship to work. To begin to ask and answer these kinds of questions, we'll of course have to make clear what we mean by work and correlations in quantum contexts. There has already been much done on these fronts [144–151].

Why ask questions about work and correlations? One motivation comes from the fact that violations of Bell inequalities (i.e., the presence of quantum correlations) are intrinsically and exclusively quantum mechanical. To understand more about these correlations, we might be interested in their relationship, if any, to energy. Another motivation comes from my supervisor, being that he suggested the particular problem for study out of his own interest. Perhaps, also, the relationship of correlations and work could find applications in the study of his other interests, like entanglement harvesting. A third motivation is that of quantum technology. Quantum correlations are useful for a variety of information processing tasks, and we would like to be able to design well for the work it will take to create those correlations, as well as for any energy they will release when broken. Criticisms of this motivation can be found in the Prologue and section 5.4 of Part I; we will elaborate on the specific ability of this study to fulfill this and other motivations in chapter 6.

We are specifically following up on a series of investigations into the unitary production of correlations in quantum systems. In 2012, Jevtic *et al.* investigated the bounds of correlatedness attainable via unitary evolution [146, 147]. Following this, Huber *et al.* developed a unitary protocol to correlate bipartite and mulitpartite systems at minimal average work cost [149]. Follow up investigations have looked at adding a nonunitary step to improve the correlations generated [150] and at how system interactions can be used to do the same [151].

One crucial element of the many and varied studies of work cost in quantum systems is appreciating its fluctuating nature. Classical work also has a distribution, of course, but in quantum systems (and especially low-dimensional ones) we would expect that the fluctuations would be much more readily comparable to the average work cost.

So, we would like to ask specifically about the protocol developed in [149]. Its average

work cost is low, but what about fluctuations in that work cost? We will, in fact, show that the fluctuations are at least of the order of the work cost. This encourages us to actively consider the fluctuations of all quantum systems, and potentially to prioritize protocols with lower fluctuations over an optimal average work cost.

To do this, we will first go into some detail about a couple of leading schemes for quantum work in chapter 2, including which definitions of work fluctuations will be relevant for our study. In chapter 3, we will follow this with discussion of what correlations are, how to measure them, and some extant results, including their minimal work cost of generation. In chapter 4, we review in detail the protocol of Huber *et al.*, and study its correlation creation and details of its work cost in chapter 5. We finish with some conclusions, limitations of the study, and comments on its effects in chapter 6.

Chapter 2

What is work, anyway?

Like many quantities in thermodynamics, writing an accurate definition of work that can be applied to all systems and setups is a slippery task. Even in classical systems, we must be careful about which objects are defined in which role. In quantum systems, there are plentiful new issues which introduce ambiguities, all stemming from the nature of a quantum probability distribution.

There have been a number of attempts to write a quantity with all the desired properties of classical work in quantum systems. There appear to be issues with each definition. The most popular, the two-time measurement scheme introduced by [143, 152], relies on projective measurements in the energy eigenbasis, limiting the ability of this scheme to measure effects from energy eigenbasis coherences. The work operator scheme, from [153], attempts to write work as a usual quantum mechanical operator, but results in a quantity which doesn't obey fluctuation theorems. Current treatments of work in thermal resource theories use quantum mechanical systems as batteries in which one stores the work that is done. This newer set of tools is not analysed deeply in this thesis, but is included in this background section for interest and completeness. For a current and analytical review of the many proposed definitions of quantum work, see [136].

Here, we first review classical work in section 2.1. We then go into some detail in each of the quantum work schemes mentioned above in section 2.2. Finally, we discuss some interpretational and statistical issues with work in section 2.3.

2.1 Classical work as a starting point

There's a lovely simple conception of what work is: energy transfer that isn't heat. We write, for macroscopic systems, that the change in energy ΔU is divided into work W and heat Q as

$$\Delta U = W + Q. \tag{2.1.1}$$

What makes energy transfer heat? One formulation of the second law (for a closed system and a reversible process) is

$$\Delta S = \frac{Q}{T}, \tag{2.1.2}$$

where S is the thermodynamic entropy and T is the temperature of the system. In an irreversible process, the change in entropy will be bounded below by Q/T. We can say that heat transfer is always accompanied by an increase in entropy, and use that as a defining characteristic. Heat is energy transfer associated with an increase in entropy. So, work is energy transfer without any increase in entropy [154].

More practically, there are several ways to write down the work. Say we have a Hamiltonian H controlled by some protocol parameter $\lambda(t)$ and dependent on a phase space parameter $z(t)$. Then the work done along the path $\vec{z}(t)$ in phase space is, as in [155],

$$W(\vec{z}(t)) = \int \mathrm{d}t \frac{\mathrm{d}\lambda}{\mathrm{d}t} \frac{\partial H(\lambda(t), \vec{z}(t))}{\partial \lambda}. \tag{2.1.3}$$

Here, the change in the system is done on (or through) the Hamiltonian. We can say also that heat is manifested through change not in the Hamiltonian but in the phase space distribution (which, one notices, also changes the entropy).

With a phase space distribution $p(\vec{z}(t))$, we can write a probability distribution for the work as

$$P(W) = \int \mathrm{d}\vec{z}\, p(\vec{z}(t))\, \delta(W - W(\vec{z}(t))). \tag{2.1.4}$$

Work for each path through phase space (i.e., for each particle in an ensemble) is well defined. The probability distribution merely incorporates the fact that there is a distribution of particles in phase space.

Defining work for each microscopic particle does pose a small issue. The laws of thermodynamics were written for macroscopic systems, those with many many particles. Their scope does not include individual particles. More accurately, quantities like the entropy and the free energy are necessarily statistical; they don't make sense to define for individual particles. Violations of strict thermodynamic laws are expected, sometimes. A

single hot particle might work its way from a cold object to a hot object, increasing the temperature difference. A few water molecules might hold tight to each other for half a millisecond. These occurences are statistically guaranteed with such large numbers of atoms and molecules. To account for this, thermodynamic laws are instead written for average values. For instance, we write

$$\Delta S \geq \frac{\langle Q \rangle}{T}, \tag{2.1.5}$$

or

$$\langle W \rangle \geq \Delta F \tag{2.1.6}$$

for the second law, where $F = U - TS$ is the free energy.

These forms of the second law don't tell us much about the scale of the deviations from average. The Jarzynski equality, which relates the work cost of non-equilibrium processes to the free energy difference of equilibrium processes,

$$\langle \mathrm{e}^{-W/T} \rangle = \mathrm{e}^{-\Delta F/T}, \tag{2.1.7}$$

tells us that in classical systems, deviations from the average work cost are in fact exponentially suppressed [155]. We'll demonstrate this briefly, because it's quite neat. The probability that the work cost of an operation is ϵ less than the change in free energy of the corresponding equilibrium process ("violating" the strict second law) is given by

$$P(W < \Delta F - \epsilon) = \int_{-\infty}^{\Delta F - \epsilon} \mathrm{d}W \; P(W). \tag{2.1.8}$$

Multiply the integrand by $\mathrm{e}^{(\Delta F - \epsilon - W)/T}$, which is larger than one on the interval of integration, since $W < \Delta F - \epsilon$ there. Then

$$\begin{aligned} P(W < \Delta F - \epsilon) &\leq \int_{-\infty}^{\Delta F - \epsilon} \mathrm{d}W \; P(W) \mathrm{e}^{(\Delta F - \epsilon - W)/T} \\ &= \mathrm{e}^{(\Delta F - \epsilon)/T} \int_{-\infty}^{\Delta F - \epsilon} \mathrm{d}W \; P(W) \mathrm{e}^{-W/T} \\ &\leq \mathrm{e}^{(\Delta F - \epsilon)/T} \underbrace{\int_{-\infty}^{\infty} \mathrm{d}W \; P(W) \mathrm{e}^{-W/T}}_{\langle \mathrm{e}^{-W/T} \rangle} \\ &= \mathrm{e}^{-\epsilon/T}. \end{aligned} \tag{2.1.9}$$

The probability of the nonequilibrium work cost being less than the free energy difference of the corresponding equilibrium process is exponentially suppressed [156]. This is a comforting result to many. We can rest assured that even in wild nonequilibrium processes, we're very unlikely to be able to do a process for free.

The Jarzynski equality has become something of a monolith of thermodynamics. The pursuit of a quantum Jarzynski equality is a defining feature of the search for a viable quantum work. For some, it is a crucial property of any quantity called work [143, 157]. It will thus figure strongly in the discussion of quantum work below.

To recap: work in classical systems is a transfer of energy unaccompanied by an increase in entropy. It is a statistical quantity, and obeys statistical second laws like (2.1.7). It has a definite value for each particle and process. It is an important motivator of what work should look like in quantum systems.

2.2 Several definitions of quantum work

Since we study quantum systems, we'd like to have a concept of work in them. But the jury's still out on what quantum work is. It's possible, in fact, that we'll ultimately need several definitions to fulfill different purposes [136, 157]. We'll start here with some very basic groundwork, identifying one of the major problems with trying to write down a quantum work, before explicating a few of the most popular attempts. For a thorough review of many recent attempts, and more excellent analysis of the problems with quantum work, see [136].

Let's start where we started with classical work. A system has energy as defined by its Hamiltonian, described by the quantum probability distribution (quantum state) over the energy eigenbasis. Over the course of a process, both the distribution and the eigenbasis may change. Consistent with above, we can call changes to the distribution heat and changes to the eigenbasis (i.e., the Hamiltonian) work. This division is justified on a similar basis: changes to the Hamiltonian do not produce von Neumann entropy, while changes to the state in general do.[1]

Now, it's not enough to have said that changes to the Hamiltonian constitute the work. How might one write down a probability distribution for the work? This is a tricky question. There are several attempts at answers, each with its own pros and cons. It's important to remember that, though we can draw similarities between each attempt at defining quantum

[1] A controversy arises already. While many take the von Neumann entropy to be the thermodynamic entropy, there is some debate over whether it truly satisfies the necessary criteria. For a view in support of the von Neumann entropy being the thermodynamic entropy, see [137]; for the opposite, see [158].

work and particular definitions of classical work, the attempts at quantum work really are different—unlike the classical definitions, which are all fundamentally the same.

Here, we briefly review just three notions of quantum work. First, the very popular two-time measurement scheme, in section 2.2.1; then the unprojected scheme, also called the work operator, in section 2.2.2; and finally quantum battery schemes in section 2.2.4. The first two schemes will be employed later, in our study of work fluctuations in correlation creation, in chapter 5. The third scheme is included for a bit more completeness in background for the interested reader.

2.2.1 Two-time measurement scheme

The two-time measurement scheme has been widely used to do quantum thermodynamics since its introduction [133, 143, 152]. The idea is to measure classical distributions in the system's energy spectrum before and after the application of a protocol. Using the initial energy distribution and a distribution of final energies conditional on the initial energy, a total work probability distribution is constructed. The motivation to have definite values of energy appears very concretely classical; there is no room in this protocol to have superpositions or coherences in the energy eigenbasis. As such, there are some issues with its utility in such cases, to be discussed in more detail below.

In detail, the two-time energy measurement quantum work scheme is this: first, projectively measure the system in the energy eigenbasis $\{|n\rangle\}$, resulting in an ensemble of pure, single-energy states, each with eigenenergy E_n. Subsequently apply the protocol of interest (noting that effects of the protocol on coherences will not be observed). Projectively measure again, resulting in states with eigenenergy E_m.

The initial probability of finding the system in state $|n\rangle$ is $P(E_n)$, given by $\mathrm{e}^{-\beta E_n}/Z$ in the case of the system initially being in a Gibbs state (where we've introduced the inverse temperature β and the partition function $Z = \mathrm{Tr}[\mathrm{e}^{-\beta \hat{H}}]$). The probability of transitioning from state $|n\rangle$ to state $|m\rangle$ by a unitary protocol $\hat{U}$ is $|\langle m|\hat{U}|n\rangle|^2$. The probability distribution of the work, given by $E_m - E_n$, is then

$$\begin{aligned} P(W) &= \sum_{m,n} P(E_n)\, P(E_m|E_n)\, \delta\big(W - (E_m - E_n)\big) \\ &= \sum_{m,n} P(E_n) \left|\langle m|\hat{U}|n\rangle\right|^2 \delta\big(W - (E_m - E_n)\big). \end{aligned} \tag{2.2.1}$$

A major benefit of this scheme is that the random variable for work obeys a quantum Jarzynski equality [143]. In the case of states diagonal in the energy eigenbasis (i.e. when

$[\hat{H}, \hat{\rho}] = 0$), the statistics of the probability distribution reproduce properties of classical work. Conceptually, it's an attractive scheme that makes quantum work somewhat straightforward.

Measure of fluctuations

To measure fluctuations in this conceptualization of quantum work, we can calculate the standard deviation of the probability distribution:

$$\sigma_W = \sqrt{\int \mathrm{d}W \, \big(W - \langle W \rangle\big)^2 \, P(W)}. \tag{2.2.2}$$

We call this quantity the two-time measurement work fluctuations.

Issues

When $[\hat{H}, \hat{\rho}] \neq 0$, an important issue arises. The average work, which may be calculated in this scheme as

$$\langle W \rangle = \int \mathrm{d}W \; W \, P(W), \tag{2.2.3}$$

is no longer equal to the difference in energy expectation values of the final and initial states,

$$\langle W \rangle \neq \mathrm{Tr}[\hat{U}^\dagger \hat{H} \hat{U} \hat{\rho}] - \mathrm{Tr}[\hat{H}\hat{\rho}]. \tag{2.2.4}$$

Having the average work equal to the difference in average energies (when there is no heat exchange) definitely sounds like a reasonable property. The two-time scheme also has this problem for the variance—when $[\hat{H}, \hat{\rho}] \neq 0$, the fluctuations are no longer equal to those one might calculate for the "operator" $\hat{U}^\dagger \hat{H} \hat{U} - \hat{H}$ [153, 159]. For details, see appendix A.

Another issue is that this scheme requires one to use projective measurements. These measurements are arguably unrealistic. Ideal projective measurements cost an infinite amount of energy [160]. Projective measurements are unphysical in quantum field theories (hence why models like the UDW of part I are used in quantum field theory). Even beyond these fundamental issues with the use of projective measurements, their use here causes real problems in the protocols that one wishes to use. There is no way to both measure the work of a protocol which, say, makes use of energy eigenbasis coherences and to observe the desired effect of the protocol at the same time. A practical solution to this is to run the protocol under the work measurement scheme to build up work statistics, and then to

run it without the work measurement scheme to observe its other effects. For some, this is nonetheless unsatisfying.

Other schemes to use measurements other than those that project in the energy eigenbasis are summarized in [136].

2.2.2 Unprojected scheme

The unprojected scheme for quantum work has been discussed in various forms. Originally, it was introduced as the work operator, $\Delta\hat{H} = \hat{U}^\dagger\hat{H}\hat{U} - \hat{H}$ [153]. We conceptualize this scheme as the difference of two correlated random variables—the final and initial energies—rather than a random variable which is the difference of two quantities. Though this scheme is unpopular in some circles, it is again being utilized for targeted purposes in e.g. [157, 161].

The statistics of this scheme are constructed just as one would with a quantum mechanical operator. The entire distribution of work is encoded in the operator and quantum state. The average is exactly

$$\langle W\rangle = \mathrm{Tr}\big[(\hat{U}^\dagger\hat{H}\hat{U} - \hat{H})\hat{\rho}\big]. \tag{2.2.5}$$

This fits particularly well with one way of dividing change in internal energy into change in work and heat. In this conception, the total change in internal energy is

$$\langle\Delta U\rangle = \mathrm{Tr}[\hat{H}_f\hat{\rho}_f - \hat{H}_i\hat{\rho}_i], \tag{2.2.6}$$

i.e. the difference in the initial and final energies as measured by the initial and final Hamiltonians. Both the state and the Hamiltonian can change, in general. As in [162], we can divide contributions to the change in internal energy along these lines, as

$$\langle\Delta U\rangle = \int_0^t \mathrm{d}t'\,\mathrm{Tr}[\hat{H}(t')\dot{\hat{\rho}}(t')] + \int_0^t \mathrm{d}t'\,\mathrm{Tr}[\dot{\hat{H}}(t')\hat{\rho}(t')]. \tag{2.2.7}$$

We can associate the latter term with change in entropy (since the state is changing) and thus with a notion of heat. The former term is associated with isoentropic change and thus work. When a process is adiabatic (i.e. when no heat is exchanged), the work is equal to the change in internal energy,

$$\langle\Delta U\rangle = \int_0^t \mathrm{d}t'\,\mathrm{Tr}[\dot{\hat{H}}(t')\hat{\rho}(t')]. \tag{2.2.8}$$

Further, when the change in the Hamiltonian can be described by the application of a unitary, we have that the work can be represented as in (2.2.5), so that

$$\langle\Delta U\rangle = \mathrm{Tr}\big[(\hat{U}^\dagger\hat{H}\hat{U} - \hat{H})\hat{\rho}\big]. \tag{2.2.9}$$

A particular motivation to consider this definition of work is that it very explicitly allows for coherent processes to contribute to the measure of work. It also avoids (at least mathematically, if not practically) difficulties with projective measurements discussed above in the two-time measurement scheme. Finally, the average work always coincides with the difference in average energies of the final and initial states, unlike the two-time measurement scheme.

Measure of fluctuations

We can measure fluctuations of unprojected work by looking at the square root of the variance of the work operator:

$$\Sigma_W = \sqrt{\mathrm{Tr}[\Delta\hat{H}^2\hat{\rho}] - \mathrm{Tr}[\Delta\hat{H}\hat{\rho}]^2}. \tag{2.2.10}$$

We can also write this in terms of the energy variance of the initial and final states, $\hat{\rho}$ and $\hat{\rho}' = \hat{U}^\dagger\hat{\rho}\hat{U}$, and their covariance:

$$\Sigma_W = \sqrt{\sigma^2_{E_i} + \sigma^2_{E_f} - 2\sigma_{E_iE_f}}, \tag{2.2.11}$$

where

$$\sigma^2_{E_i} = \mathrm{Tr}[\hat{H}^2\hat{\rho}] - \mathrm{Tr}[\hat{H}\hat{\rho}]^2, \tag{2.2.12}$$

$$\sigma^2_{E_f} = \mathrm{Tr}[\hat{H}^2\hat{\rho}'] - \mathrm{Tr}[\hat{H}\hat{\rho}']^2, \tag{2.2.13}$$

and the covariance of the energies is given by the convex correlator

$$\begin{aligned}\sigma_{E_iE_f} &= \langle\hat{H}(\hat{U}^\dagger\hat{H}\hat{U})\rangle - \langle\hat{H}\rangle\langle\hat{U}^\dagger\hat{H}\hat{U}\rangle \\ &= \mathrm{Tr}[\hat{H}\hat{U}^\dagger\hat{H}\hat{U}\hat{\rho}] - \mathrm{Tr}[\hat{H}\hat{\rho}]\mathrm{Tr}[\hat{H}\hat{\rho}'].\end{aligned} \tag{2.2.14}$$

Issues

The major issue with this scheme is that the unprojected work cannot be used to write a Jarzynski equality. The importance of this feature has been hotly debated [142, 143, 153]. A thorough discussion of the competing issues and features of both this unprojected scheme and the two-time scheme can be found in [157].

Generally, practical measurement procedures for this work are not discussed. It is used as a theoretical conception. Other work schemes explicitly consider measurement techniques, such as Gaussian measurement [163, 164], POVM dependent on the initial state [165], and collective measurement schemes [157].

2.2.3 When $[\hat{H}, \hat{\rho}] = 0$: fluctuations used in this thesis

As mentioned in section 2.2.1, the average work of the two-time measurement scheme corresponds to the average work of the unprojected scheme when $\hat{\rho}$ is diagonal in the energy eigenbasis (when $[\hat{H}, \hat{\rho}] = 0$). The fluctuations of each scheme also coincide in this case.

In this thesis, we will study the fluctuations in work cost of a specific unitary protocol acting on global thermal states, which do indeed commute with the global Hamiltonian. It thus does not matter whether we take (2.2.2) or (2.2.10) as our quantity measuring the fluctuations.

For completeness, we show their equivalence in appendix A.

2.2.4 Quantum battery schemes

In the growing field of quantum resource theories, the resource theory of thermal operations deals with making quantum thermodynamics very rigorous and genuinely quantum; for an overview, see [166]. One main issue that these efforts are trying to address is that work in quantum systems has been conceptualized using classical batteries and classical probability distributions. A quantum battery scheme does not trouble itself with trying to write down a probability distribution for the work, but instead aims to include quantum work as a part of relations like a genuinely quantum second law and Jarzynski equality. Moreover, it achieves those things!

The setup, briefly, is this. We have a system of interest, a bath, and a battery—all quantum systems with their own Hamiltonians and Hilbert spaces [141]. We restrict ourselves to unitary operations on the total system, and require that they commute with the total Hamiltonian (because of conservation of energy). Additionally, it is required that the unitary commutes with operations that translate the state of the battery (ensuring that it cannot be used as a source of entropy). Then, the change in energy of the battery is the work. But, we don't necessarily care about the specific value of this work, or its distribution. We allow the battery to have coherences in the energy eigenbasis, and don't trouble ourselves really about what that means for a discrete value of work. This approach really prioritizes a conception of work as something which is transferred between quantum systems, in quantum ways.

The results of this setup include writing the second law as an equality (without projective measurements or classical probability distributions), writing a condition on an operation on the system to preserve thermality, and writing a quantum Jarzynski equality [141].

2.3 What's average about average work? (and other interpretational issues)

There are a few points of contention in what exactly one aims to measure with a measure of work. Conceptually, what does one means when one asks for an average value of work? And how is this tied to interpretational issues in quantum mechanics?

In classical statistical mechanics, probability distributions describe statistical ensembles—generally many particles which, as a whole, follow a pattern of behaviour like a Maxwell-Boltzmann distribution. The path of any individual particle is uncertain in the sense that we don't have detailed knowledge about its path. Hence, we might use the Maxwell-Boltzmann distribution as a probability distribution, from which we could draw some statistical knowledge about the work done on any individual particle. We can say that, in classical systems, the probability distributions are completely *epistemic.* They represent a lack of knowledge. In this case, we aren't completely acquainted with each particle's position. We still know that they have a definite position, and a definite work value, and so on.

In quantum mechanics, there is contention as to what a probability distribution really means. Some hold that the quantum state is also epistemic. Then, quantum objects would, in fact, have definite properties. Superposition would be an aspect of probability, representative of some kind of deficit in our knowledge, rather than a "real" physical phenomenon. In this view, one may be motivated to consider transitions between eigenstates as a physically accurate and encompassing view of what really happens during a protocol on a quantum system. One could think that having an epistemic view of the quantum state motivates the two-time measurement scheme for quantum work.

A related interpretation of quantum mechanics is the statistical one, where quantum states represent statistical ensembles much like classical ones. This interpretation is the exact analogue of the classical scenario which motivates the two-time measurement scheme. In this case, the average work is the work averaged over many runs or members of the ensemble. If we require that the work done in an individual run of the protocol is a difference of final and initial eigenstate (or if this is what is prescribed by our interpretation), then we have exactly the two-time measurement scheme. Even in advance of requiring a statistical interpretation of quantum mechanics, the two-time scheme makes a quantum state into an ensemble using projective measurements and many copies of a state to build a classical probability distribution.

What if the quantum state is neither a statistical ensemble nor an epistemic object? What if the state is *ontic*? Then any individual quantum object could in some sense really

be in superposition. One could take this interpretation as motivation to consider that there is some uncertainty or distribution of work even in single runs of protocols on individual quantum objects. We would not, then, take as a given that work must be the difference of final and initial energy eigenstates. An average value of work would be an average over a single quantum state assigned to a single quantum object; it would consider superpositions in the energy eigenbasis to matter even in single runs of a protocol. This, of course, would support the unprojected work scheme.

The difference in schemes and associated interpretations is emphasized by when they are equivalent. If the state commutes with the Hamiltonian, $[\hat{H}, \hat{\rho}] = 0$, then the moments of the two-time measurement scheme and the unprojected work scheme are equivalent (see Appendix A). It is how each scheme values coherences in the energy eigenbasis that truly makes a difference. One might say that the two-time measurement scheme is the one which adheres more closely to classical ideals, while the unprojected scheme appears to incorporate some aspects of quantum probability.

The quantum battery schemes used in thermal resource theories appear very careful to not play into interpretational issues. They take work to be a transfer of energy between a system of interest and a battery, and allow the battery to be a quantum object. They aren't particularly interested in the value of the work, but in the behaviour of the systems on the whole, and being able to describe what operations are allowed. This approach is more operational and less restrictive than either the two-time measurement or unprojected approaches.

Chapter 3

Correlations in quantum thermodynamics

In thermodynamics, we're interested in properties of systems which are useful for tasks. Having knowledge about a system is certainly useful; the more knowledge we have about a probability distribution, the better a task we can make to extract something useful like work from it. Correlations between probability distributions over different systems have been shown to be a useful tool in tasks like quantum teleportation and various quantum algorithms [167]. We are thus interested in the thermodynamic nature of correlations. How much work does it cost to generate them? How much work can we extract from them? Much has been done on these questions in quantum systems [144–146, 148–151, 168].

These questions dig perhaps at something deeper than how much work it takes to enact certain protocols. We already have in classical thermodynamics that the entropy is important. The Gibbs entropy, though associated with classical probability distributions, is however not immediately associated with correlations between systems. The von Neumann entropy, on the other hand, is a deeply information-theoretic quantity that can be employed to measure correlations between systems. Further, it appears to show up in important relations in quantum thermodynamics (though there is contention that it is always the correct entropy to use [169]). This is one way to think about the apparently stronger association between correlations and thermodynamics in the quantum literature as opposed to the classical.

It's also true that quantum correlations are different from classical correlations. Difference makes them interesting; many are interested specifically in the fact that quantum correlations are stronger than classical. They can be used to perform different and often more powerful tasks.

In this chapter, we will review in a little detail what correlations are and how we measure them in quantum systems in section 3.1. We will also review some specific results about the relationship of work and correlations in section 3.2.

3.1 What are correlations, anyway?

Correlation between probability distributions indicates some level of coincidence between the distributions. The more highly correlated, the more like each other they are. When we speak of correlations in the context of a physical theory, we mean something more specific than this. Classical (or quantum) correlations are those that can arise between systems under the constraints of that physical theory. The wild thing about quantum correlations is not just that they can be very strong, but that their strength is not permitted by the physical interactions possible in classical mechanics. The canonical example of this is Bell's inequality, where in a specific physical setup, two variables are only able to be correlated to a certain degree under the laws of classical mechanics. When quantum mechanics is allowed, the correlations increase significantly, and the systems are called entangled [170, 171].

In practice, it's not trivial to measure how correlated two systems are, especially when looking for quantum correlations. There are many measures one can use, and in the case of entanglement, the ordering of a set of states from most to least entangled can change depending on which measure one uses [172, 173]. Here, we will try to say something practical about how one can try to measure total, classical, and quantum correlations in bipartite quantum systems.

Total correlations

The mutual information I is used to measure the total correlations between two quantum systems:

$$I = S[\hat{\rho}_{\mathrm{A}}] + S[\hat{\rho}_{\mathrm{B}}] - S[\hat{\rho}], \tag{3.1.1}$$

where $S[\hat{\rho}] = -\mathrm{Tr}[\hat{\rho}\log\hat{\rho}]$ is the von Neumann entropy, $\hat{\rho}$ is the quantum state over the whole system, and $\hat{\rho}_{\mathrm{A(B)}} = \mathrm{Tr}_{\mathrm{B(A)}}\hat{\rho}$ are the partial states. It is a measure of how much information one can learn about system B by uncovering a bit of information about system A.

In the later parts of this thesis, we will focus exclusively on correlations as measured by the mutual information.

Quantum correlations

The most famous of quantum correlations is of course entanglement. This somewhat mysticized property of systems has been attributed as the reason for quantum advantages small and large. Entanglement can be used for a variety of powerful information processing tasks like quantum teleportation [167] and is generally thought to be a signature of behaviour that is not simulatable in classical systems. It is neither easy to philosophize about nor to quantify. There are many scalar measures of entanglement, none of which give the same order (from most to least entangled) to any given set of states [174]. One such entanglement measure is the entanglement entropy, which measures how entangled a pure bipartite state is by looking at how mixed the state on the subsystem is:

$$S_{\mathrm{EE}}[\hat{\rho}] = S[\hat{\rho}_{\mathrm{A}}]. \tag{3.1.2}$$

Another sometimes measure of quantum correlation is known as quantum discord [175, 176]. Its significance is somewhat contentious. It is thought by some to be a useful quantum resource [177, 178], but its necessity in creating those quantum advantages is disputed [179, 180]. It has been identified as a signature of more-body entanglement in certain systems (entanglement between more parties than are a part of the discord) [181, 182]. Its role as a measure of correlation is in fact not trivial, as it can under certain circumstances be increased by operations acting on only one party, but it nonetheless appears to measure something which can, in some cases, be used for computational tasks [183]. For more on how to compute discord, see [176].

Classical correlations

In classical systems, the mutual information may be used without hesitation to measure correlations. In quantum systems, the same is true, but it is no longer immediately clear which of the correlations can be attributed to dynamics which are classical or those which are uniquely quantum. One attempt at identifying the correlations which are specifically classical in quantum systems comes from [184]. There, total correlations are divided into two parts. Entanglement is measured with the relative entropy of entanglement, which measures how far a state is from being separable,

$$E(\hat{\rho}) = \min_{\hat{\sigma} \in D} S[\hat{\rho}||\hat{\sigma}], \tag{3.1.3}$$

where D is the set of all separable states and $S[\hat{\rho}||\hat{\sigma}] = -S[\hat{\rho}] - \mathrm{Tr}[\hat{\rho} \log \hat{\sigma}]$ is the relative entropy. Classical correlations are measured using a quantity which attempts to identify

only those correlations still present after a measurement is performed on a subsystem. This somewhat involved measure is as follows:

$$C_{\mathrm{B}}(\hat{\rho}) = \max_{\hat{B}_i^\dagger \hat{B}_i} S[\hat{\rho}_{\mathrm{A}}] - \sum_i p_i S[\hat{\rho}_{\mathrm{A}}^i], \tag{3.1.4}$$

with $\hat{B}_i^\dagger \hat{B}_i$ a POVM (positive operator-valued measurement) on the subsystem B, $\hat{\rho}_{\mathrm{A}} = \mathrm{Tr}_{\mathrm{B}}[\hat{B}_i \hat{\rho} \hat{B}_i^\dagger]/\mathrm{Tr}[\hat{B}_i \hat{\rho} \hat{B}_i^\dagger]$, and $\sum_i \hat{B}_i \hat{\rho}_{\mathrm{A}} \hat{B}_i^\dagger = \sum_i p_i \hat{\rho}_{\mathrm{A}}^i$. A similar definition exists for $C_{\mathrm{A}}(\hat{\rho})$, with equality between the two when $S[\hat{\rho}_{\mathrm{A}}] = S[\hat{\rho}_{\mathrm{B}}]$.

When there is no discord, the sum of these measures of entanglement and classical correlations are equal to the mutual information,

$$I(\hat{\rho}) = E(\hat{\rho}) + C_{\mathrm{B}}(\hat{\rho}). \tag{3.1.5}$$

In at least some situations where there is discord, the mutual information is larger than the sum of these measures: $I > E + C_{\mathrm{B}}$.

3.2 Work and correlations

Some fundamental questions can be asked about the relationship between work and correlations. Is there a lower bound on the work cost needed to develop a certain amount of correlations? What about work that can be extracted from them?

In non-interacting systems, these questions have been thoroughly addressed for average work. In [159], the extractable work of states which are locally thermal is investigated. States which are entangled are shown to attain the maximum possible value for extractable work, while classically correlated and separable states are fundamentally limited from doing so. The setup of this study ensures that there are only two possible sources of work: the correlations between systems as well as advantages from activation of a collection of passive states. Passive states are ones from which no work can be extracted; a thermal state is an example. When one has multiple copies of a thermal state, however, the eigenvalues may be swapped between systems to potentially cleverly extract some energy. This is activation. The difference in energy extraction between the entangled, classically correlated, and separable states clearly indicates that entanglement stores work.

The work needed to generate correlations in non-interacting systems using a specific protocol was investigated in [149]. We will delve much more deeply into the content of this paper in the next two chapters—it suffices for now to say that a unitary protocol to generate correlations cannot operate on the absolute minimum possible work cost. That

requires a non-unitary cooling step, as explained in [150]. It is in this work that a minimum bound on the work cost of generating correlations is written,

$$I \leq \beta W, \tag{3.2.1}$$

where β is the inverse temperature of the initial thermal state and W is the average work cost of the operation.

This relation depends critically on the correlations being generated in a non-interacting system, so that the initial thermal state is separable. If this is not the case, it is possible to generate a value I of mutual information at average work cost less than I/β [151].

A final comment on the subject: as with all thermodynamic relations, drawing fundamental conclusions is perhaps not as satisfying as we'd like it to be, since the work cost is always dependent on the Hamiltonian. There are many quantum systems with degenerate Hamiltonians. In these cases, there is no minimum work cost to generate correlations. Additionally, when the Hamiltonian has interaction terms, these facts can again be uprooted. The relationship is not quite so simple as the pretty (3.2.1) might lead us to believe.

Chapter 4

A unitary protocol to create correlations

If we are interested in the relationship of correlations and work cost, then we must have a protocol to develop correlations. There are many ways to do so—plenty of unitaries are able to entangle two parties. In [149], a unitary protocol was introduced which can maximally correlate two parties of the same dimension. In this chapter, we will review this protocol, including its setup, general form for d-dimensional subsystems, and specific form for two qubits.

4.1 Thermal and Gibbs states

First, we briefly define thermal and Gibbs states. The Gibbs distribution is

$$\hat{\tau}(\beta) = \frac{\mathrm{e}^{-\beta\hat{H}}}{\mathrm{Tr}[\mathrm{e}^{-\beta\hat{H}}]}, \tag{4.1.1}$$

for inverse temperature β and Hamiltonian $\hat{H}$. When a system reaches this distribution by a thermalization process (i.e. waiting for the system to equilibrate with a bath of inverse temperature β), we call this a thermal state. If the state has been reached by some other process, we call it a Gibbs state. When $\hat{H}$ is the global Hamiltonian, we call the state global; when $\hat{H}$ is local, we call it local. More specifically, we denote the local Gibbs state on subsystem A by

$$\hat{\tau}_{\mathrm{A}}(\beta') = \frac{\mathrm{e}^{-\beta\hat{H}_{\mathrm{A}}}}{\mathrm{Tr}[\mathrm{e}^{-\beta\hat{H}_{\mathrm{A}}}]}. \tag{4.1.2}$$

We need these somewhat nitpicky definitions to speak accurately about the function of this protocol, which is able to achieve maximal generation of correlations. Speaking generally, and assuming that a bipartite non-interacting system begins in a global thermal state, then any protocol which will create maximal correlations for a given amount of work input will produce local Gibbs states. That is, the protocol will take

$$\hat{\rho} = \hat{\tau}(\beta) \longrightarrow \hat{\rho}' \tag{4.1.3}$$

such that

$$\mathrm{Tr}_{\mathrm{A}}[\hat{\rho}'] = \hat{\tau}_{\mathrm{B}}(\beta') \qquad \mathrm{Tr}_{\mathrm{B}}[\hat{\rho}'] = \hat{\tau}_{\mathrm{A}}(\beta'). \tag{4.1.4}$$

Why does a maximal correlation-generating unitary protocol need to do this? We aim to maximize the mutual information. For a bipartite quantum system $\hat{\rho}$ with partial subsystems' density matrices written as $\hat{\rho}_{\mathrm{A}} = \mathrm{Tr}_{\mathrm{B}}(\hat{\rho})$, $\hat{\rho}_{\mathrm{B}} = \mathrm{Tr}_{\mathrm{A}}(\hat{\rho})$, the mutual information is given by

$$I(\hat{\rho}) = S[\hat{\rho}_{\mathrm{A}}] + S[\hat{\rho}_{\mathrm{B}}] - S[\hat{\rho}], \tag{4.1.5}$$

where $S[\hat{\rho}] = -\mathrm{Tr}[\hat{\rho}\log\hat{\rho}]$ is the von Neumann entropy. Under a unitary protocol, $S[\hat{\rho}]$ will not change. Thus, to maximize creation of mutual information, we must maximize $S[\hat{\rho}_{\mathrm{A}}]$ and $S[\hat{\rho}_{\mathrm{B}}]$—which the local Gibbs state does.

4.2 A family of correlating unitaries

Huber et al. prove (in Appendix A1 of [149]; reviewed here in Appendix B) the existence of a unitary which transforms a d^2-dimensional bipartite system in a global thermal state to a state which is locally Gibbs. The system is non-interacting, meaning that the global thermal state will be a product state, i.e., initially there are no correlations. In the body of their paper, they investigate the particular unitary which produces infinite temperature local Gibbs states—that is, which produces maximally correlated global states. Here, we will first introduce the broad class of unitaries which perform this global to local Gibbs state function. We will call this family of unitaries $\hat{U}_{\mathrm{corr}}$. Then, we will particularize to a two-qubit system, and write out the family of unitaries explicitly, re-stating some results of [149] from a different mathematical perspective.

To see what the family of correlating unitaries $\hat{U}_{\mathrm{corr}}$ is, we need to make use of gener-

alized Bell states, which we now introduce. Using the 'clock' operators $\hat{X}$ and $\hat{Z}$,

$$\hat{X} = \sum_{n=0}^{d-1} |(n+1) \bmod d\rangle \langle n| , \tag{4.2.1}$$

$$\hat{Z} = \sum_{n=0}^{d-1} \mathrm{e}^{2n\pi \mathrm{i}/d} |n\rangle \langle n| , \tag{4.2.2}$$

we can write the generalized Bell states as

$$|\phi_{m,n}\rangle = \hat{Z}^m \otimes \hat{X}^n |\phi\rangle , \tag{4.2.3}$$

where $|\phi\rangle = d^{-1/2} \sum_{n=0}^{d-1} |nn\rangle$ and d is the dimension of each subsystem (so that the dimension of the total system is d^2). We can write these states alternatively as

$$|\phi_{m,n}\rangle = \sum_{k=0}^{d-1} \mathrm{e}^{2km\pi \mathrm{i}/d} |k\rangle \otimes |k+n\rangle , \tag{4.2.4}$$

which can be seen to be Bell states by noting that the label n gives the difference between the state of the first and second system and the label m gives the spacing of the phases on the $|k\rangle \otimes |k+n\rangle$.

Now, these unitaries $\hat{U}_{\mathrm{corr}}$ which transform global thermal states to local Gibbs states are those which perform rotations within the subspaces

$$S_i = \mathrm{span} \{ |\phi_{0,i}\rangle , |\phi_{1,i}\rangle , \ldots , |\phi_{d-1,i}\rangle \} . \tag{4.2.5}$$

Again, a review of this proof from [149] may be found in Appendix B. The bases of these subspaces are those Bell states for which the difference between the label of the energy eigenstates of the first and second qubit is constant and equal to i, e.g. for two qubits, we have the zero difference subspace S_0 and the unit difference subspace S_1

$$S_0 = \mathrm{span} \{ |00\rangle + |11\rangle , |00\rangle - |11\rangle \} , \tag{4.2.6}$$

$$S_1 = \mathrm{span} \{ |01\rangle + |10\rangle , |01\rangle - |10\rangle \} . \tag{4.2.7}$$

4.2.1 An explicit form for two qubits

We now particularize and write out the unitary explicitly for a system of two qubits. The family of correlating unitaries $\hat{U}_{\mathrm{corr}}$ can be represented as a tensor product of two rotations

$\hat{R}_0$ and $\hat{R}_1$ in the bases (4.2.6) and (4.2.7) respectively:

$$\begin{aligned}\hat{U}_{\text{corr}} &= \hat{R}_0 \otimes \hat{R}_1 \\ &= \begin{bmatrix} \cos\theta & -\mathrm{e}^{-\mathrm{i}\delta}\sin\theta \\ \mathrm{e}^{\mathrm{i}\delta}\sin\theta & \cos\theta \end{bmatrix} \otimes \begin{bmatrix} \cos\phi & -\mathrm{e}^{-\mathrm{i}\gamma}\sin\phi \\ \mathrm{e}^{\mathrm{i}\gamma}\sin\phi & \cos\phi \end{bmatrix},\end{aligned} \tag{4.2.8}$$

where θ, δ, γ, and ϕ are real parameters that will be investigated in detail below. In the global energy eigenbasis $\{\,|00\rangle, |01\rangle, |10\rangle, |11\rangle\,\}$, $\hat{U}_{\text{corr}}$ takes the form

$$\hat{U}_{\text{corr}} = \begin{bmatrix} \cos\theta + \mathrm{i}\sin\delta\sin\theta & 0 & 0 & \cos\delta\sin\theta \\ 0 & \cos\phi + \mathrm{i}\sin\gamma\sin\phi & \cos\gamma\sin\phi & 0 \\ 0 & -\cos\gamma\sin\phi & \cos\phi - \mathrm{i}\sin\gamma\sin\phi & 0 \\ -\cos\delta\sin\theta & 0 & 0 & \cos\theta - \mathrm{i}\sin\delta\sin\theta \end{bmatrix}. \tag{4.2.9}$$

We explained above that the protocol for correlation creation acts on thermal states. For two identical qubits, the populations of states $|01\rangle$ and $|10\rangle$ in a thermal state are equal. This means that a rotation in the subspace S_1—controlled by the parameters ϕ and γ—will have no net effect on the state. For the rest of this thesis, we are thus able to neglect ϕ and γ completely, as they do not figure at all into properties of process.

The study of this unitary protocol in [149] focuses on the average work cost of implementing it—here, with the explicit form of the unitary rather than only its action on the diagonals in the energy eigenbasis, we can compute the relative magnitude of the work fluctuations as compared to the average work cost.

Chapter 5

Work cost fluctuations in correlation creation in two qubits

In the context of the difficulty of defining work in quantum systems and the importance of the relationship of work to correlations, discussed in chapters 2 and 3, we would like to investigate the work cost of creating correlations. Specifically, the protocol developed in [149] and reviewed in chapter 4 is designed to create correlations between two non-interacting parties which are initially uncorrelated. Its average work cost is low—it plays a crucial role in a protocol which in fact creates correlations at optimal work cost, $W = I/\beta$ [150].

As noted, however, work in quantum systems is about more than the average work cost. How important are fluctuations in the work cost in this protocol? We seek to answer this question by conducting an investigation of the protocol in a slightly different mode than was done in [149]. We look explicitly at the unitary and the final state produced, rather than only the marginals. We use this information to calculate the work fluctuations of the protocol, as well as the mutual information and work cost as a function of properties of the final state output.

As a result of this investigation, we show that the fluctuations in the work cost of this particular protocol are significant—they are at least of the order of the average work cost. This result motivates giving higher consideration to work fluctuations in practical contexts, rather than solely prioritizing minimizing average work cost of a protocol.

In this chapter, we will first outline the setup of the study in section 5.1. We give a detailed study of the mutual information created in the protocol, the average work cost, and the final temperature in section 5.2. Finally, in section 5.3, we calculate the fluctuations in work cost and the change in standard deviation of the energy from the initial to final

state. We provide some discussion on conceptual issues of calculating fluctuations in this particular context.

5.1 Setup

We study bipartite correlation creation in a system of two identical qubits, with free Hamiltonian

$$\hat{H} = \frac{\omega}{2}\left(\hat{\sigma}_z^{(\mathrm{A})} + \hat{\sigma}_z^{(\mathrm{B})}\right), \tag{5.1.1}$$

where ω is the energy gap of each qubit.

To implement the unitary protocol discussed in chapter 4, the system must initially be in a thermal state. We call the inverse temperature of the initial state β_{in}, so the initial state is

$$\hat{\rho} = \frac{\mathrm{e}^{-\beta_{\mathrm{in}}\hat{H}}}{\mathrm{Tr}[\mathrm{e}^{-\beta_{\mathrm{in}}\hat{H}}]} = \hat{\tau}_{\mathrm{A}}(\beta_{\mathrm{in}}) \otimes \hat{\tau}_{\mathrm{B}}(\beta_{\mathrm{in}}), \tag{5.1.2}$$

where $\hat{\tau}_{\mathrm{A(B)}}(\beta_{\mathrm{in}})$ is the local Gibbs state on subsystem A (B), as in equation (4.1.2). In the computational basis $\{|00\rangle, |01\rangle, |10\rangle, |11\rangle\}$, this initial state is

$$\hat{\rho} = \frac{1}{Z}\begin{bmatrix} \mathrm{e}^{-\beta_{\mathrm{in}}\omega} & 0 & 0 & 0 \\ 0 & 1 & 0 & 0 \\ 0 & 0 & 1 & 0 \\ 0 & 0 & 0 & \mathrm{e}^{\beta_{\mathrm{in}}\omega} \end{bmatrix}, \tag{5.1.3}$$

where $Z = \mathrm{Tr}[\mathrm{e}^{-\beta_{\mathrm{in}}\hat{H}}] = (\mathrm{e}^{-\beta_{\mathrm{in}}\omega/2} + \mathrm{e}^{\beta_{\mathrm{in}}\omega/2})^2$ is the partition function.

To create correlations in this completely separable initial state, we apply the correlating unitary, yielding

$$\hat{\rho}' = \hat{U}_{\mathrm{corr}}\hat{\rho}\hat{U}_{\mathrm{corr}}^{\dagger} = \frac{1}{Z}\begin{bmatrix} A_- & 0 & 0 & B_+ \\ 0 & 1 & 0 & 0 \\ 0 & 0 & 1 & 0 \\ B_- & 0 & 0 & A_+ \end{bmatrix}, \tag{5.1.4}$$

where

$$A_\pm = \mathrm{e}^{\pm\beta_{\mathrm{in}}\omega} \mp 2\sinh[\beta_{\mathrm{in}}\omega]\cos^2\delta\sin^2\theta, \tag{5.1.5}$$

$$B_\pm = 2\sinh[\beta_{\mathrm{in}}\omega]\cos\delta\sin\theta(\cos\theta \pm \mathrm{i}\sin\delta\sin\theta). \tag{5.1.6}$$

As mentioned at the end of chapter 4, the parameters ϕ and γ of the unitary (4.2.9) controlling the rotation in the subspace S_1 as in equation (4.2.6) have no effect on the final state.

The final local states of each system are found by tracing out the other:

$$\mathrm{Tr}_{\mathrm{B}}[\hat{\rho}'] = \frac{1}{Z}\begin{bmatrix} A_- + 1 & 0 \\ 0 & A_+ + 1 \end{bmatrix}, \tag{5.1.7}$$

$$\mathrm{Tr}_{\mathrm{A}}[\hat{\rho}'] = \frac{1}{Z}\begin{bmatrix} A_- + 1 & 0 \\ 0 & A_+ + 1 \end{bmatrix}. \tag{5.1.8}$$

These are in fact Gibbs states, as desired, for the local Hamiltonian $\hat{H}_{\mathrm{A/B}} = \frac{1}{2}\omega\hat{\sigma}_z^{(\mathrm{A})/(\mathrm{B})}$. We can find the local temperature β_{out} of these local Gibbs states by letting the right hand side of the above expression for the state of the subsystem equal the usual expression for a Gibbs state of temperature β_{out}, as

$$\frac{1}{Z}\begin{bmatrix} A_- + 1 & 0 \\ 0 & A_+ + 1 \end{bmatrix} = \frac{1}{Z}\begin{bmatrix} \mathrm{e}^{\beta_{\mathrm{out}}\omega/2} & 0 \\ 0 & \mathrm{e}^{-\beta_{\mathrm{out}}\omega/2}. \end{bmatrix} \tag{5.1.9}$$

The final local temperature is then

$$\beta_{\mathrm{out}} = \frac{2}{\omega}\,\mathrm{arctanh}\left[\frac{A_+ - A_-}{Z}\right]. \tag{5.1.10}$$

5.2 Work, mutual information, and other quantities

Given the initial and final states of the two qubits in terms of the parameters of the unitary, we can calculate a great deal of information. Laying these details of the protocol out in terms of the parameters of the unitary will allow us to make several concrete relations between them. A summary of what we discuss is presented in figure 5.1: the maximum mutual information is produced when the final local inverse temperature is zero; the average work cost is bounded above by $2\omega\tanh[\beta_{\mathrm{in}}\omega/2]$; the final local inverse temperature is in the range $[-\beta_{\mathrm{in}}, \beta_{\mathrm{in}}]$.

First, we will detail the average work cost of the protocol and discuss the sets of unitaries which have the same average work cost. Then, we discuss the limits on the final temperature, and finally the mutual information produced.

5.2.1 Average work cost and the family of unitaries

As discussed in chapter 2, we can write the average work cost of a unitary protocol as the difference in expectation value of energy between the final and initial states:

$$W = \mathrm{Tr}[\hat{H}(\hat{\rho}' - \hat{\rho})]. \tag{5.2.1}$$

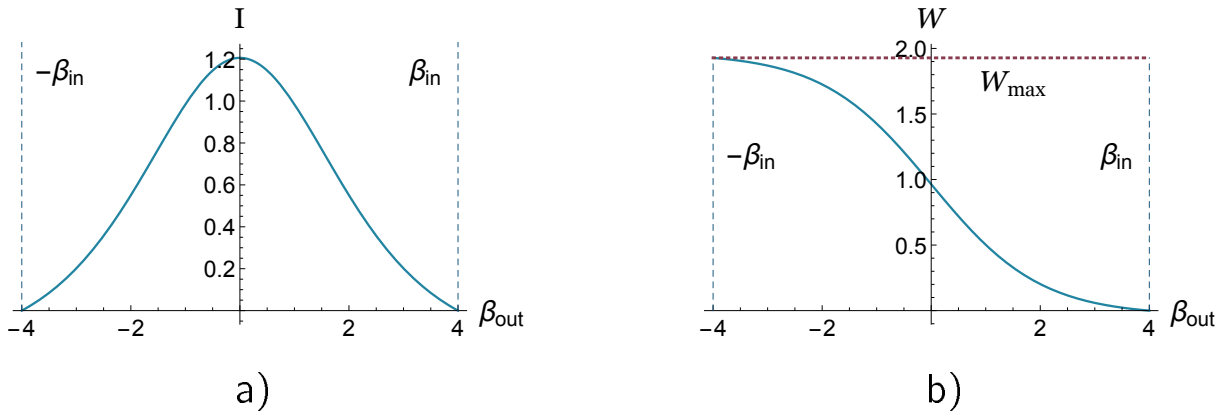

Figure 5.1: a) Mutual information created as a function of the final temperature β_{out}. The bounds on reachable β_{out} are marked by vertical dashed lines. b) The average work cost of the correlation-creating protocol as a function of the final local inverse temperature. The horizontal dotted line marks the upper bound on the average work cost, as in equation (5.2.3).

This is the average work cost for both the two-time measurement and unprojected work schemes when, as in our case, $[\hat{H}, \hat{\rho}] = 0$.

We can express this average work cost in multiple ways. Substituting in our expressions (5.1.3) and (5.1.3) for the initial and final states, we arrive at

$$W = 2\omega \tanh[\beta_{\text{in}}\omega/2] \cos^2 \delta \sin^2 \theta, \tag{5.2.2}$$

with an upper bound of

$$W \leq 2\omega \tanh[\beta_{\text{in}}\omega/2]. \tag{5.2.3}$$

We can also write the average work cost as a function only of the initial and final local temperatures:

$$W = \omega \left(\tanh[\beta_{\text{in}}\omega/2] - \tanh[\beta_{\text{out}}\omega/2]\right). \tag{5.2.4}$$

In equation (5.2.2), we see that several values of θ and δ could give the same value of the average work cost W. If we fix the value of W, we can in fact derive a relationship between θ and δ, which defines families of unitaries (where θ and δ vary across the family) which cost the same amount of average work:

$$\theta(\delta) = \arcsin\left[\sqrt{\frac{W \coth(\beta_{\text{in}}\omega/2)}{2\omega}} \sec\delta\right]. \tag{5.2.5}$$

These θ-δ curves are shown in figure 5.2.

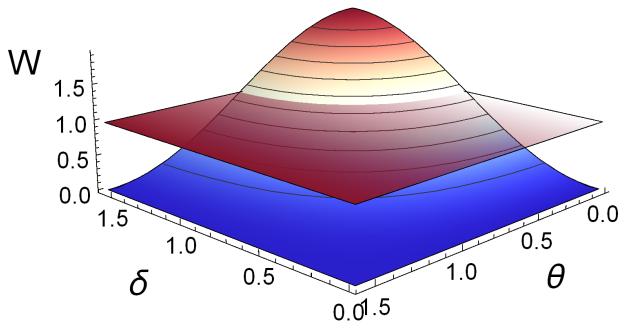

Figure 5.2: Average work cost plotted as a function of parameters of the unitary θ and δ. Lines shown are of constant average work cost, defined in equation (5.2.5). The plane indicates maximum creation of correlations, where $\beta_{\text{out}} = 0$ and the average work cost is given by equation (5.2.9). Above this plane, the final local temperature is negative, with $\beta_{\text{out}} = -\beta_{\text{in}}$ at the top of the plot.

5.2.2 Final temperature

The final local states have local temperature given by equation (5.1.10). Expanding this expression, we find an explicit dependence of the final temperature on the parameters θ and δ of the unitary:

$$\beta_{\text{out}} = \frac{2}{\omega} \operatorname{arctanh}\left[\tanh\left[\frac{\beta_{\text{in}}\omega}{2}\right](1 - 2\cos^2\delta\sin^2\theta)\right]. \tag{5.2.6}$$

This gives us explicit limits on the final local temperature in terms of the initial temperature: $\beta_{\text{out}} \in [-\beta_{\text{in}}, \beta_{\text{in}}]$.

This expression for β_{out} indicates that the θ-δ curves defined by (5.2.5) not only define curves of constant average work cost but also of constant final temperature. There is, however, an ambiguity here, as the average work cost is symmetric in the final temperature about $\beta_{\text{out}} = 0$. That is, the average work cost to reach the final local temperature β_{out} is the same as to reach $-\beta_{\text{out}}$.

5.2.3 Mutual information

The mutual information of the bipartite system is initially zero, as we begin in a global thermal state of a non-interacting system, i.e., a product state. The final mutual information is calculated explicitly from its definition (4.1.5). In terms of the initial and final

temperatures, it is

$$I = \log\left[\frac{\mathrm{e}^{\beta_{\mathrm{in}}\omega\tanh[\beta_{\mathrm{in}}\omega/2]}}{\cosh^2[\beta_{\mathrm{in}}\omega/2]}\right] + \log\left[\frac{\mathrm{e}^{\beta_{\mathrm{out}}\omega\tanh[\beta_{\mathrm{out}}\omega/2]}}{\cosh^2[\beta_{\mathrm{out}}\omega/2]}\right]. \tag{5.2.7}$$

The maximum correlations will be created when the final local temperature is infinite (when $\beta_{\mathrm{out}} = 0$). This corresponds to a Bell state being created over the two qubits. The maximum depends on the initial temperature as

$$I_{\max} = \log\left[\frac{\mathrm{e}^{\beta_{\mathrm{in}}\omega\tanh[\beta_{\mathrm{in}}\omega/2]}}{\cosh^2[\beta_{\mathrm{in}}\omega/2]}\right]. \tag{5.2.8}$$

The average work cost of reaching this maximum, from equation (5.2.4), is

$$W_{(I_{\max})} = \omega\tanh[\beta_{\mathrm{in}}\omega/2]. \tag{5.2.9}$$

5.3 Measures of work fluctuations

Having studied the average work cost, final temperature, and the mutual information created in the protocol, we now wish to ask: what are the fluctuations in the work cost? Do they matter? As discussed in earlier sections, the uncertainty in the work cost of a protocol is not often considered in the literature. This is ultimately a practical question. How reliable is the work cost of this protocol?

In this section, we calculate two measures of the work fluctuations of this protocol, discussed earlier in section 2.2. We find that the measures of fluctuations are nontrivial when the protocol creates maximal correlations in low-temperature initial states.

5.3.1 Work fluctuations

We can calculate the fluctuations in the work cost using the expression of either the two-time measurement scheme, (2.2.2) or the unprojected scheme, (2.2.10). In terms of the parameters of the unitary, we have

$$\sigma_W^2 = \frac{\omega^2\cos^2\delta\sin^2\delta}{(1+\mathrm{e}^{\beta\omega})^2}\big(3 + 2\mathrm{e}^{\beta\omega} + 3\mathrm{e}^{\beta\omega} + (\mathrm{e}^{\beta\omega}-1)^2(1 - 4\cos^2\delta\sin^2\theta)\big). \tag{5.3.1}$$

In terms of the initial and final inverse temperatures, we can also write

$$\sigma_W^2 = \omega^2\big(\operatorname{sech}^2(\beta_{\mathrm{out}}\omega/2) - 2\tanh(\beta_{\mathrm{out}}\omega/2)\operatorname{csch}\beta_{\mathrm{in}}\omega\big). \tag{5.3.2}$$

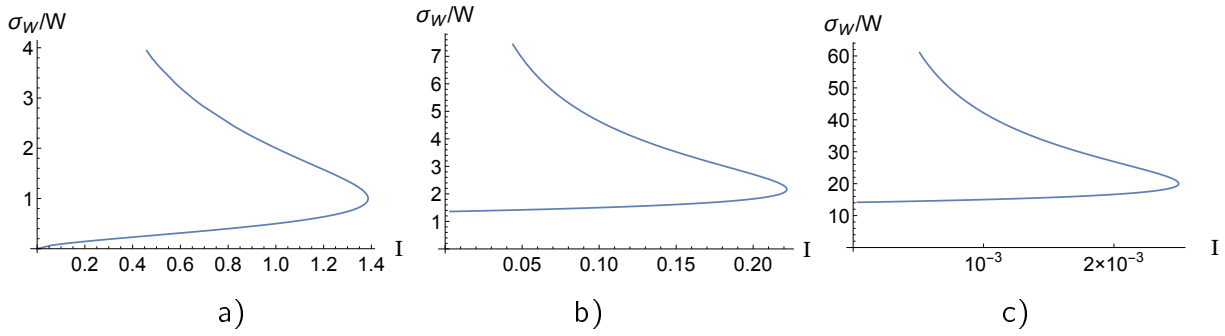

Figure 5.3: The ratio of work fluctuations to average work cost versus the mutual information created in the protocol. Average work cost increases along the curve from top to bottom; $\beta_{\text{out}} = 0$ at the point of maximum creation of mutual information. From left to right, $\beta_{\text{in}} = 100\omega^{-1}$, ω^{-1}, $0.1\omega^{-1}$. The ratio of fluctuations to average work cost is of order one for the lowest temperature initial state, and increases as the initial temperature increases.

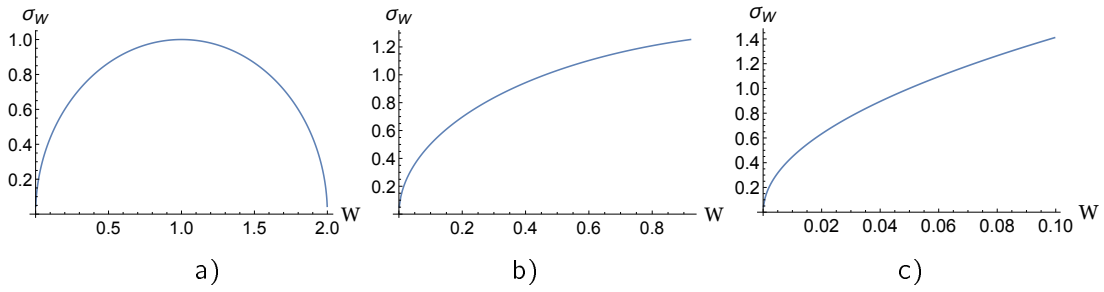

Figure 5.4: Work fluctuations σ_W versus average work cost, for $\omega = 1$ and initial temperatures, from left to right, of $\beta_{\text{in}} = 100\omega^{-1}$, ω^{-1}, and $0.1\omega^{-1}$.

To get a sense of the importance of these fluctuations, we plot the ratio of σ_W to the average work cost W as a function of the mutual information created in figure 5.3. In these plots, the average work cost increases along the curve from top to bottom, with $W = \omega \tanh[\beta_{\text{in}}\omega/2]$ at the point of maximal mutual information. Note that the region of the curve below maximal I is where the final local temperature is negative, and therefore that the point of $I = 0$ corresponds to $\beta_{\text{out}} = -\beta_{\text{in}}$ (not to an identity process). We see that the ratio of fluctuations to the average work cost is at least of order one for maximum creation of correlations!

We also plot the fluctuations as a function of the average work cost in figure 5.4. They can be seen to increase significantly in magnitude for higher initial temperatures, even as the average work cost decreases dramatically.

Measurement issues

Though our two conceptualizations of work are identical for the purpose of calculating fluctuations, they are not completely free of differences. We can ask: how are we actually measuring these quantities?

In the case of the two-time measurement scheme, how can we create any mutual information in the protocol if we are performing two projective measurements? These measurements in the energy eigenbasis will certainly erase any coherences in the basis. We offer two responses to this excellent question. The first is yes, attempting to measure the work cost at the same time as creating correlations will fail. This certainly raises questions of the accuracy of the measurement scheme, if it cannot measure the work when correlations are actually created. The second is that one may consider the measurement scheme to be applied many times outside of the actual run of the protocol to create useful correlations, building up a probability distribution. Then statistical knowledge like the average work and fluctuations in the work cost may be used for any given implementation of the protocol.

In the unprojected scheme, the name of course suggests that no projective measurements are formed. In fact, there is nothing built into the formalism about how one would measure the energy of the system at all, which leaves any analysis about how measurement would impact the work value measured ambiguous.

Again, this encourages the consideration of other schemes for work statistics, especially those which include fully developed schemes for measurement [136]. One would still generally expect that any measurement performed on the system will alter it somehow, and thus disturb the correlations we so painstakingly created. We might, then, in many schemes of work need to rely on a statistical knowledge of work generated in applications of the protocol separate from those we intend to use to actually generate useful correlations.

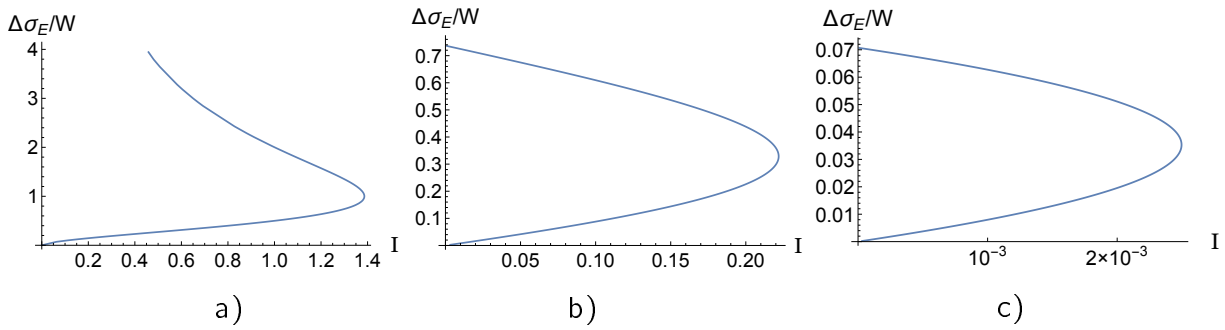

Figure 5.5: The ratio of change in standard deviation of energy to average work cost versus the mutual information created in the protocol. Average work cost increases along the curve from top to bottom; $\beta_{\text{out}} = 0$ at the point of maximum creation of mutual information. From left to right, $\beta_{\text{in}} = 100\omega^{-1}$, ω^{-1}, $0.1\omega^{-1}$. Though the behaviour of this measure is similar to that of the other measures of fluctuations at low initial temperature, its magnitude decreases significantly as the initial temperature increases, in contrast to the behaviour in figure 5.3. This suggests that a great deal of the uncertainty in the work cost of the protocol comes from the uncertainty in the energy of the initial state, especially when the initial temperature is high, as opposed to being from the application of the unitary.

5.3.2 Change in the standard deviation of energy

Finally, we provide an indication of the uncertainty in energy of the state developed by application of the protocol (rather than a measure of the uncertainty in work cost of the protocol). This somewhat heuristic measure is the change in the standard deviation of the energy distribution of each state:

$$\Delta\sigma_E = \sigma_{E_f} - \sigma_{E_i}, \tag{5.3.3}$$

with

$$\sigma_{E_i}^2 = \text{Tr}[\hat{H}^2\hat{\rho}] - \text{Tr}[\hat{H}\hat{\rho}]^2, \tag{5.3.4}$$

$$\sigma_{E_f}^2 = \text{Tr}[\hat{H}^2\hat{\rho}'] - \text{Tr}[\hat{H}\hat{\rho}']^2. \tag{5.3.5}$$

We aim to literally subtract the contribution from the uncertainty in the initial state from the uncertainty in the work cost.

The behaviour of this measure of uncertainty is very different from the other measure of fluctuations in the work cost, as shown in figure 5.5. When the initial temperature is low, the difference between the measures is negligible, but the change in standard deviation

decreases as the initial temperature increases. This indicates that a substantial amount of the uncertainty in the work cost of the unitary protocol is due more to the temperature of the initial state rather than to the application of the unitary itself. This doesn't mitigate the uncertainty in the work cost of applying the unitary. It does, however, caution us as to the existence of a protocol which will have lower uncertainty for application to high temperature initial states.

Chapter 6

Discussion and conclusions

In this part of the thesis, we have presented an analysis of uncertainty in work cost of a unitary protocol to generate correlations in a system of two non-interacting qubits. We have provided some background on the very active field of quantum work and the study of correlations in the context of quantum thermodynamics. We have added some detail to what is known about the protocol of Huber *et al.*, initially put forth in ref. [149]. In particular, we studied the fluctuations in the work cost and analysed a little where they originate.

Our main result is that the ratio of work fluctuations to average work cost is of order at least one for maximal generation of correlations. This isn't great, practically speaking. If you have a strict energy budget with which to develop correlations, large work fluctuations could easily break it. Additionally, we find that for initial thermal states with higher temperature, this ratio increases. The small change in standard deviation of energy from the initial to final state indicates, however, that this can be substantially attributed to the already large energy fluctuations present in the initial state, rather than to the protocol. As another practical note, these high temperature states have little room to develop correlations anyway, as their local states are already quite close to the infinite temperature state.

Given these results, we may thus suggest that it would be prudent to consider using a protocol which is not optimal in its average work cost (or maximal in its correlation creation) but which nonetheless has a more reliable work cost.

There are at least two limitations to drawing this conclusion from our work. The first arises from looking at the problem in an even more practical light. Given that it is difficult to correlate a highly mixed system, it is desirable to start from a state which is as pure as possible. Before one correlates, one thus ought to cool the system, as proposed in

[150]. Because of the increase in correlations able to be obtained, adding the cooling step allows this adjusted protocol to in fact saturate the inequality $I \leq \beta W$ for non-interacting systems. The work cost of cooling is high. In fact, the work cost to cool from an initial temperature of $\beta_{\text{in}} = 0.1\omega$ to $\beta = 10\omega$ (that is, from $T = 10\omega^{-1}$ to $T = 0.1\omega^{-1}$) is ten times the work cost of applying the maximally correlating unitary to the resulting state. In this more practical case, the fluctuations in the work cost quickly dwindle in their relevance to the total work cost of the protocol.

Another limitation arises from the ongoing discussion about work in quantum systems. It is not, after all, completely clear that the fluctuations we measure are exactly those that would be observed in a specific experimental setup, especially if projective measurements are not used. Given the sheer number of proposals surrounding an apt definition for quantum work, drawing any certain conclusions about what one will see in an experiment seems to be treading on unsteady ground.

As for future work, this particular problem could be investigated in a little more depth. What is the dimensional dependence of the importance of fluctuations? What if the system has a small interaction? Or begins out of equilibrium? How do these fluctuations change for the development of multipartite correlations? And, perhaps building on [150], what is the specific cost of developing entanglement?

The conclusion which can be drawn from this study in a slightly wider context is mostly an encouragement to people who study quantum systems to consider the variance of the work cost in addition to the average work cost, to get a better sense of how much energy a protocol will cost in practice. This is arguably a trend in the field [136, 161]. Thus, the encouragement that can be derived from the study is not a contribution which is unique to it. The details of the study of a potentially useful unitary protocol to develop correlations may prove useful to folks doing other detailed studies, or (perhaps a stretch) to those interested in implementing the protocol. However, our judgement is that the study is primarily valuable as a part of this larger trend to be more careful about what we mean when we talk about work in quantum systems.

As in the study conducted in Part I, we have contributed to an ever larger body of work which aims to support the exploration and exploitation of quantum systems. In both studies, there are motivations apart from quantum technology. Studying quantum systems is interesting! There are neat things to learn! The universe is a fascinating place, and physics is no exception. But personal interest and appeals to universal wonder are not the end of the story. They themselves are not even apolitical or without effect—advertising our personal wonder attracts new folks to study physics to stoke their own wonder, which generally means also contributing to projects like quantum technology. Regardless of whether we intend to support projects like unethical mining, many of us are

doing so in our pursuit of our dreams. It wouldn't do to try and manage this effect by dismissing or trying to do away with our own wonder and intrigue about the world. But we can temper these dreams with reality. We can acknowledge the world that our stated and unstated goals are helping to create. We can use that to revisit our motivations, use some of the tools presented here to analyse their relationship to parts of society frequently considered to be outside of physics, and discuss it openly—to ask if that's the world you really want.

References

[1] Emma McKay, Adrian Lupascu, and Eduardo Martín-Martínez. Finite sizes and smooth cutoffs in superconducting circuits. *Physical Review A*, 96(5), nov 2017. doi:10.1103/physreva.96.052325. iii, vi

[2] Emma McKay, Nayeli A. Rodríguez-Briones, and Eduardo Martín-Martínez. Fluctuations of work cost in optimal generation of correlations. *Physical Review E*, 98(3), sep 2018. doi:10.1103/physreve.98.032132. iii

[3] LSPIRG. Know the land, 2018. URL http://www.lspirg.org/knowtheland/. [Online - accessed Nov 13-18]. v

[4] Jeremy Kahn. Why quantum computers will be super awesome, someday. Bloomberg Businessweek, 2018. URL https://www.bloomberg.com/news/articles/2018-06-29/why-quantum-computers-will-be-super-awesome-someday-quicktake. [Online - accessed Nov 9-18]. xx

[5] David P. DiVincenzo. Scientists and citizens: getting to quantum technologies. *Ethics and Information Technology*, 19(4):247–251, aug 2017. doi:10.1007/s10676-017-9435-3. xx

[6] Ronald de Wolf. The potential impact of quantum computers on society. *Ethics and Information Technology*, 19(4):271–276, sep 2017. doi:10.1007/s10676-017-9439-z. xxi

[7] Christopher Coenen and Armin Grunwald. Responsible research and innovation (RRI) in quantum technology. *Ethics and Information Technology*, 19(4):277–294, aug 2017. doi:10.1007/s10676-017-9432-6. xxi, xxii, xxiii, xxvi

[8] Scott Aaronson. The limits of quantum computers. *Scientific American*, 298(3):62–69, mar 2008. doi:10.1038/scientificamerican0308-62. xxi

[9] David Poulin, M. B. Hastings, Dave Wecker, Nathan Wiebe, Andrew C. Doherty, and Matthias Troyer. The trotter step size required for accurate quantum simulation of quantum chemistry. xxi

[10] Amir Fruchtman and Iris Choi. Technical roadmap for fault-tolerant quantum computing. resreport, University of Oxford, 2016. URL https://www.nqit.ox.ac.uk/sites/www.nqit.ox.ac.uk/files/2016-11/NQIT%20Technical%20Roadmap.pdf. xxi

[11] J. Heisler, P.M. Glibert, J.M. Burkholder, D.M. Anderson, W. Cochlan, W.C. Dennison, Q. Dortch, C.J. Gobler, C.A. Heil, E. Humphries, A. Lewitus, R. Magnien, H.G. Marshall, K. Sellner, D.A. Stockwell, D.K. Stoecker, and M. Suddleson. Eutrophication and harmful algal blooms: A scientific consensus. *Harmful Algae*, 8(1):3–13, dec 2008. doi:10.1016/j.hal.2008.08.006. xxi

[12] A.L. Smit, P.S. Bindraban, J.J. Schröder, J.G. Conjin, and H.G. van der Meer. Phosphorus in agriculture: gloval resources, trends, and developments. resreport 282, Steering Committee Technology Assessment of the Ministry of Agriculture, Nature, and Food Quality, The Netherlands, 2009. URL http://edepot.wur.nl/12571.

[13] Zareen Pervez Bharucha. Sustainable food production: Facts and figures. SciDevNet, 2013. URL https://www.scidev.net/global/food-security/feature/sustainable-food-production-facts-and-figures.html. [Online - accessed Nov 12-18]. xxi

[14] Government of Canada. Inaugural competition 1 results. Canada First Research Excellence Fund, 2016. URL http://www.cfref-apogee.gc.ca/results-resultats/competition_1-eng.aspx. [Online - accessed Nov 12-18]. xxii

[15] Government of Canada. Inaugural competition 2 results. Canada First Research Excellence Fund, 2018. URL http://www.cfref-apogee.gc.ca/results-resultats/index-eng.aspx. [Online - accessed Nov 12-18]. xxii

[16] A De Touzalin, C Marcus, F Heijman, I Cirac, R Murray, and T Calarco. Quantum manifesto. a new era of technology. *European Comission*, 2016. xxiii

[17] Wolfgang P Schleich, Kedar S Ranade, Christian Anton, Markus Arndt, Markus Aspelmeyer, Manfred Bayer, Gunnar Berg, Tommaso Calarco, Harald Fuchs, Elisabeth Giacobino, et al. Quantum technology: from research to application. *Applied Physics B*, 122(5):130, 2016. xxiii

[18] Quirin Schiermeier. The great arctic oil race begins. *Nature*, 482(7383):13–14, jan 2012. doi:10.1038/482013a. xxiv

[19] Ty McCormick. Arctic sovereignty: A short history. Foreign Policy, 2014. URL https://foreignpolicy.com/2014/05/07/arctic-sovereignty-a-short-history/. [Online - accessed Nov 11-18]. xxiv

[20] Offfice of Naval Research, Naval Ice Center, Oceanographer of the Navy, and Arctic Research Commission. Naval operations in an ice-free arctic symposium: Final report, April 2001. URL https://www.star.nesdis.noaa.gov/star/documents/2007IceSymp/FinalArcticReport_2001.pdf. xxiv

[21] W.R. Morrison. Canadian arctic sovereignty. In *The Canadian Encyclopedia*. Historica Canada, 2018. URL https://www.thecanadianencyclopedia.ca/en/article/arctic-sovereignty. [Online - accessed Nov 11-18]. xxiv, xxv

[22] Dennis Patterson. Canada must assert sovereignty over the arctic while there's still time. The National Post, 2017. URL https://nationalpost.com/opinion/canadas-must-assert-sovereignty-over-the-arctic-while-theres-still-time. [Online - accessed Nov 11-18]. xxiv

[23] Nunavut Alert. Alert, nunavut — Wikipedia, the free encyclopedia, 2018. URL https://en.wikipedia.org/wiki/Alert,_Nunavut. [Online; accessed 02-March-2018]. xxiv

[24] Surveys with autonomous underwater vehicles (auvs), 2016. URL http://science.gc.ca/eic/site/063.nsf/eng/h_6829914E.html. xxiv

[25] Canada's extended continental shelf program, 2016. URL http://science.gc.ca/eic/site/063.nsf/eng/h_98773CA7.html. xxiv

[26] Pauline Wakeham. At the intersection of apology and sovereignty: The arctic exile monument project. *Cultural Critique*, 87:84–143, 2014. URL https://muse.jhu.edu/article/549351. xxiv

[27] Peter Kulchyski Frank Tester. *Tammarniit (Mistakes): Inuit Relocation in the Eastern Arctic, 1939-63*. UNIV OF BRITISH COLUMBIA, 2002. ISBN 0774804521. URL https://www.ebook.de/de/product/23187129/frank_tester_peter_kulchyski_tammarniit_mistakes_inuit_relocation_in_the_eastern_arctic_1939_63.html. xxiv

[28] Sandra E. Smith J. Douglas Porteous. *Domicide*. PAPERBACKSHOP UK IMPORT, 2001. ISBN 0773522581. URL https://www.ebook.de/de/product/4315350/j_douglas_porteous_sandra_e_smith_domicide.html. xxiv

[29] Exercising our arctic sovereignty, 2015. URL https://www.northernstrategy.gc.ca/sov/index-eng.asp. [Online - accessed November 7-18]. xxiv

[30] Department of National Defence. Government of canada announces contract award to the university of waterloo for research and development in support of arctic surveillance, 2018. URL https://www.canada.ca/en/department-national-defence/news/2018/04/government-of-canada-announces-contract-award-to-the-university-of-waterloo-for-research-and-de
html. [Online - accessed November 7-2018]. xxiv, xxv

[31] Mary-Ann Russon. Canada developing quantum radar to detect stealth aircraft. BBC News, 2018. URL https://www.bbc.com/news/technology-43877682. [Online - accessed November 8-18]. xxv

[32] Sandra Harding. *Whose Science? Whose Knowledge?* Cornell University Press, 1991. ISBN 0801497469. URL https://www.ebook.de/de/product/4293196/sandra_harding_whose_science_whose_knowledge.html. xxvi

[33] Sandra Harding. *Objectivity and Diversity*. The University of Chicago Press, 2015. ISBN 022624136X. URL https://www.ebook.de/de/product/22824905/sandra_harding_objectivity_and_diversity.html. xxvi, 51

[34] Heather Douglas. *Science, Policy, and the Value-Free Ideal*. UNIV OF PITTSBURGH PR, 2009. ISBN 0822960265. URL https://www.ebook.de/de/product/8106576/heather_douglas_science_policy_and_the_value_free_ideal.html. xxvii

[35] Barbara L. Whitten. (baby) steps toward feminist physics. *Journal of Women and Minorities in Science and Engineering*, 18 (2):115–134, 2012. ISSN 1072-8325. xxvii

[36] Thomas S. Kuhn. *The Structure of Scientific Revolutions*. The University of Chicago Press, 1962. ISBN 0226458113. URL https://www.ebook.de/de/product/16779638/thomas_s_kuhn_the_structure_of_scientific_revolutions.html. xxvii

[37] Ludwik Fleck. *Genesis and Development of a Scientific Fact*. The University of Chicago Press, 1981. ISBN 0226253252. URL https://www.ebook.de/de/product/3627047/ludwik_fleck_genesis_and_development_of_a_scientific_fact.html. xxvii

[38] Alejandro Pozas-Kerstjens and Eduardo Martín-Martínez. Harvesting correlations from the quantum vacuum. *Physical Review D*, 92(6), sep 2015. doi:10.1103/physrevd.92.064042. 3, 21

[39] W. G. Unruh. Notes on black-hole evaporation. *Physical Review D*, 14(4):870–892, aug 1976. doi:10.1103/physrevd.14.870. 3, 18, 20, 23

[40] Alejandro Pozas-Kerstjens and Eduardo Martín-Martínez. Entanglement harvesting from the electromagnetic vacuum with hydrogenlike atoms. *Physical Review D*, 94(6), sep 2016. doi:10.1103/physrevd.94.064074. 3, 21, 23

[41] J. Bourassa, J. M. Gambetta, A. A. Abdumalikov, O. Astafiev, Y. Nakamura, and A. Blais. Ultrastrong coupling regime of cavity QED with phase-biased flux qubits. *Physical Review A*, 80(3), sep 2009. doi:10.1103/physreva.80.032109. 3

[42] B. Peropadre, P. Forn-Díaz, E. Solano, and J. J. García-Ripoll. Switchable ultrastrong coupling in circuit QED. *Physical Review Letters*, 105(2), jul 2010. doi:10.1103/physrevlett.105.023601. 3, 11, 12, 29

[43] T. Niemczyk, F. Deppe, H. Huebl, E. P. Menzel, F. Hocke, M. J. Schwarz, J. J. Garcia-Ripoll, D. Zueco, T. Hmmer, E. Solano, A. Marx, and R. Gross. Circuit quantum electrodynamics in the ultrastrong-coupling regime. *Nature Physics*, 6(10):772–776, jul 2010. doi:10.1038/nphys1730. 3, 7, 23

[44] P. Forn-Díaz, J. J. García-Ripoll, B. Peropadre, J.-L. Orgiazzi, M. A. Yurtalan, R. Belyansky, C. M. Wilson, and A. Lupascu. Ultrastrong coupling of a single artificial atom to an electromagnetic continuum in the nonperturbative regime. *Nature Physics*, 13(1):39–43, oct 2016. doi:10.1038/nphys3905. 3, 8, 9, 10, 11, 12, 17, 26, 27, 29, 46

[45] A. Wallraff, D. I. Schuster, A. Blais, L. Frunzio, R.-S. Huang, J. Majer, S. Kumar, S. M. Girvin, and R. J. Schoelkopf. Strong coupling of a single photon to a superconducting qubit using circuit quantum electrodynamics. *Nature*, 431(7005):162–167, sep 2004. doi:10.1038/nature02851. 5, 8, 9, 11

[46] Ulrich Weiss. *Quantum Dissipative Systems*. World Scientific Publishing Company, 2012. ISBN 9814374911. URL https://www.ebook.de/de/product/16842249/ulrich_weiss_quantum_dissipative_systems.html. 3, 4, 8, 9, 12, 15

[47] Marlan O. Scully and M. Suhail Zubairy. *Quantum optics*. Cambridge University Press, 1997. doi:10.1017/cbo9780511813993. 3, 11, 23

[48] P. Forn-Díaz, J. Lisenfeld, D. Marcos, J. J. García-Ripoll, E. Solano, C. J. P. M. Harmans, and J. E. Mooij. Observation of the bloch-siegert shift in a qubit-oscillator system in the ultrastrong coupling regime. *Physical Review Letters*, 105(23), nov 2010. doi:10.1103/physrevlett.105.237001. 3

[49] F. Yoshihara, K. Harrabi, A. O. Niskanen, Y. Nakamura, and J. S. Tsai. Decoherence of flux qubits due to1/fFlux noise. *Physical Review Letters*, 97(16), oct 2006. doi:10.1103/physrevlett.97.167001. 3, 29

[50] B. Peropadre, D. Zueco, D. Porras, and J. J. García-Ripoll. Nonequilibrium and nonperturbative dynamics of ultrastrong coupling in open lines. *Physical Review Letters*, 111(24), dec 2013. doi:10.1103/physrevlett.111.243602. 3, 8, 10, 12, 47

[51] Eduardo Martín-Martínez. Causality issues of particle detector models in QFT and quantum optics. *Phys. Rev. D*, 92(10), nov 2015. doi:10.1103/physrevd.92.104019. 4, 12, 23, 28

[52] Jorma Louko and Alejandro Satz. How often does the unruh–DeWitt detector click? regularization by a spatial profile. *Classical and Quantum Gravity*, 23(22):6321–6343, oct 2006. doi:10.1088/0264-9381/23/22/015. 4, 23

[53] A. A. Houck, D. I. Schuster, J. M. Gambetta, J. A. Schreier, B. R. Johnson, J. M. Chow, L. Frunzio, J. Majer, M. H. Devoret, S. M. Girvin, and R. J. Schoelkopf. Generating single microwave photons in a circuit. *Nature*, 449(7160):328–331, sep 2007. doi:10.1038/nature06126. 5, 28, 48

[54] Z. H. Peng, S. E. de Graaf, J. S. Tsai, and O. V. Astafiev. Tuneable on-demand single-photon source in the microwave range. *Nat. Commun.*, 7:12588, aug 2016. doi:10.1038/ncomms12588. 28

[55] B. T. H. Varcoe, S. Brattke, M. Weidinger, and H. Walther. Preparing pure photon number states of the radiation field. *Nature*, 403(6771):743–746, feb 2000. doi:10.1038/35001526. 5

[56] D. I. Schuster, A. A. Houck, J. A. Schreier, A. Wallraff, J. M. Gambetta, A. Blais, L. Frunzio, J. Majer, B. Johnson, M. H. Devoret, S. M. Girvin, and R. J. Schoelkopf. Resolving photon number states in a superconducting circuit. *Nature*, 445(7127):515–518, feb 2007. doi:10.1038/nature05461. 7

[57] Michele Campisi, Jukka Pekola, and Rosario Fazio. Nonequilibrium fluctuations in quantum heat engines: theory, example, and possible solid state experiments. *New Journal of Physics*, 17(3): 035012, mar 2015. doi:10.1088/1367-2630/17/3/035012. 7

[58] A. J. Leggett, S. Chakravarty, A. T. Dorsey, Matthew P. A. Fisher, Anupam Garg, and W. Zwerger. Dynamics of the dissipative two-state system. *Reviews of Modern Physics*, 59(1):1–85, jan 1987. doi:10.1103/revmodphys.59.1. 8, 10

[59] E.T. Jaynes and F.W. Cummings. Comparison of quantum and semiclassical radiation theories with application to the beam maser. *Proceedings of the IEEE*, 51(1):89–109, 1963. doi:10.1109/proc.1963.1664. 8

[60] M. D. Reed, L. DiCarlo, B. R. Johnson, L. Sun, D. I. Schuster, L. Frunzio, and R. J. Schoelkopf. High-fidelity readout in circuit quantum electrodynamics using the jaynes-cummings nonlinearity. *Physical Review Letters*, 105(17), oct 2010. doi:10.1103/physrevlett.105.173601. 8, 9

[61] C. Sabín, J. León, and J. J. García-Ripoll. Detecting ground-state qubit self-excitations in circuit QED: A slow quantum anti-zeno effect. *Physical Review B*, 84(2), jul 2011. doi:10.1103/physrevb.84.024516. 8, 9, 23

[62] H. S. Sehmi, W. Langbein, and E. A. Muljarov. Optimizing the drude-lorentz model for material permittivity: Method, program, and examples for gold, silver, and copper. *Physical Review B*, 95 (11), mar 2017. doi:10.1103/physrevb.95.115444. 9, 29

[63] Mark Mitchison (https://physics.stackexchange.com/users/14105/mark mitchison). What is the relationship between the drude form and the exponential form of ohmic spectral density? Physics Stack Exchange. URL https://physics.stackexchange.com/q/200277. URL:https://physics.stackexchange.com/q/200277 (version: 2015-08-15). 9

[64] I. Lizuain, J. Casanova, J. J. García-Ripoll, J. G. Muga, and E. Solano. Zeno physics in ultrastrong-coupling circuit QED. *Physical Review A*, 81(6), jun 2010. doi:10.1103/physreva.81.062131. 9

[65] Guillermo Díaz-Camacho, Alejandro Bermudez, and Juan José García-Ripoll. Dynamical polaron ansatz: A theoretical tool for the ultrastrong-coupling regime of circuit qed. *Phys. Rev. A*, 93(4), apr 2016. doi:10.1103/physreva.93.043843. 10, 11, 12, 46

[66] Alexandre Blais, Ren-Shou Huang, Andreas Wallraff, S. M. Girvin, and R. J. Schoelkopf. Cavity quantum electrodynamics for superconducting electrical circuits: An architecture for quantum computation. *Phys. Rev. A*, 69(6), jun 2004. doi:10.1103/physreva.69.062320. 11

[67] J. E. Mooij. Josephson persistent-current qubit. *Science*, 285(5430):1036–1039, aug 1999. doi:10.1126/science.285.5430.1036. 12

[68] Mikhail V. Feigel'man, Lev. B. Ioffe, Vadim B. Geshkenbein, and Gianni Blatter. Andreev spectroscopy for superconducting phase qubits. *Journal of Low Temperature Physics*, 118(5/6):805–816, 2000. doi:10.1023/a:1004664000417. 12

[69] B. S. DeWitt. Quantum gravity: The new synthesis. In S. W. Hawking and W. Israel, editors, *General Relativity: An Einstein Centenary Survey*, pages 680–745. Cambridge University Press, 1979. 18, 21, 23

[70] Hiroomi Umezawa. *Advanced Field Theory: Micro, Macro, and Thermal Physics*. SPRINGER VERLAG GMBH, 1992. ISBN 1563960818. URL https://www.ebook.de/de/product/18514513/hiroom_umezawa_h_umezawa_advanced_field_theory_micro_macro_and_thermal_physics.html. 19

[71] Franco Strocchi. *An Introduction to Non-Perturbative Foundations of Quantum Field Theory*. OXFORD UNIV PR, 2013. ISBN 0199671575. URL https://www.ebook.de/de/product/20281265/franco_strocchi_an_introduction_to_non_perturbative_foundations_of_quantum_field_theory.html. 22, 23

[72] P. C. W. Davies N. D. Birrell. *Quantum Fields in Curved Space*. Cambridge University Press, 1984. ISBN 0521278589. URL https://www.ebook.de/de/product/3757654/n_d_birrell_p_c_w_davies_quantum_fields_in_curved_space.html. 19

[73] Keith K. Ng. Unruh-dewitt detector response along static and circular geodesic trajectories for schwarzschild-ads black holes. Master's thesis, University of Waterloo, 2014. 19

[74] Mathieu Cliche. Information propagation and entanglement generation between two unruh-dewitt detectors. Master's thesis, University of Waterloo, 2010.

[75] Allison Sachs. Entanglement harvesting and divergences in unruh-dewitt detector pairs. Master's thesis, University of Waterloo, 2017.

[76] David Cecil Murphy Ostapchuk. Entanglement in non-inertial frames. Master's thesis, University of Waterloo, 2008. 19

[77] Benito A Juárez-Aubry and Jorma Louko. Onset and decay of the 1+1 hawking-unruh effect: what the derivative-coupling detector saw. *Classical and Quantum Gravity*, 31(24):245007, nov 2014. doi:10.1088/0264-9381/31/24/245007. 20

[78] Jorma Louko. Unruh-dewitt detector response across a rindler firewall is finite. *Journal of High Energy Physics*, 2014(9), sep 2014. doi:10.1007/jhep09(2014)142. 20

[79] Eduardo Martín-Martínez and Jorma Louko. Particle detectors and the zero mode of a quantum field. *Physical Review D*, 90(2), jul 2014. doi:10.1103/physrevd.90.024015. 20

[80] Stephen A. Fulling. Nonuniqueness of canonical field quantization in riemannian space-time. *Physical Review D*, 7(10):2850–2862, may 1973. doi:10.1103/physrevd.7.2850. 20

[81] P C W Davies. Scalar production in schwarzschild and rindler metrics. *Journal of Physics A: Mathematical and General*, 8(4):609–616, apr 1975. doi:10.1088/0305-4470/8/4/022. 20

[82] Stefan Hollands and Ko Sanders. Entanglement measures and their properties in quantum field theory. 21

[83] Benni Reznik, Alex Retzker, and Jonathan Silman. Violating bell's inequalities in vacuum. *Physical Review A*, 71(4), apr 2005. doi:10.1103/physreva.71.042104. 21

[84] Benni Reznik. Entanglement from the vacuum. *Foundations of Physics*, 33(1):167–176, 2003. doi:10.1023/a:1022875910744.

[85] Antony Valentini. Non-local correlations in quantum electrodynamics. *Physics Letters A*, 153(6-7): 321–325, mar 1991. doi:10.1016/0375-9601(91)90952-5. 21

[86] Allison Sachs, Robert B. Mann, and Eduardo Martín-Martínez. Entanglement harvesting and divergences in quadratic unruh-DeWitt detector pairs. *Physical Review D*, 96(8), oct 2017. doi:10.1103/physrevd.96.085012. 21

[87] Petar Simidzija and Eduardo Martín-Martínez. Nonperturbative analysis of entanglement harvesting from coherent field states. *Physical Review D*, 96(6), sep 2017. doi:10.1103/physrevd.96.065008. 21

[88] Petar Simidzija and Eduardo Martín-Martínez. All coherent field states entangle equally. *Physical Review D*, 96(2), jul 2017. doi:10.1103/physrevd.96.025020. 21

[89] Grant Salton, Robert B Mann, and Nicolas C Menicucci. Acceleration-assisted entanglement harvesting and rangefinding. *New Journal of Physics*, 17(3):035001, mar 2015. doi:10.1088/1367-2630/17/3/035001. 21

[90] Laura J. Henderson, Robie A. Hennigar, Robert B. Mann, Alexander R. H. Smith, and Jialin Zhang. Harvesting entanglement from the black hole vacuum, 2017.

[91] Shingo Kukita and Yasusada Nambu. Harvesting large scale entanglement in de sitter space with multiple detectors. *Entropy*, 19(9):449, aug 2017. doi:10.3390/e19090449. 21

[92] Eduardo Martín-Martínez, Eric G. Brown, William Donnelly, and Achim Kempf. Sustainable entanglement production from a quantum field. *Physical Review A*, 88(5), nov 2013. doi:10.1103/physreva.88.052310. 21

[93] Eric G Brown, William Donnelly, Achim Kempf, Robert B Mann, Eduardo Martín-Martínez, and Nicolas C Menicucci. Quantum seismology. *New Journal of Physics*, 16(10):105020, oct 2014. doi:10.1088/1367-2630/16/10/105020. 21

[94] Richard Lopp and Eduardo Martín-Martínez. Light, matter, and quantum randomness generation: A relativistic quantum information perspective. *Optics Communications*, 423:29–47, sep 2018. doi:10.1016/j.optcom.2018.03.056. 21

[95] Petar Simidzija and Eduardo Martín-Martínez. Information carrying capacity of a cosmological constant. *Physical Review D*, 95(2), jan 2017. doi:10.1103/physrevd.95.025002. 21

[96] Eduardo Martín-Martínez and Nicolas C Menicucci. Entanglement in curved spacetimes and cosmology. *Classical and Quantum Gravity*, 31(21):214001, oct 2014. doi:10.1088/0264-9381/31/21/214001. 21

[97] B L Hu, Shih-Yuin Lin, and Jorma Louko. Relativistic quantum information in detectors–field interactions. *Classical and Quantum Gravity*, 29(22):224005, oct 2012. doi:10.1088/0264-9381/29/22/224005.

[98] E. Martin-Martinez. Relativistic quantum information: developments in quantum information in general relativistic scenarios, 2011. 21

[99] John Earman. The unruh effect for philosophers. *Studies in History and Philosophy of Science Part B: Studies in History and Philosophy of Modern Physics*, 42(2):81–97, 2011. 21

[100] James Ladyman. Structural realism. In Edward N. Zalta, editor, *The Stanford Encyclopedia of Philosophy*. Metaphysics Research Lab, Stanford University, winter 2016 edition, 2016.

[101] Steven French. Identity and individuality in quantum theory. In Edward N. Zalta, editor, *The Stanford Encyclopedia of Philosophy*. Metaphysics Research Lab, Stanford University, fall 2015 edition, 2015. 21

[102] Mark Srednicki. Entropy and area. *Physical Review Letters*, 71(5):666–669, aug 1993. doi:10.1103/physrevlett.71.666. 22

[103] Christoph Holzhey, Finn Larsen, and Frank Wilczek. Geometric and renormalized entropy in conformal field theory. *Nuclear Physics B*, 424(3):443–467, aug 1994. doi:10.1016/0550-3213(94)90402-2. 22

[104] Achim Kempf. Fields over unsharp coordinates. *Physical Review Letters*, 85(14):2873–2876, oct 2000. doi:10.1103/physrevlett.85.2873. 23

[105] Achim Kempf and Robert Martin. Information theory, spectral geometry, and quantum gravity. *Physical Review Letters*, 100(2), jan 2008. doi:10.1103/physrevlett.100.021304.

[106] Michael McGuigan. Finite black hole entropy and string theory. *Physical Review D*, 50(8):5225–5231, oct 1994. doi:10.1103/physrevd.50.5225. 23

[107] Rafael D Sorkin and Yasaman K Yazdi. Entanglement entropy in causal set theory. *Classical and Quantum Gravity*, 35(7):074004, mar 2018. doi:10.1088/1361-6382/aab06f. 23

[108] Steven Johnston. Correction terms for propagators and d'alembertians due to spacetime discreteness. *Classical and Quantum Gravity*, 32(19):195020, sep 2015. doi:10.1088/0264-9381/32/19/195020. 23

[109] D. H. Douglass and R. Meservey. Energy gap measurements by tunneling between superconducting films. i. temperature dependence. *Physical Review*, 135(1A):A19–A23, jul 1964. doi:10.1103/physrev.135.a19. 23

[110] Sebastian Schlicht. Considerations on the unruh effect: causality and regularization. *Classical and Quantum Gravity*, 21(19):4647–4660, sep 2004. doi:10.1088/0264-9381/21/19/011. 23

[111] Paul Langlois. Causal particle detectors and topology. *Annals of Physics*, 321(9):2027–2070, sep 2006. doi:10.1016/j.aop.2006.01.013. 23

[112] Álvaro M. Alhambra, Achim Kempf, and Eduardo Martín-Martínez. Casimir forces on atoms in optical cavities. *Physical Review A*, 89(3), mar 2014. doi:10.1103/physreva.89.033835. 23

[113] Eduardo Martín-Martínez, Miguel Montero, and Marco del Rey. Wavepacket detection with the unruh-DeWitt model. *Physical Review D*, 87(6), mar 2013. doi:10.1103/physrevd.87.064038. 23

[114] Eduardo Martin-Martinez and Pablo Rodriguez-Lopez. Relativistic quantum optics: On the relativistic invariance of the light-matter interaction models. doi:10.1103/PhysRevD.97.105026. 23

[115] Shin Takagi. Vacuum noise and stress induced by uniform acceleration: Hawking-unruh effect in rindler manifold of arbitrary dimension. *Progress of Theoretical Physics Supplement*, 88:1–142, 1986. 23

[116] Dionigi M T Benincasa, Leron Borsten, Michel Buck, and Fay Dowker. Quantum information processing and relativistic quantum fields. *Classical and Quantum Gravity*, 31(7):075007, mar 2014. doi:10.1088/0264-9381/31/7/075007. 23

[117] Antony Richard Lee. *Localised systems in relativistic quantum information*. PhD thesis, University of Nottingham, 2013. 28

[118] I. Chiorescu, P. Bertet, K. Semba, Y. Nakamura, C. J. P. M. Harmans, and J. E. Mooij. Coherent dynamics of a flux qubit coupled to a harmonic oscillator. *Nature*, 431(7005):159–162, sep 2004. doi:10.1038/nature02831. 29

[119] Jonas Bylander, Simon Gustavsson, Fei Yan, Fumiki Yoshihara, Khalil Harrabi, George Fitch, David G. Cory, Yasunobu Nakamura, Jaw-Shen Tsai, and William D. Oliver. Noise spectroscopy through dynamical decoupling with a superconducting flux qubit. *Nature Physics*, 7(7):565–570, may 2011. doi:10.1038/nphys1994.

[120] M. Stern, G. Catelani, Y. Kubo, C. Grezes, A. Bienfait, D. Vion, D. Esteve, and P. Bertet. Flux qubits with long coherence times for hybrid quantum circuits. *Physical Review Letters*, 113(12), sep 2014. doi:10.1103/physrevlett.113.123601.

[121] J.-L. Orgiazzi, C. Deng, D. Layden, R. Marchildon, F. Kitapli, F. Shen, M. Bal, F. R. Ong, and A. Lupascu. Flux qubits in a planar circuit quantum electrodynamics architecture: Quantum control and decoherence. *Physical Review B*, 93(10), mar 2016. doi:10.1103/physrevb.93.104518. 29

[122] Chunqing Deng, Jean-Luc Orgiazzi, Feiruo Shen, Sahel Ashhab, and Adrian Lupascu. Observation of floquet states in a strongly driven artificial atom. *Physical Review Letters*, 115(13), sep 2015. doi:10.1103/physrevlett.115.133601. 30, 43

[123] J. Raftery, A. Vrajitoarea, G. Zhang, Z. Leng, S. J. Srinivasan, and A. A. Houck. Direct digital synthesis of microwave waveforms for quantum computing, 2017. 30

[124] Judith Marshall. Tailings dam spills at mount polley and mariana chronicles of disasters foretold, 2018. URL https://www.policyalternatives.ca/sites/default/files/uploads/publications/BC%20Office/2018/08/CCPA-BC_TailingsDamSpills.pdf. 48

[125] Flávio Fonseca do Carmo, Luciana Hiromi Yoshino Kamino, Rogério Tobias Junior, Iara Christina de Campos, Felipe Fonseca do Carmo, Guilherme Silvino, Kenedy Junio da Silva Xavier de Castro, Mateus Leite Mauro, Nelson Uchoa Alonso Rodrigues, Marcos Paulo de Souza Miranda, and Carlos Eduardo Ferreira Pinto. Fundão tailings dam failures: the environment tragedy of the largest technological disaster of brazilian mining in global context. *Perspectives in Ecology and Conservation*, 15(3):145–151, jul 2017. doi:10.1016/j.pecon.2017.06.002. 48

[126] Christopher J. Ayres. The international trade in conflict minerals: coltan. *Critical perspectives on international business*, 8(2):178–193, may 2012. doi:10.1108/17422041211230730. 48

[127] Hannes Hofmann, Martin C. Schleper, and Constantin Blome. Conflict minerals and supply chain due diligence: An exploratory study of multi-tier supply chains. *Journal of Business Ethics*, 147(1): 115–141, nov 2015. doi:10.1007/s10551-015-2963-z. 48

[128] Emily Chasan. Corporate news: Conflict-mineral audits barely scratch surface, Sep 19 2014. URL http://search.proquest.com.proxy.lib.uwaterloo.ca/docview/1562988447?accountid=14906. Name - Intel Corp; Schulte Roth & Zabel; EY Global Services Ltd; Copyright - (c) 2014 Dow Jones & Company, Inc. Reproduced with permission of copyright owner. Further reproduction or distribution is prohibited without permission; Last updated - 2017-11-21.

[129] Colin Fitzpatrick, Elsa Olivetti, T. Reed Miller, Richard Roth, and Randolph Kirchain. Conflict minerals in the compute sector: Estimating extent of tin, tantalum, tungsten, and gold use in ICT products. *Environmental Science & Technology*, 49(2):974–981, dec 2014. doi:10.1021/es501193k.

[130] Iain Marlow and Omar el Akkad. Smartphones: Blood stains at our fingertips. The Globe and Mail, 2010. URL https://www.theglobeandmail.com/technology/smartphones-blood-stains-at-our-fingertips/article1318713/. [Online - accessed Nov 9-18].

[131] Ngombe Leon-Kabamba, Nlandu Roger Ngatu, Sakatolo Jean-Baptiste Kakoma, Christophe Nyembo, Etongola Papy Mbelambela, Reiko Juliana Moribe, Stanislas Wembonyama, Brigitta Danuser, and Numbi Oscar-Luboya. Respiratory health of dust-exposed congolese coltan miners. *International Archives of Occupational and Environmental Health*, 91(7):859–864, jun 2018. doi:10.1007/s00420-018-1329-0. 48

[132] Brian Merchant. *"Life and death in Apples forbidden city" in The One Device: The Secret History of the iPhone*. LITTLE BROWN & CO INC, 2017. ISBN 031654616X. URL https://www.theguardian.com/technology/2017/jun/18/foxconn-life-death-forbidden-city-longhua-suicide-apple-iphone-brian-merchant-one-device-extrac [content warning: suicide]. 48

[133] John Goold, Marcus Huber, Arnau Riera, Lídia del Rio, and Paul Skrzypczyk. The role of quantum information in thermodynamics—a topical review. *J. Phys. A: Math. Theor.*, 49(14):143001, feb 2016. doi:10.1088/1751-8113/49/14/143001. 52, 58

[134] Sai Vinjanampathy and Janet Anders. Quantum thermodynamics. *Contemporary Physics*, 57(4): 545–579, jul 2016. doi:10.1080/00107514.2016.1201896. 52

[135] F. Binder, L. A. Correa, C. Gogolin, J. Anders, and G. Adesso, editors. *Thermodynamics in the Quantum Regime: Recent Progree and Outlook*. Springer International Publishing, 2018. ISBN 978-3-319-99046-0. 52

[136] Elisa Bäumer, Matteo Lostaglio, Mart Perarnau-Llobet, and Rui Sampaio. Fluctuating work in coherent quantum systems: proposals and limitations. 52, 54, 57, 60, 81, 85

[137] O. J. E. Maroney. The physical basis of the gibbs-von neumann entropy. 52, 57

[138] Michele Campisi and Peter Hnggi. Comment on "experimental verification of a jarzynski-related information-theoretic equality by a single trapped ion". *Physical Review Letters*, 121(8), aug 2018. doi:10.1103/physrevlett.121.088901. 52

[139] David Wallace. Thermodynamics as control theory. *Entropy*, 16(2):699–725, jan 2014. doi:10.3390/e16020699.

[140] Manabendra Nath Bera, Andreas Winter, and Maciej Lewenstein. Thermodynamics from information. 52

[141] Alvaro M. Alhambra, Lluis Masanes, Jonathan Oppenheim, and Christopher Perry. Fluctuating work: From quantum thermodynamical identities to a second law equality. *Phys. Rev. X*, 6(4):–, oct 2016. doi:10.1103/physrevx.6.041017. 52, 62

[142] A. E. Allahverdyan. Nonequilibrium quantum fluctuations of work. *Physical Review E*, 90(3), sep 2014. doi:10.1103/physreve.90.032137. 52, 61

[143] Peter Talkner, Eric Lutz, and Peter Hänggi. Fluctuation theorems: Work is not an observable. *Phys. Rev. E*, 75(5):–, may 2007. doi:10.1103/physreve.75.050102. 52, 54, 57, 58, 61

[144] Jonathan Oppenheim, Michał Horodecki, Paweł Horodecki, and Ryszard Horodecki. Thermodynamical approach to quantifying quantum correlations. *Physical Review Letters*, 89(18), oct 2002. doi:10.1103/physrevlett.89.180402. 52, 65

[145] R. Dillenschneider and E. Lutz. Energetics of quantum correlations. *EPL (Europhysics Letters)*, 88 (5):50003, dec 2009. doi:10.1209/0295-5075/88/50003.

[146] Sania Jevtic, David Jennings, and Terry Rudolph. Quantum mutual information along unitary orbits. *Phys. Rev. A*, 85(5):–, may 2012. doi:10.1103/physreva.85.052121. 52, 65

[147] Sania Jevtic, David Jennings, and Terry Rudolph. Maximally and minimally correlated states attainable within a closed evolving system. *Phys. Rev. Lett.*, 108(11):–, mar 2012. doi:10.1103/physrevlett.108.110403. 52

[148] Ken Funo, Yu Watanabe, and Masahito Ueda. Thermodynamic work gain from entanglement. *Phys. Rev. A*, 88(5):–, nov 2013. doi:10.1103/physreva.88.052319. 65

[149] Marcus Huber, Martí Perarnau-Llobet, Karen V Hovhannisyan, Paul Skrzypczyk, Claude Klöckl, Nicolas Brunner, and Antonio Acín. Thermodynamic cost of creating correlations. *New J. Phys.*, 17(6):065008, jun 2015. doi:10.1088/1367-2630/17/6/065008. 52, 68, 70, 71, 72, 73, 74, 84, 107, 113

[150] David Edward Bruschi, Martí Perarnau-Llobet, Nicolai Friis, Karen V. Hovhannisyan, and Marcus Huber. Thermodynamics of creating correlations: Limitations and optimal protocols. *Phys. Rev. E*, 91(3):–, mar 2015. doi:10.1103/physreve.91.032118. 52, 69, 74, 85

[151] Nicolai Friis, Marcus Huber, and Martí Perarnau-Llobet. Energetics of correlations in interacting systems. *Phys. Rev. E*, 93(4):–, apr 2016. doi:10.1103/physreve.93.042135. 52, 65, 69

[152] Jorge Kurchan. A quantum fluctuation theorem. 54, 58

[153] A. E. Allahverdyan and Th. M. Nieuwenhuizen. Fluctuations of work from quantum subensembles: The case against quantum work-fluctuation theorems. *Phys. Rev. E*, 71(6):–, jun 2005. doi:10.1103/physreve.71.066102. 54, 59, 60, 61

[154] Daniel V. Schroeder. *An Introduction to Thermal Physics*. Pearson, 1999. ISBN 0-201-38027-7. URL https://www.amazon.com/Introduction-Thermal-Physics-Daniel-Schroeder/dp/0201380277?SubscriptionId=AKIAIOBINVZYXZQZ2U3A&tag=chimbori05-20&linkCode=xm2&camp=2025&creative=165953&creativeASIN=0201380277. 55

[155] C. Jarzynski. Nonequilibrium equality for free energy differences. *Physical Review Letters*, 78(14): 2690–2693, apr 1997. doi:10.1103/physrevlett.78.2690. 55, 56

[156] José Hoyos. Nonequilibrium microthermodynamics, 2016. URL http://www.ifsc.usp.br/~hoyos/courses/2016/FCI0319/Jarzynski.pdf. 57

[157] Martí Perarnau-Llobet, Elisa Bumer, Karen V. Hovhannisyan, Marcus Huber, and Antonio Acín. No-go theorem for the characterization of work fluctuations in coherent quantum systems. *Phys. Rev. Lett.*, 118(7):–, feb 2017. doi:10.1103/physrevlett.118.070601. 57, 60, 61

[158] Meir Hemmo and Orly Shenker. Von neumann's entropy does not correspond to thermodynamic entropy. *Philosophy of Science*, 73(2):153–174, apr 2006. doi:10.1086/510816. 57

[159] Martí Perarnau-Llobet, Karen V. Hovhannisyan, Marcus Huber, Paul Skrzypczyk, Nicolas Brunner, and Antonio Acín. Extractable work from correlations. *Phys. Rev. X*, 5(4):–, oct 2015. doi:10.1103/physrevx.5.041011. 59, 68

[160] Yelena Guryanova, Nicolai Friis, and Marcus Huber. Ideal projective measurements have an infinite energy cost. 59

[161] Nicolai Friis and Marcus Huber. Precision and work fluctuations in gaussian battery charging. *Quantum*, 2:61, apr 2018. doi:10.22331/q-2018-04-23-61. 60, 85

[162] Wolfgang Niedenzu, Victor Mukherjee, Arnab Ghosh, Abraham G. Kofman, and Gershon Kurizki. Quantum engine efficiency bound beyond the second law of thermodynamics. *Nature Communications*, 9(1), jan 2018. doi:10.1038/s41467-017-01991-6. 60

[163] Gabriele De Chiara, Augusto J Roncaglia, and Juan Pablo Paz. Measuring work and heat in ultracold quantum gases. *New Journal of Physics*, 17(3):035004, mar 2015. doi:10.1088/1367-2630/17/3/035004. 61

[164] Augusto J. Roncaglia, Federico Cerisola, and Juan Pablo Paz. Work measurement as a generalized quantum measurement. *Physical Review Letters*, 113(25), dec 2014. doi:10.1103/physrevlett.113.250601. 61

[165] Takahiro Sagawa. Second law-like inequalities with quantum relative entropy: An introduction. In *Kinki University Series on Quantum Computing*, pages 125–190. World Scientific, oct 2012. URL arxiv.org/abs/1202.0983. 61

[166] Nelly Ng and Mischa P. Woods. Resource theory of quantum thermodynamics: Thermal operations and second laws. 62

[167] Isaac L. Chuang Michael A. Nielsen. *Quantum Computation and Quantum Information*. Cambridge University Pr., 2001. ISBN 1107002176. URL https://www.ebook.de/de/product/13055864/michael_a_nielsen_isaac_l_chuang_quantum_computation_and_quantum_information.html. 65, 67

[168] Wojciech Hubert Zurek. Quantum discord and maxwell's demons. *Physical Review A*, 67(1), jan 2003. doi:10.1103/physreva.67.012320. 65

[169] Oscar C O Dahlsten, Renato Renner, Elisabeth Rieper, and Vlatko Vedral. Inadequacy of von neumann entropy for characterizing extractable work. *New Journal of Physics*, 13(5):053015, may 2011. doi:10.1088/1367-2630/13/5/053015. 65

[170] John St. Bell J. S. Bell. *Speakable and Unspeakable in Quantum Mechanics*. Cambridge University Press, 2004. ISBN 0521523389. URL https://www.ebook.de/de/product/2991829/j_s_bell_john_st_bell_speakable_and_unspeakable_in_quantum_mechanics.html. 66

[171] John F. Clauser, Michael A. Horne, Abner Shimony, and Richard A. Holt. Proposed experiment to test local hidden-variable theories. *Physical Review Letters*, 23(15):880–884, oct 1969. doi:10.1103/physrevlett.23.880. 66

[172] Fumiaki Morikoshi, Marcelo Franca Santos, and Vlatko Vedral. Accessibility of physical states and non-uniqueness of entanglement measure. doi:10.1088/0305-4470/37/22/013. 66

[173] Adam Miranowicz and Andrzej Grudka. Ordering two-qubit states with concurrence and negativity. *Physical Review A*, 70(3), sep 2004. doi:10.1103/physreva.70.032326. 66

[174] Bob Coecke, Tobias Fritz, and Robert W. Spekkens. A mathematical theory of resources. *Information and Computation*, 250:59–86, oct 2016. doi:10.1016/j.ic.2016.02.008. 67

[175] Harold Ollivier and Wojciech H. Zurek. Quantum discord: A measure of the quantumness of correlations. *Physical Review Letters*, 88(1), dec 2001. doi:10.1103/physrevlett.88.017901. 67

[176] Vlatko Vedral. Foundations of quantum discord. 67

[177] Helena C. Braga, Clodoaldo C. Rulli, Thiago R. de Oliveira, and Marcelo S. Sarandy. Maxwell's demons in multipartite quantum correlated systems. *Physical Review A*, 90(4), oct 2014. doi:10.1103/physreva.90.042338. 67

[178] Tan Kok Chuan Bobby and Tomasz Paterek. Separable states improve protocols with finite randomness. *New Journal of Physics*, 16(9):093063, sep 2014. doi:10.1088/1367-2630/16/9/093063. 67

[179] Gian Luca Giorgi. Quantum discord and remote state preparation. *Physical Review A*, 88(2), aug 2013. doi:10.1103/physreva.88.022315. 67

[180] Zhaohui Wei and Shengyu Zhang. Quantum game players can have advantage without discord. 67

[181] Kavan Modi, Aharon Brodutch, Hugo Cable, Tomasz Paterek, and Vlatko Vedral. The classical-quantum boundary for correlations: Discord and related measures. *Reviews of Modern Physics*, 84 (4):1655–1707, nov 2012. doi:10.1103/revmodphys.84.1655. 67

[182] Eric G. Brown, Eric J. Webster, Eduardo Martín-Martínez, and Achim Kempf. Purified discord and multipartite entanglement. *Annals of Physics*, 337:153–162, oct 2013. doi:10.1016/j.aop.2013.06.015. 67

[183] Borivoje Dakić, Yannick Ole Lipp, Xiaosong Ma, Martin Ringbauer, Sebastian Kropatschek, Stefanie Barz, Tomasz Paterek, Vlatko Vedral, Anton Zeilinger, Časlav Brukner, and Philip Walther. Quantum discord as resource for remote state preparation. *Nature Physics*, 8(9):666–670, aug 2012. doi:10.1038/nphys2377. 67

[184] L Henderson and V Vedral. Classical, quantum and total correlations. *Journal of Physics A: Mathematical and General*, 34(35):6899–6905, aug 2001. doi:10.1088/0305-4470/34/35/315. 67

[185] T. Ando. Majorization, doubly stochastic matrices, and comparison of eigenvalues. *Linear Algebra Appl.*, 118:163–248, jun 1989. doi:10.1016/0024-3795(89)90580-6. 109

[186] John Watrous. *The Theory of Quantum Information*. Cambridge University Pr., 2018. ISBN 1107180562. URL https://www.ebook.de/de/product/30782492/john_watrous_the_theory_of_quantum_information.html. 109

[187] Giuseppe Vitagliano, Claude Klöckl, Marcus Huber, and Nicolai Friis. Trade-off between work and correlations in quantum thermodynamics, 2018. 111, 113

[188] Fanny Dufossé and Bora Uçar. Notes on birkhoff–von neumann decomposition of doubly stochastic matrices. *Linear Algebra Appl.*, 497:108–115, may 2016. doi:10.1016/j.laa.2016.02.023. 112

[189] Propagation of uncertainty. Propagation of uncertainty — Wikipedia, the free encyclopedia, 2018. URL https://en.wikipedia.org/wiki/Propagation_of_uncertainty. [Online; accessed 02-March-2018]. 117

APPENDICES

Appendix A

Equivalence of two-time measurement and unprojected scheme work fluctuations when $[\hat{H}, \hat{\rho}] = 0$

In chapter 2, we reviewed two quite different notions of work in a quantum scenario. The two-time energy measurement and the unprojected work schemes do, however, have identical first and second moments when the Hamiltonian commutes with the initial state of the system. Thus, our analysis corresponds to both underlying schemes—they appear to not have significant conceptual difference in this case. In this appendix, we will show concretely that in this case, the expressions for the average work and the work fluctuations in both schemes are identical.

The two-time energy measurement scheme, described in section 2.2.1, constructs a classical probability distribution of work, taking the random variable to be the difference in final and initial eigenenergies of the system. The scheme relies on projective measurements conducted before and after the application of the protocol. The probability distribution is, for a general unitary process $\hat{U}$,

$$P(W) = \sum_{m,n} P(E_n) \left| \langle m| \hat{U} |n\rangle \right|^2 \delta\big(W - (E_m - E_n)\big). \tag{A.0.1}$$

The average work cost is

$$\langle W\rangle_{\mathrm{TT}} = \int \mathrm{d}W\; W\, P(W) \tag{A.0.2}$$

$$= \int \mathrm{d}W\; W \sum_{m,n} P(E_n)\big|\,\langle m|\,\hat{U}\,|n\rangle\,\big|^2 \delta\big(W-(E_m-E_n)\big) \tag{A.0.3}$$

$$= \sum_{m,n} (E_m - E_n) P(E_n)\big|\,\langle m|\,\hat{U}\,|n\rangle\,\big|^2, \tag{A.0.4}$$

where we have integrated over the delta function.

Similarly, the second moment, which is the square of what we have called the fluctuations, is given by

$$\sigma^2_{\mathrm{TT}} = \int \mathrm{d}W\; (W - \langle W\rangle_{\mathrm{TT}})^2 P(W) \tag{A.0.5}$$

$$= \int \mathrm{d}W\; (W^2 - 2W\langle W\rangle_{\mathrm{TT}} + \langle W\rangle^2_{\mathrm{TT}}) P(W) \tag{A.0.6}$$

$$= \int \mathrm{d}W\; W^2 P(W) - 2\langle W\rangle_{\mathrm{TT}} \int \mathrm{d}W\; W\, P(W) + \langle W\rangle^2_{\mathrm{TT}} \tag{A.0.7}$$

$$= \int \mathrm{d}W\; W^2 P(W) - \langle W\rangle^2_{\mathrm{TT}}, \tag{A.0.8}$$

where we have used that $\int \mathrm{d}W\, P(W) = 1$. Substituting in the probability distribution and integrating over W, we obtain

$$\sigma^2_{\mathrm{TT}} = \sum_{m,n} (E_m - E_n)^2 P(E_n)\big|\,\langle m|\,\hat{U}\,|n\rangle\,\big|^2 - \langle W\rangle^2_{\mathrm{TT}}. \tag{A.0.9}$$

The average work cost in the unprojected work scheme is the expectation value of the work operator $\Delta\hat{H} = \hat{U}\hat{H}\hat{U}^\dagger - \hat{H}$:

$$\langle W\rangle_{\mathrm{UP}} = \mathrm{Tr}[\Delta\hat{H}\hat{\rho}]. \tag{A.0.10}$$

The second moment is the variance of this operator,

$$\sigma^2_{\mathrm{UP}} = \mathrm{Tr}[\Delta\hat{H}^2\hat{\rho}] - \mathrm{Tr}[\Delta\hat{H}\hat{\rho}]^2. \tag{A.0.11}$$

Starting from these equations, we will now show the equivalence of the first and second moments of both schemes in the case where $[\hat{H}, \hat{\rho}] = 0$.

We will write the energy eigenbasis as $\{|n\rangle\}$, the Hamiltonian as $\hat{H} = \sum_n E_n |n\rangle\langle n|$, and the initial diagonal state as $\hat{\rho} = \sum_n \rho_n |n\rangle\langle n|$ (so that $P(E_n) = \rho_n$). Let us expand the trace in the expectation value of the work operator,

$$\langle W\rangle_{\mathrm{UP}} = \mathrm{Tr}[\Delta\hat{H}\hat{\rho}] = \sum_n \langle n|\,(\hat{U}\hat{H}\hat{U}^\dagger - \hat{H})\hat{\rho}\,|n\rangle\,, \tag{A.0.12}$$

and write the spectral decomposition of the Hamiltonian,

$$\mathrm{Tr}[\Delta\hat{H}\hat{\rho}] = \sum_{n,m} \langle n|\,\hat{U}E_m\,|m\rangle\langle m|\,\hat{U}^\dagger\hat{\rho}\,|n\rangle - \langle n|\,E_m\,|m\rangle\langle n|\,\hat{\rho}\,|n\rangle\,, \tag{A.0.13}$$

and the initial state,

$$\begin{aligned}
\mathrm{Tr}[\Delta\hat{H}\hat{\rho}] &= \sum_{n,m,i} \langle n|\,\hat{U}E_m\,|m\rangle\langle m|\,\hat{U}^\dagger\rho_i\,|i\rangle\langle i|n\rangle - \langle n|\,E_m\,|m\rangle\langle n|\,\rho_i\,|i\rangle\langle i|n\rangle && \text{(A.0.14)}\\
&= \sum_{n,m} \langle n|\,\hat{U}E_m\,|m\rangle\langle m|\,\hat{U}^\dagger\rho_n\,|n\rangle - \langle n|\,E_m\,|m\rangle\langle m|\,\rho_n\,|n\rangle && \text{(A.0.15)}\\
&= \sum_{n,m} E_m\rho_n\big|\,\langle m|\,\hat{U}\,|n\rangle\,\big|^2 - \sum_n \langle n|\,E_n\rho_n\,|n\rangle && \text{(A.0.16)}\\
&= \sum_{n,m} E_m\rho_n\big|\,\langle m|\,\hat{U}\,|n\rangle\,\big|^2 - \sum_n \langle n|\,E_n\rho_n\hat{U}\hat{U}^\dagger\,|n\rangle && \text{(A.0.17)}\\
&= \sum_{n,m} E_m\rho_n\big|\,\langle m|\,\hat{U}\,|n\rangle\,\big|^2 - \langle n|\,E_n\rho_n\hat{U}\,|m\rangle\langle m|\,\hat{U}^\dagger\,|n\rangle && \text{(A.0.18)}\\
&= \sum_{n,m} (E_m - E_n)\rho_n\big|\,\langle m|\,\hat{U}\,|n\rangle\,\big|^2 = \langle W\rangle_{\mathrm{TT}}. && \text{(A.0.19)}
\end{aligned}$$

In the third from last line, we used that $\hat{U}\hat{U}^\dagger = \mathbb{1}$; in the second from last line, we used that $\sum_m |m\rangle\langle m| = \mathbb{1}$. Thus, the average work cost in the unprojected scheme is equal to that of the two-time measurement scheme (A.0.4) when the initial state is diagonal in the energy eigenbasis.

Now for the second moment. Let us again start from the definition for the unprojected work scheme:

$$\begin{aligned}
\sigma_{\mathrm{UP}} &= \mathrm{Tr}[\Delta\hat{H}^2\hat{\rho}] - \mathrm{Tr}[\Delta\hat{H}\hat{\rho}]^2 && \text{(A.0.20)}\\
&= \mathrm{Tr}[\Delta\hat{H}^2\hat{\rho}] - \langle W\rangle^2_{\mathrm{UP}}. && \text{(A.0.21)}
\end{aligned}$$

We already know that $\langle W \rangle_{\mathrm{UP}} = \langle W \rangle_{\mathrm{TT}}$ in this case, so let's focus on the first term. First, expand $\Delta \hat{H}^2$

$$\mathrm{Tr}[\Delta \hat{H}^2 \hat{\rho}] = \mathrm{Tr}[(\hat{U}\hat{H}\hat{U}^\dagger - \hat{H})^2 \hat{\rho}] \tag{A.0.22}$$

$$= \mathrm{Tr}[(\hat{U}\hat{H}\hat{U}^\dagger \hat{U}\hat{H}\hat{U}^\dagger - \hat{H}\hat{U}\hat{H}\hat{U}^\dagger - \hat{U}\hat{H}\hat{U}^\dagger \hat{H} + \hat{H}^2)\hat{\rho}] \tag{A.0.23}$$

$$= \mathrm{Tr}[\hat{U}\hat{H}^2\hat{U}^\dagger \hat{\rho}] - \mathrm{Tr}[\hat{H}\hat{U}\hat{H}\hat{U}^\dagger \hat{\rho}] - \mathrm{Tr}[\hat{U}\hat{H}\hat{U}^\dagger \hat{H}\hat{\rho}] + \mathrm{Tr}[\hat{H}^2\hat{\rho}]. \tag{A.0.24}$$

The middle two terms are equal if $[\hat{H}, \hat{\rho}] = 0$:

$$\mathrm{Tr}[\Delta \hat{H}^2 \hat{\rho}] = \mathrm{Tr}[\hat{U}\hat{H}^2\hat{U}^\dagger \hat{\rho}] - 2\mathrm{Tr}[\hat{U}\hat{H}\hat{U}^\dagger \hat{H}\hat{\rho}] + \mathrm{Tr}[\hat{H}^2\hat{\rho}]. \tag{A.0.25}$$

Now, expand the trace, and substitute in the spectral decomposition of the Hamiltonian (noting that $\hat{H}^2 = \sum_n E_n^2 |n\rangle \langle n|$):

$$\mathrm{Tr}[\Delta \hat{H}^2 \hat{\rho}] = \sum_{n,m,i} \langle n| \hat{U} E_m^2 |m\rangle \langle m| \hat{U}^\dagger \hat{\rho} |n\rangle - 2 \langle n| \hat{U} E_m |m\rangle \langle m| \hat{U}^\dagger E_i |i\rangle \langle i| \hat{\rho} |n\rangle + \langle n| E_m^2 |m\rangle \langle m| \hat{\rho} |n\rangle . \tag{A.0.26}$$

Substituting in the spectral decomposition of the initial state, the terms simplify in much the same way as for the average work:

$$\mathrm{Tr}[\Delta \hat{H}^2 \hat{\rho}] = \sum_{n,m} E_m^2 \rho_n \big| \langle m| \hat{U} |n\rangle \big|^2 - 2E_m E_n \rho_n \big| \langle m| \hat{U} |n\rangle \big|^2 + E_n^2 \rho_n \big| \langle m| \hat{U} |n\rangle \big|^2 \tag{A.0.27}$$

$$= \sum_{n,m} (E_m - E_n)^2 \rho_n \big| \langle m| \hat{U} |n\rangle \big|^2, \tag{A.0.28}$$

so that the second moment of the unprojected scheme is

$$\sigma_{\mathrm{UP}} = \sum_{n,m} (E_m - E_n)^2 \rho_n \big| \langle m| \hat{U} |n\rangle \big|^2 - \langle W \rangle_{\mathrm{UP}}^2 \tag{A.0.29}$$

$$= \sigma_{\mathrm{TT}}. \tag{A.0.30}$$

This completes the demonstration that the first and second moments of work in the two-time measurement and unprojected schemes are identical when the initial state commutes with the Hamiltonian.

Appendix B

Proof of the existence of the correlating unitary $\hat{U}_{\mathbf{corr}}$

In this appendix, we provide a detailed restatement of the proof in Appendix A.1 of [149], which proves that the correlating unitary we use acts as we claim. Namely, we wish to show that, for a bipartite system of dimension d^2 composed of two subsystems A and B, of local dimension d, a unitary consisting of rotations in the subspaces spanned by the generalized Bell states (4.2.3),

$$S_j = \text{span}\left\{ |\phi_{0,j}\rangle, |\phi_{1,j}\rangle, \ldots, |\phi_{d,j}\rangle \right\}, \tag{B.0.1}$$

will transform a global thermal state of inverse temperature β_{in} to a local Gibbs state of some local inverse temperature β_{out}. Additionally, we will show that the unitary may be tailored to reach a specific final temperature.

Under the assumption that there is no interaction Hamiltonian between the two parts of the system, we will work in the eigenbasis of the local Hamiltonians that we notate as $\{|ij\rangle\}$.

Let us first summarize the steps of the proof. We will begin by showing that the action of rotating the initial global thermal state in the subspaces S_j produces global coherences in the energy eigenbasis, but no local coherences. This proves that the action of the unitary takes global thermal states to locally diagonal states (a necessary condition for the local final states to be Gibbs). We will deduce, then, that the action of the global unitary on the local subsystems may be described by a particular type of transformation called circulant doubly stochastic transformation (CDST). We use this to rewrite the global unitary action on the subsystems in terms of a general CDST. Rewriting the general transformation in

this way will allow for the calculation of the specific map needed to take a global thermal state of inverse temperature β_{in} to a local Gibbs state of inverse temperature β_{out}.

Let us briefly review notation. We call the initial global state $\hat{\rho}$. This is a global thermal state. The global state after the application of the unitary is $\hat{\rho}'$, generally not in a global Gibbs state. The local states of subsystem A and B are denoted $\hat{\rho}_{\text{A}}$ and $\hat{\rho}_{\text{B}}$, with primes similarly denoting the local states after application of the unitary. We notate matrix elements of $\hat{\rho}$ as follows

$$\hat{\rho} = \sum_{i,j,k,l=0}^{d-1} \rho_{ij,kl} \left|ij\right\rangle \left\langle kl\right| . \tag{B.0.2}$$

Since there is some amount of index gymnastics in this appendix, when the value of an index gets too long we use a bracket notation like $\rho_{(d-1)(d-1),(d-1)(d-1)}$ to separate the first and second indices and the third and fourth indices. Matrix elements of the state $\hat{\rho}_{\text{A}}$ are denoted by $\alpha_{i,j}$. They are given by partial tracing system B from the bipartite density matrix $\hat{\rho}$:

$$\alpha_{i,j} = \sum_{k=0}^{d-1} \rho_{ik,jk}. \tag{B.0.3}$$

Now, the action of the unitary on the global state is to mix elements within each subspace S_j. A particular rotation in a subspace S_j will, in general, act on elements of the form

$$\rho_{n(n+j),m(m+j)}. \tag{B.0.4}$$

For example, consider rotations in the subspace S_1. This is the space spanned by the generalized Bell states

$$\left|\phi_{n,1}\right\rangle = \sum_{k=0}^{d-1} \mathrm{e}^{2k\pi \mathrm{i}/d} \left|k\right\rangle \left|k+1\right\rangle . \tag{B.0.5}$$

or

$$\begin{aligned}
\left|\phi_{0,1}\right\rangle &= \frac{1}{\sqrt{d}}\big(\left|01\right\rangle + \left|12\right\rangle + \left|23\right\rangle + \cdots \big), \\
\left|\phi_{1,1}\right\rangle &= \frac{1}{\sqrt{d}}\big(\left|01\right\rangle + \mathrm{e}^{2\pi \mathrm{i}/d} \left|12\right\rangle + \mathrm{e}^{4\pi \mathrm{i}/d} \left|23\right\rangle + \cdots \big), \\
\left|\phi_{2,1}\right\rangle &= \frac{1}{\sqrt{d}}\big(\left|01\right\rangle + \mathrm{e}^{4\pi \mathrm{i}/d} \left|12\right\rangle + \mathrm{e}^{8\pi \mathrm{i}/d} \left|23\right\rangle + \cdots \big), \\
&\vdots
\end{aligned} \tag{B.0.6}$$

and so on. The action of rotating in S_1 will only affect density matrix elements like $\rho_{01,01}$, $\rho_{01,23}$, $\rho_{23,12}$, ..., or, in general, matrix elements of the form $\rho_{n(n+1),m(m+1)}$.

We wish to show that the off-diagonal elements of $\hat{\rho}'$ do not contribute to the partial trace, ensuring that the local states $\hat{\rho}'_{\mathrm{A}}$ and $\hat{\rho}'_{\mathrm{B}}$ maintain their diagonal nature, i.e., the unitary does not create coherences in the local states. To prove this we will use the observation made above.

Since the initial global state is thermal, it is diagonal in the Hamiltonian eigenbasis. That implies that matrix elements of the global state which are non-zero after application of the unitary are of the form $\rho'_{n(n+j),m(m+j)}$, and matrix elements contributing to the local state $\hat{\rho}'_{\mathrm{A}}$ are of the form $\rho'_{ik,jk}$. Thus, the matrix elements of the final global state which are both nonzero and contribute to the local state have $n+j=m+j$, i.e. $n=m$, that is, diagonal elements of $\hat{\rho}'$. Global diagonal matrix elements only contribute to local matrix elements which are also diagonal. Thus, the action of the unitary on a global thermal state does not create coherences in the local states. Hence, since the local states were initially diagonal (because the systems are non-interacting) then the local states remain diagonal after the application of the unitary.

To continue the proof, let us introduce the notion of doubly-stochastic transformations. A matrix T is doubly stochastic in a given basis if and only if its matrix elements satisfy

$$T_{ij} > 0 \qquad \text{and} \tag{B.0.7}$$

$$\sum_i T_{ij} = \sum_j T_{ij} = 1. \tag{B.0.8}$$

A stochastic transformation of a vector preserves the sum of its components: considering $x = Ty$ for x and $y \in \mathbb{R}^d$, we have that

$$\begin{aligned} \sum_{i=0}^{d-1} x_i &= \sum_{i,j=0}^{d-1} T_{ij} y_j \\ &= \sum_{j=0}^{d-1} y_j \left(\sum_{i=0}^{d-1} T_{ij} \right) \\ &= \sum_{j=0}^{d-1} y_j. \end{aligned} \tag{B.0.9}$$

In fact, all matrices which preserve the sum of vector elements satisfy $\sum_i T_{ij} = 1$ [185]. The final property, $\sum_j T_{ij} = 1$, is the defining characteristic of unital matrices, that is, matrices whose action preserves the 'fully mixed' vector $[1, 1, \ldots, 1]^\intercal$ [186].

A global unitary transformation on $\hat{\rho}$ preserves its trace. All unitary transformations are also unital. This implies that the diagonals of the global state undergo a doubly stochastic transformation, that is,

$$\mathrm{diag}(\hat{\rho}') = T\,\mathrm{diag}(\hat{\rho}), \tag{B.0.10}$$

where $\mathrm{diag}(\hat{\rho}) = [\rho_{00,00}, \rho_{01,01}...]^\intercal$ and T is a doubly stochastic matrix. This will be useful for the rest of the proof.

Indeed, we can further visualize the action of the unitary through the fact that the rotations in each subspace S_j only act on diagonal matrix elements $\rho_{n(n+j),n(n+j)}$, $n = 0, \ldots, d-1$. We thus have that the unitary implements doubly stochastic transformations on each set of diagonal matrix elements belonging to different subspaces S_j:

$$\begin{bmatrix} \rho'_{0j,0j} \\ \rho'_{1(1+j),1(1+j)} \\ \vdots \\ \rho'_{(d-1)(d-1+j),(d-1)(d-1+j)} \end{bmatrix} = T^{(j)} \begin{bmatrix} \rho_{0j,0j} \\ \rho_{1(1+j),1(1+j)} \\ \vdots \\ \rho_{(d-1)(d-1+j),(d-1)(d-1+j)} \end{bmatrix}, \tag{B.0.11}$$

where $T^{(j)}$ is a doubly stochastic matrix corresponding to the elements belonging to the subspace S_j.

For convenience, let us write a shorthand for the above vectors:

$$\mathrm{diag}(\hat{\rho})_{S_j} = \begin{bmatrix} \rho_{0j,0j} \\ \rho_{1(1+j),1(1+j)} \\ \vdots \\ \rho_{(d-1)(d-1+j),(d-1)(d-1+j)} \end{bmatrix}. \tag{B.0.12}$$

We can actually write the partial trace by summing over these vectors, as

$$\mathrm{diag}(\hat{\rho}_{\mathrm{A}}) = \sum_{j=0}^{d-1} \mathrm{diag}(\hat{\rho})_{S_j}. \tag{B.0.13}$$

To see this, compare the elements of the vectors $\mathrm{diag}(\hat{\rho})_{S_j}$ with the partial trace as in (B.0.3).

Then the action of the unitary on the local state can be finally written as

$$\mathrm{diag}(\hat{\rho}'_{\mathrm{A}}) = \sum_{j=0}^{d-1} T^{(j)}\,\mathrm{diag}(\hat{\rho})_{S_j}. \tag{B.0.14}$$

The action on the second subsystem can be expressed in terms of the same doubly stochastic matrices $T^{(j)}$ by making use of the permutation operator $\Pi = \sum_k |k\rangle |k\rangle \langle k+1| \langle k+1|$, which shifts coefficients $\rho_{ij,kl}$ to apply to different elements as

$$\Pi \rho_{ij,kl} |ij\rangle \langle kl| \Pi^\dagger = \rho_{ij,kl} |(i+i)(j+1)\rangle \langle (k+1)(l+1)| \tag{B.0.15}$$

For the rest of this paper, we will employ a shorthand notation to use with the vector $\mathrm{diag}(\hat{\rho})_{S_j}$ as,

$$\Pi^j \,\mathrm{diag}(\hat{\rho})_{S_j} = \begin{bmatrix} \rho_{(-j)0,(-j)0} \\ \rho_{(1-j)1,(1-j)1} \\ \vdots \\ \rho_{(d-1-j)(d-1),(d-1-j)(d-1)} \end{bmatrix}, \tag{B.0.16}$$

where all indices are taken to be $\bmod d$, so that, for instance $\rho_{(-1)0,(-1)0} = \rho_{(d-1)0,(d-1)0}$. Then the diagonals of subsystem B can be written as

$$\mathrm{diag}(\hat{\rho}_\mathrm{B}) = \sum_{j=0}^{d-1} \Pi^j \,\mathrm{diag}(\hat{\rho})_{S_j}. \tag{B.0.17}$$

We thus write the action of the unitary on the second subsystem as

$$\mathrm{diag}(\hat{\rho}'_\mathrm{B}) = \sum_{j=0}^{d-1} \Pi^j (T^{(j)} \,\mathrm{diag}(\hat{\rho})_{S_j}). \tag{B.0.18}$$

If the action of the specified unitary is symmetric on both subsystems (guaranteed in our case because the local Hamiltonians of both qubits are the same [187]), this directly implies that the doubly stochastic matrices $T^{(j)}$ commute with the permutation operator Π, i.e., the $T^{(j)}$ are circulant. To find a particular transformation that allows us to set the temperature of the local states to any arbitrary $1/\beta_\mathrm{out}$ it is enough to pick all the rotations on the different subspaces S_j to have the 'same angle', that is to take all the $T^{(j)}$ to have the same matrix elements to one another. We can then write

$$\mathrm{diag}(\mathrm{Tr}_\mathrm{B}[\hat{\rho}']) = T \sum_{j=0}^{d-1} \mathrm{diag}(\hat{\rho})_{S_j}, \tag{B.0.19}$$

$$\mathrm{diag}(\mathrm{Tr}_\mathrm{A}[\hat{\rho}']) = T \sum_{j=0}^{d-1} \Pi^j \,\mathrm{diag}(\hat{\rho})_{S_j}. \tag{B.0.20}$$

We can write T (or any doubly stochastic matrix) in terms of a convex combination of permutation matrices (Birkhoff-von Neumann decomposition [188]), the coefficients of which can be calculated from the initial and final temperatures of the system. Concretely,

$$T = \sum_{i=0}^{d-1} \eta_i \Pi^i, \tag{B.0.21}$$

where the η_i satisfy $\eta_i > 0 \,\forall\, i$ and $\sum_i \eta_i = 1$. The diagonal elements of the local states after application of the unitary will thus be given by

$$\mathrm{diag}(\hat{\rho}'_{\mathrm{A}}) = \sum_{i=0}^{d-1} \eta_i \Pi^i \sum_{j=0}^{d-1} \mathrm{diag}(\hat{\rho})_{S_j}, \tag{B.0.22}$$

$$\mathrm{diag}(\hat{\rho}'_{\mathrm{B}}) = \sum_{i=0}^{d-1} \eta_i \Pi^i \sum_{j=0}^{d-1} \Pi^j \,\mathrm{diag}(\hat{\rho})_{S_j}. \tag{B.0.23}$$

Let us again focus on the state of subsystem A to determine the coefficients η_i from a given initial and desired final temperature. We can rewrite the right hand side of (B.0.22) as

$$\begin{aligned}\sum_{i=0}^{d-1} \eta_i \Pi^i \begin{bmatrix} \alpha_{00} \\ \alpha_{11} \\ \vdots \\ \alpha_{(d-1)(d-1)} \end{bmatrix} &= \eta_0 \begin{bmatrix} \alpha_{00} \\ \alpha_{11} \\ \vdots \\ \alpha_{(d-1)(d-1)} \end{bmatrix} + \eta_1 \begin{bmatrix} \alpha_{(d-1)(d-1)} \\ \alpha_{00} \\ \vdots \\ \alpha_{(d-2)(d-2)} \end{bmatrix} + \eta_2 \begin{bmatrix} \alpha_{(d-2)(d-2)} \\ \alpha_{(d-1)(d-1)} \\ \vdots \\ \alpha_{(d-3)(d-3)} \end{bmatrix} + \cdots \\ &= \begin{bmatrix} \eta_0\alpha_{00} + \eta_1\alpha_{11} + \cdots \\ \eta_0\alpha_{11} + \eta_1\alpha_{22} + \cdots \\ \eta_0\alpha_{22} + \eta_1\alpha_{33} + \cdots \\ \vdots \\ \eta_0\alpha_{(d-1)(d-1)} + \eta_1\alpha_{00} + \cdots \end{bmatrix},\end{aligned} \tag{B.0.24}$$

so that we can write each new diagonal element of the local state as

$$\alpha'_{jj} = \sum_{i=0}^{d-1} \eta_i \alpha_{(i+j)(i+j)}. \tag{B.0.25}$$

Recalling, again, that both the final and initial local states are Gibbs allows us to rewrite

initial and final diagonal matrix elements of the local states as

$$\frac{\mathrm{e}^{-\beta_{\mathrm{out}}E_j}}{Z'} = \sum_{i=0}^{d-1} \eta_i \frac{\mathrm{e}^{-\beta_{\mathrm{in}}E_{i+j}}}{Z}$$
$$\Rightarrow \mathrm{e}^{-\beta_{\mathrm{out}}E_j} = \frac{Z'}{Z} \sum_{i=0}^{d-1} \eta_i \mathrm{e}^{-\beta_{\mathrm{in}}E_{i+j}}, \tag{B.0.26}$$

where we have defined the partition functions $Z = \mathrm{Tr}[\mathrm{e}^{-\mathrm{i}\beta_{\mathrm{in}}\hat{H}}]$ and $Z' = \mathrm{Tr}[\mathrm{e}^{-\mathrm{i}\beta_{\mathrm{out}}\hat{H}}]$. This establishes a simple linear relationship between all the η_i and the final and initial temperatures that can easily be inverted to find all possible transformations $\eta_i(\beta_{\mathrm{in}}, \beta_{\mathrm{out}})$ (the solution is not unique). Not all collections of coefficients determined by pairs of temperatures β_{in} and β_{out} yield valid transformations (i.e., if the η_i compatible with (B.0.26) were negative). This means that there may be some sets of initial and final temperatures for which the unitary transformation that we desire is not possible. For Hamiltonians with uniform energy spacings, the final temperature is limited to be in the range $[-\beta_{\mathrm{out}}, \beta_{\mathrm{out}}]$. For Hamiltonians with nonuniform energy spacings, this range is further constricted. There is, then, a minimum local temperature that the application of this unitary can produce; beginning in a global thermal state of inverse temperature β_{in}, we must have $\beta_{\mathrm{out}} < \tilde{\beta}$ for some $\tilde{\beta} < \beta_{\mathrm{in}}$ [187]. This is not a significant roadblock since then this transformation is sufficient to reach any $\beta_{\mathrm{out}} < \tilde{\beta}$.

This completes the proof. In summary, we have presented here a pedagogical summary of the result in Appendix A.1 of [149]. Repeating the steps in [149], we have shown that the unitary which performs rotations in the subspaces (4.2.5) transforms global thermal states to states which have local Gibbs distributions. We have shown how the protocol in [149] gives a method to calculate the transformation acting on the local state, assuming that the rotation in each subspace S_j is the same.

Notice that there is a relevant difference between the method used in the body of the paper and the method from [149] that we summarized in this appendix. The latter does not fully specify the global unitary, only the local transformations. In the body of the paper, we use the general form for the global unitary that yields local transformations as the ones desired in this appendix. We additionally do not assume that the rotations in each subspace are the same, although we found that one of the rotations is indeed irrelevant.

Appendix C

How important are the correlations between the initial and final energies?

One can write the unprojected fluctuations as

$$\Sigma_W = \sqrt{\sigma_{E_i}^2 + \sigma_{E_f}^2 - 2\sigma_{E_i E_f}}, \tag{C.0.1}$$

where $\sigma_{E_{i/f}}^2$ is the variance of the initial (final) energy and $\sigma_{E_i E_f}$ is the covariance, or convex correlator, of the initial and final energies. This expression conceptualizes of the initial and final energies as random variables, with their own variances and a covariance between them.

This covariance is a bit of a nuanced quantity. It measures correlations in the energies *in time*. Usually, in quantum mechanics, we measure correlations between quantities at the same instant. We may take two approaches to calculate the covariance. The first considers the initial and final states to not live in the same Hilbert space—then, the covariance is trivially zero. The second considers them to live in the same Hilbert space, resulting in a nonzero covariance.

Of course, we know that the states are physically related; we evolve $\hat{\rho}$ into $\hat{\rho}'$ by the application of a unitary. It makes sense, then, to consider the correlations between them. We might then want to calculate the unprojected work fluctuations without the inclusion of the covariance simply to provide an estimation of how significant this factor is.

For both of these reasons, in this appendix we demonstrate the importance of considering the correlations between the initial and final energies, by calculating the unprojected work fluctuations without them.

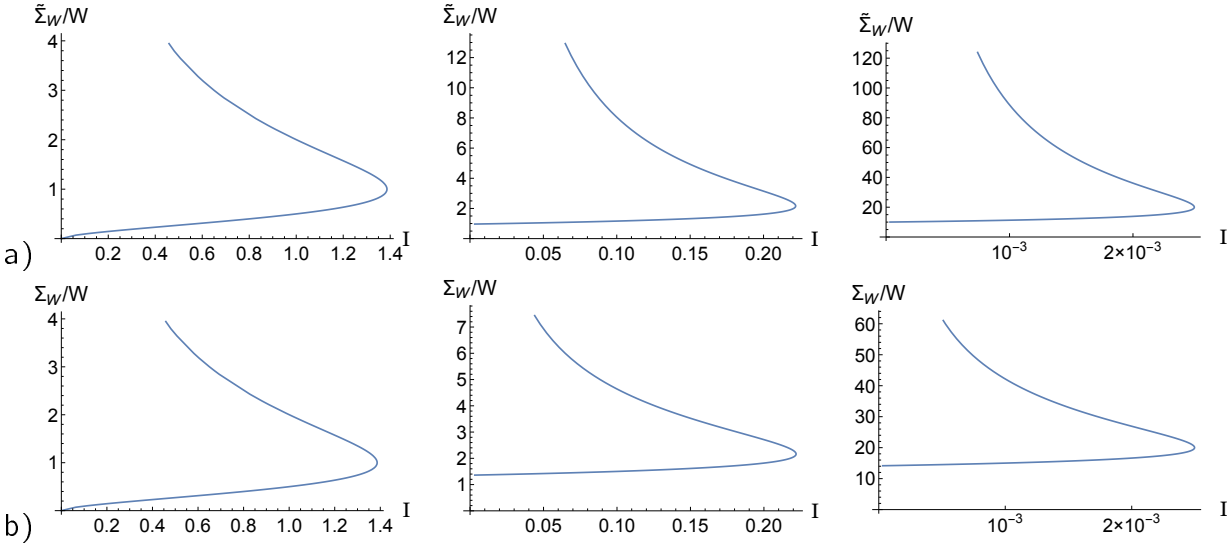

Figure C.1: The ratio of unprojected work fluctuations to average work cost versus the mutual information created in the protocol. Average work cost increases along the curve from top to bottom; $\beta_{\text{out}} = 0$ at the point of maximum creation of mutual information. From left to right, $\beta_{\text{in}} = 100\omega^{-1}$, ω^{-1}, $0.1\omega^{-1}$. Fluctuations are shown in a) without time correlations and in b) with time correlations. At high temperatures, the ratio of fluctuations to average work cost without considering correlations between ρ and ρ' is much larger than those when correlations are included. This gives an indication of the closeness of the initial and final states when the initial temperature is high.

The uncorrelated measure of fluctuations is larger than the two-time fluctuations of figure 5.3, but shows similar key characteristics—the ratio of fluctuations to average work cost is at least order unity for maximum creation of correlations, and increases as the initial temperature increases.

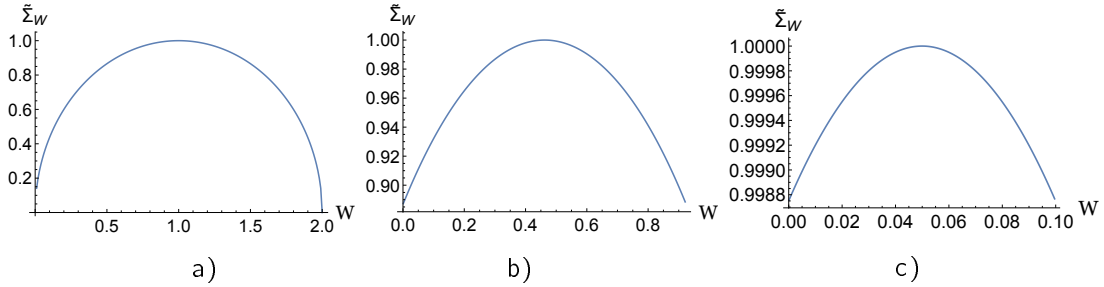

Figure C.2: Unprojected uncorrelated fluctuations plotted as a function of the average work cost. From left to right, $\beta_{\text{in}} = 100\omega^{-1}$, ω^{-1}, $0.1\omega^{-1}$. This uncorrelated measure is dramatically different from the correlated one, shown in figure 5.4, at higher temperatures. Notably, it is nonzero for zero work done, indicating that it is measuring the static energy variance of a state rather than work done in a dynamical process.

If we consider the correlations between $\hat{\rho}$ and $\hat{\rho}'$ to be irrelevant (or mathematically unfounded), then the independent unprojected work fluctuations are given by

$$\tilde{\Sigma}_W = \sqrt{\sigma_{E_i}^2 + \sigma_{E_f}^2}, \tag{C.0.2}$$

with energy variances

$$\sigma_{E_i}^2 = \text{Tr}[\hat{H}^2\hat{\rho}] - (\text{Tr}[\hat{H}\hat{\rho}])^2, \tag{C.0.3}$$

$$\sigma_{E_f}^2 = \text{Tr}[\hat{H}^2\hat{\rho}'] - (\text{Tr}[\hat{H}\hat{\rho}'])^2. \tag{C.0.4}$$

We can rewrite $\tilde{\Sigma}_W$ as

$$\tilde{\Sigma}_W = \sqrt{\text{Tr}[\hat{H}^2(\hat{\rho} + \hat{\rho}')] - (\text{Tr}[\hat{H}\hat{\rho}])^2 - (\text{Tr}[\hat{H}\hat{\rho}'])^2}. \tag{C.0.5}$$

Upon some subsitution and manipulation, we can arrive at an expression of this measure of fluctuations in terms of the final inverse temperature,

$$\tilde{\Sigma}_W = \omega \,\text{sech}[\beta_{\text{out}}\omega/2], \tag{C.0.6}$$

and in terms of the average work cost W and initial inverse temperature,

$$\tilde{\Sigma}_W = \sqrt{\omega^2 - \left(W - \omega \tanh\left[\frac{\beta_{\text{in}}\omega}{2}\right]\right)^2}. \tag{C.0.7}$$

This last expression allows us to bound the independent unprojected work fluctuations as

$$\omega \operatorname{sech}[\beta_{\text{in}}\omega/2] \leq \tilde{\Sigma}_W \leq \omega. \tag{C.0.8}$$

$\tilde{\Sigma}_W$ achieves the upper bound when the protocol creates maximal correlations, as the average work cost for $I_{\max}$ is $\omega \tanh[\beta_{\text{in}}\omega/2]$.

The ratio of this measure of fluctuations to the average work cost as a function of the mutual information created by the protocol is plotted in panel a) of figure C.1. The key characteristics noted in section 5.3.1 for the two-time measurement work fluctuations are present here; namely that the ratio is at least of order one for maximal creation of correlations, and that this ratio increases as the initial temperature of the state increases. Interestingly, this measure of fluctuations is about twice as large as the two-time fluctuations.

In figure C.2, we plot the uncorrelated fluctuations versus the average work cost. Here is where we see the feature of these fluctuations which makes them unphysical, or at least not very useful. As the initial temperature increases, the maximum of the uncorrelated fluctuations stays the same; the minimum value increases dramatically. For high initial temperature states, $\tilde{\Sigma}$ is nonzero even for a zero work process! This indicates that what the quantity measures is mostly the energy variance of the individual states, and not the variance of the difference of the random variables. This is to be expected from a quantity which does not follow the rules of error propagation and instead abandons the clearly important covariance term [189].